Appendix A.18:

Travis Country Dr – CPT 29778

Table 1: Site Description for Travis Country Dr (CPT 29778 – CC LIQ 8).

Attribute	Yes/No			Description/Date	Symbol in Figure 1
	10-m Buffer	20-m Buffer	50-m Buffer		
Near a body of surface water or other free face features?	No	No	No	The center of the site is 52 m away from a creek (~1.5-m-high, E-W free face) and 1250 m away from the Avon River (~2.0-m-high, NW-SE free face).	NA
Lateral spreading observed during the CES?	No	No	No	Absence of ground cracks indicates no lateral spreading, as observed by the mapping team.[1]	NA
Nearby buildings or structures?	Yes	Yes	Yes	Building coverage of the 10-m, 20-m, and 50-m buffers is 18%, 21%, and 18%, respectively. Buildings are in the N half of the 10-m and 20-m buffers and in all quadrants of the 50-m buffer.	White Fill + Brown Outline
Sloping land?	No	No	No	Flat land, residential area.	NA
Step changes in the ground surface?	No	No	No	NA	NA
Retaining walls?	No	No	No	NA	NA
Vegetation?	Yes	Yes	Yes	Trees and bushes cover 31% of the 10-m buffer, 16% of the 20-m buffer and 22% of the 50-m buffer. They are in the E half of the 10-m buffer and throughout all quadrants of the 20-m and 50-m buffers.	White Fill + Green Outline
Anthropogenic changes to the site between the LiDAR surveys?	Yes	Yes	Yes	Roadwork in the S portion of the three buffers was performed sometime between Sep 2015 and Nov 2015. Patches of new asphalt pavement are visible for Aug 2012; this repair might have occurred after Feb 2011 EQ and prior to Jun 2011 EQ, as observed from the aerial photography. Equipment in backyard in the NE quadrant of the 50-m buffer is present in Apr 2012 but is no longer visible in Sep 2015.	Roadwork: Orange Outline
Other important factors?	Yes	Yes	Yes	Two low-motor-vehicle-volume, two-way roadways occupy 19% of the 50-m buffer, whereas only one low-motor-vehicle-volume, two-way roadway covers 10% and 28% of the 10-m and 20-m buffers, respectively. The roads affect the S half of all the buffers. Recreational Vehicle (RV) is parked in the NW quadrant of the 50-m buffer. Bench is in the NW quadrant of the 50-m buffer.	Road: Gray Fill + Red Outline; RV: White Fill + Purple Outline; Bench: White Fill + Yellow Outline

Note: Buffer is the area within a circle of a specified radius with CPT investigations done at its center (172.691683°, -43.489401°).

[1] Canterbury Geotechnical Database. (2012). "Observed Ground Crack Locations", Map Layer CGD0400 - 23 July 2012, retrieved July 09, 2018 from https://canterburygeotechnicaldatabase.projectorbit.com/

Figure 1: Site plan with areas where LiDAR survey data is considered.

Note 1: Four patches (outlined in red) in free field were initially selected for settlement assessment as areas free of vegetation and structures. Further analyses such as proximity of a patch to a CPT, proximity of a patch to a property subjected to addition and/or demolition of a structure, front yard/backyard alterations (e.g., ploughing, rubble, scrap), aerial distribution of sediment ejecta, and density of LiDAR points for 2003 resulted in Patches A and B being selected for detailed settlement assessment and other patches being discarded in detailed settlement assessment. In addition, since significant amounts of ejecta were observed on roads in the CES, the entire portion of the road within the 50-m buffer was considered for settlement assessment. Roads as hard, relatively flat surfaces provide many ground-classified points. Therefore, it is very useful to compare settlement estimates on roads with settlement estimates in free field.

Table 2: LiDAR flight error adjustments, global adjustments for the difference between average LiDAR point elevations and benchmark survey elevations, and vertical tectonic movement adjustments.

	Adjustments (mm)		
Earthquake Event(s)	LiDAR Flight Error	Global Offset[2]	Tectonic Vertical Movement
Sep-10	0	-3	0
Feb-11	0	16	-40
Jun-11	0	38	-30
Dec-11	-100	-65	-10
CES	-100	-14	-80
Post Sep 2010 LiDAR survey affected by ejecta?			No

Note: The negative sign indicates the subtraction from the ground surface subsidence, while the positive sign indicates the addition to the ground surface subsidence.

Table 3a: LiDAR Measurement Error for Patch A.

Surveys	Buffer	Area Averaged Difference Indicating Repeat Measurement Error (mm)	$\sigma^*_{\text{individual LiDAR points}}$ (mm)	%Reduction in σ due to Area Averaging of LiDAR Points
Post Feb 2011: Mar 2011 and May 2011	10-m	NA	59	NA
	20-m	NA		
	50-m	NA		
Post Dec 2011: Feb 2012 and Oct 2015	10-m	32	70	[46,46]
	20-m	32		
	50-m	32		

*Standard deviation.

[2] Russell, J., & van Ballegooy, S. (2015). *Canterbury Earthquake Sequence: Increased liquefaction vulnerability assessment methodology*. New Zealand: Tonkin & Taylor Ltd.

Table 3b: LiDAR Measurement Error for Patch B.

Surveys	Buffer	Area Averaged Difference Indicating Repeat Measurement Error (mm)	$\sigma^*_{individual\ LiDAR\ points}$ (mm)	%Reduction in σ due to Area Averaging of LiDAR Points
Post Feb 2011: Mar 2011 and May 2011	10-m	NA	59	NA
	20-m	NA		
	50-m	NA		
Post Dec 2011: Feb 2012 and Oct 2015	10-m	NA	70	[30,30]
	20-m	NA		
	50-m	21		

*Standard deviation.

Table 3c: LiDAR Measurement Error for Road.

Surveys	Buffer	Area Averaged Difference Indicating Repeat Measurement Error (mm)	$\sigma^*_{individual\ LiDAR\ points}$ (mm)	%Reduction in σ due to Area Averaging of LiDAR Points
Post Feb 2011: Mar 2011 and May 2011	10-m	NA	59	NA
	20-m	NA		
	50-m	NA		
Post Dec 2011: Feb 2012 and Oct 2015	10-m	11	70	[14,33]
	20-m	10		
	50-m	23		

*Standard deviation.

Table 4a: Ground surface subsidence adjustments for Patch A due to LiDAR measurement error.

Earthquake Event(s)	$\sigma_{pre\text{-}EQ\ LiDAR\ survey}$ (mm)	$\sigma_{post\text{-}EQ\ LiDAR\ survey}$ (mm)	σ_{total} (mm)	Area Average Adjusted σ (mm) **
Sep-10	158	56	134	±61
Feb-11	56	59	59	±27
Jun-11	59	61	62	±28
Dec-11	61	70	87	±40
CES	158	70	124	±57

**Based on the highest %Reduction in Table 3a.

Table 4b: Ground surface subsidence adjustments for Patch B due to LiDAR measurement error.

Earthquake Event(s)	$\sigma_{pre\text{-}EQ\ LiDAR\ survey}$ (mm)	$\sigma_{post\text{-}EQ\ LiDAR\ survey}$ (mm)	σ_{total} (mm)	Area Average Adjusted σ (mm) **
Sep-10	158	56	134	±40
Feb-11	56	59	59	±18
Jun-11	59	61	62	±19
Dec-11	61	70	87	±26
CES	158	70	124	±37

**Based on the highest %Reduction in Table 3b.

Table 4c: Ground surface subsidence adjustments for Road due to LiDAR measurement error.

Earthquake Event(s)	$\sigma_{pre\text{-}EQ\ LiDAR\ survey}$ (mm)	$\sigma_{post\text{-}EQ\ LiDAR\ survey}$ (mm)	σ_{total} (mm)	Area Average Adjusted σ (mm) **
Sep-10	158	56	134	±44
Feb-11	56	59	59	±19
Jun-11	59	61	62	±20
Dec-11	61	70	87	±28
CES	158	70	124	±41

**Based on the highest %Reduction in Table 3d.

Table 5a: Raw liquefaction-related ground surface subsidence for Patch A using original LiDAR points.

	Average Ground Surface Subsidence (mm)		
Earthquake Event(s)	10-m Buffer	20-m Buffer	50-m Buffer
Sep-10	NA	NA	NA
Feb-11	116	116	116
Jun-11	55	55	55
Dec-11	91	91	91
CES	NA	NA	NA

Table 5b: Raw liquefaction-related ground surface subsidence for Patch B using original LiDAR points.

	Average Ground Surface Subsidence (mm)		
Earthquake Event(s)	10-m Buffer	20-m Buffer	50-m Buffer
Sep-10	NA	NA	-60
Feb-11	NA	NA	134
Jun-11	NA	NA	1
Dec-11	NA	NA	84
CES	NA	NA	160

Table 5c: Raw liquefaction-related ground surface subsidence for Road using original LiDAR points.

	Average Ground Surface Subsidence (mm)		
Earthquake Event(s)	10-m Buffer	20-m Buffer	50-m Buffer
Sep-10	140	92	72
Feb-11	31	46	41
Jun-11	38	42	36
Dec-11	85	80	75
CES	294	260	224

Table 6a: Corrected liquefaction-related ground surface subsidence for Patch A using original LiDAR points with the calculated adjustments in Table 2.

	Average Calculated Ground Surface Subsidence (mm)		
Earthquake Event(s)	10-m Buffer	20-m Buffer	50-m Buffer
Sep-10	NA	NA	NA
Feb-11	92 ± 25	92 ± 25	92 ± 25
Jun-11	63 ± 25	63 ± 25	63 ± 25
Dec-11	-84 ± 50	-84 ± 50	-84 ± 50
CES	NA	NA	NA

Notes: Plus/minus values are same as those in Table 4a, but rounded to the nearest 25; Positive overall values indicate ground surface subsidence, while negative overall values indicate ground surface uplift.

Table 6b: Corrected liquefaction-related ground surface subsidence for Patch B using original LiDAR points with the calculated adjustments in Table 2.

	Average Calculated Ground Surface Subsidence (mm)		
Earthquake Event(s)	10-m Buffer	20-m Buffer	50-m Buffer
Sep-10	NA	NA	-63 ± 50
Feb-11	NA	NA	110 ± 25
Jun-11	NA	NA	9 ± 25
Dec-11	NA	NA	-91 ± 25
CES	NA	NA	-35 ± 50

Notes: Plus/minus values are same as those in Table 4b, but rounded to the nearest 25; Positive overall values indicate ground surface subsidence, while negative overall values indicate ground surface uplift.

Table 6c: Corrected liquefaction-related ground surface subsidence for Road using original LiDAR points with the calculated adjustments in Table 2.

	Average Calculated Ground Surface Subsidence (mm)		
Earthquake Event(s)	10-m Buffer	20-m Buffer	50-m Buffer
Sep-10	137 ± 50	89 ± 50	69 ± 50
Feb-11	7 ± 25	22 ± 25	17 ± 25
Jun-11	46 ± 25	50 ± 25	44 ± 25
Dec-11	-91 ± 25	-95 ± 25	-101 ± 25
CES	99 ± 50	66 ± 50	30 ± 50

Notes: Plus/minus values are same as those in Table 4d, but rounded to the nearest 25; Positive overall values indicate ground surface subsidence, while negative overall values indicate ground surface uplift.

Table 7a: Corrected liquefaction-related ground surface subsidence for Patch A using LiDAR DEMs.

	Estimated Ground Surface Subsidence (mm)								
	10-m Buffer			20-m Buffer			50-m Buffer		
Earthquake Event(s)	16th %ile	50th %ile	84th %ile	16th %ile	50th %ile	84th %ile	16th %ile	50th %ile	84th %ile
Sep-10	50	50	50	50	50	50	50	50	50
Feb-11	100	100	100	100	100	100	100	100	100
Jun-11	50	50	50	50	50	50	50	50	50
Dec-11	<50	50	50	<50	50	50	<50	50	50
CES	250	250	250	250	250	250	250	250	250

Note: These percentiles are not the exact statistical measures; they indicate the spatial variability of ground surface subsidence.

Table 7b: Corrected liquefaction-related ground surface subsidence for Patch B using LiDAR DEMs.

	Estimated Ground Surface Subsidence (mm)								
	10-m Buffer			20-m Buffer			50-m Buffer		
Earthquake Event(s)	16th %ile	50th %ile	84th %ile	16th %ile	50th %ile	84th %ile	16th %ile	50th %ile	84th %ile
Sep-10	NA	NA	NA	NA	NA	NA	50	50	50
Feb-11	NA	NA	NA	NA	NA	NA	50	50	100
Jun-11	NA	NA	NA	NA	NA	NA	50	50	50
Dec-11	NA	NA	NA	NA	NA	NA	<50	50	50
CES	NA	NA	NA	NA	NA	NA	150	150	150

Note: These percentiles are not the exact statistical measures; they indicate the spatial variability of ground surface subsidence.

Table 7c: Corrected liquefaction-related ground surface subsidence for Road using LiDAR DEMs.

	Estimated Ground Surface Subsidence (mm)								
	10-m Buffer			20-m Buffer			50-m Buffer		
Earthquake Event(s)	16th %ile	50th %ile	84th %ile	16th %ile	50th %ile	84th %ile	16th %ile	50th %ile	84th %ile
Sep-10	50	100	100	50	100	150	50	100	150
Feb-11	50	50	50	50	50	50	50	50	50
Jun-11	50	50	50	50	50	50	50	50	50
Dec-11	<50	<50	50	<50	<50	50	<50	<50	50
CES	150	150	150	100	150	200	100	150	200

Note: These percentiles are not the exact statistical measures; they indicate the spatial variability of ground surface subsidence.

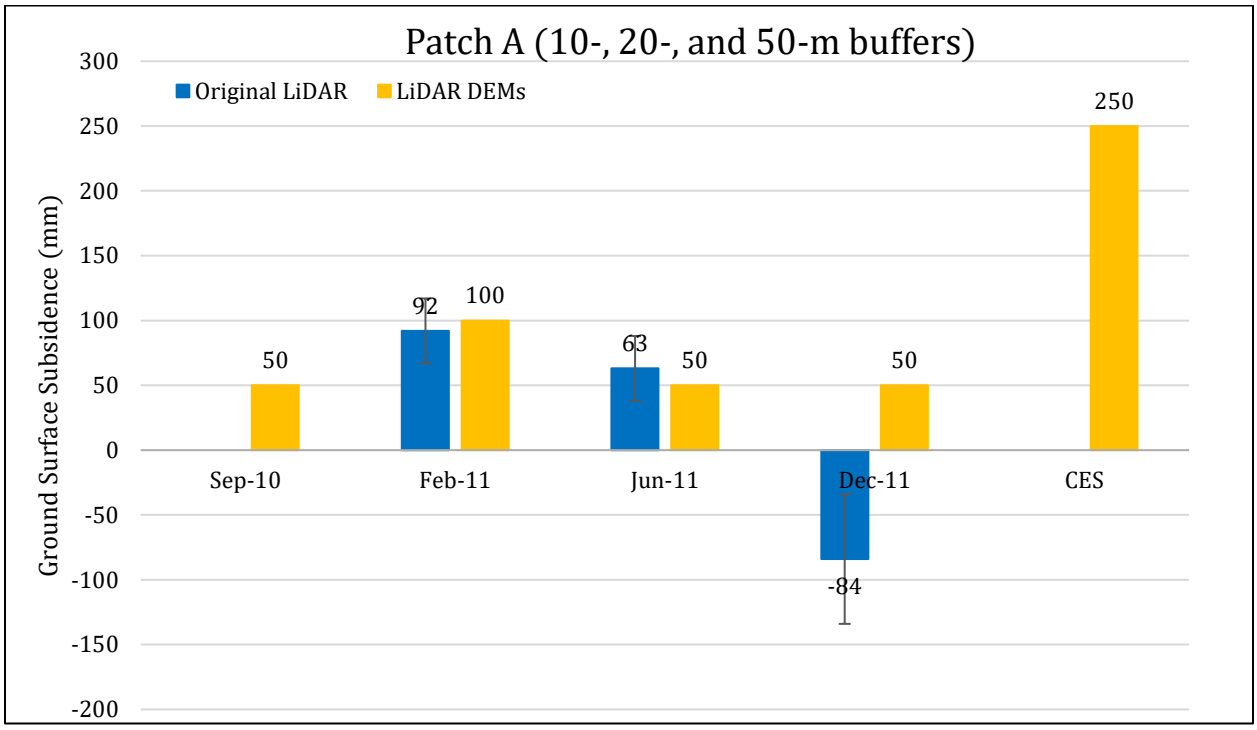

Figure 2: Comparison between ground surface subsidence determined from original LiDAR survey points and ground surface subsidence (50th %ile) estimated using LiDAR DEMs for Patch A.

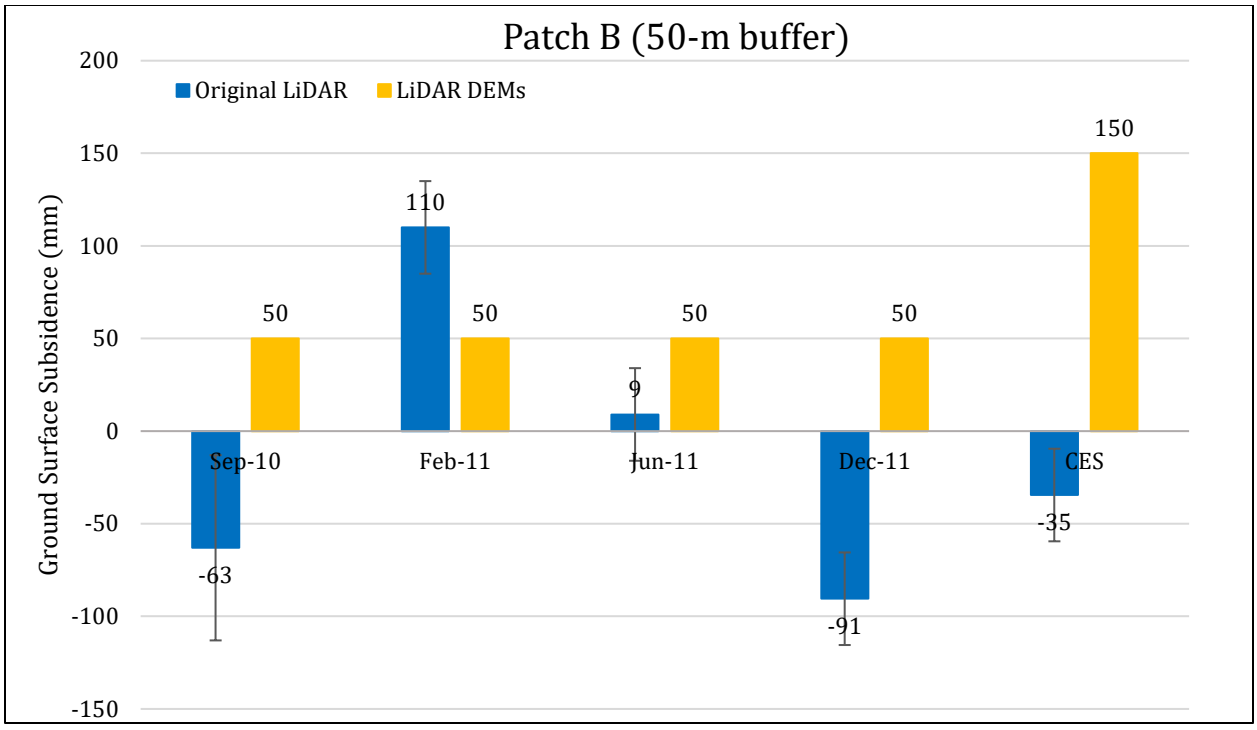

Figure 3: Comparison between ground surface subsidence determined from original LiDAR survey points and ground surface subsidence (50th %ile) estimated using LiDAR DEMs for Patch B.

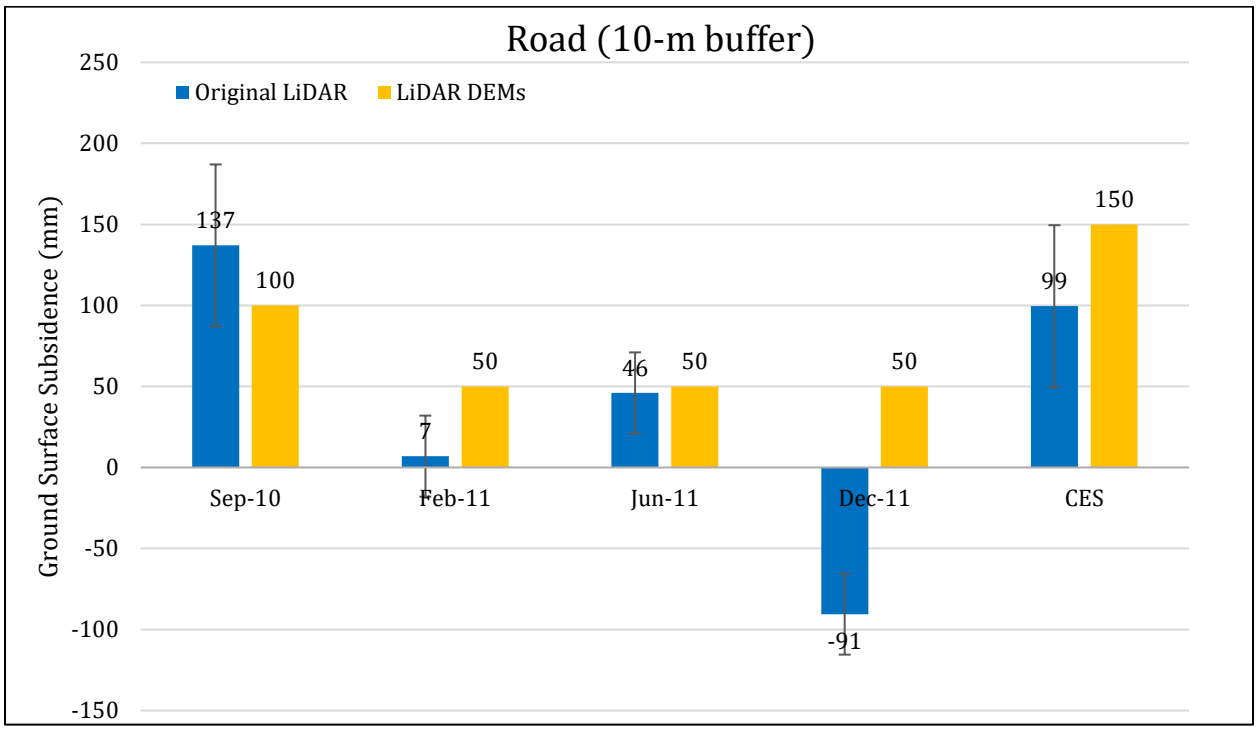

Figure 4: Comparison between ground surface subsidence determined from original LiDAR survey points and ground surface subsidence (50th %ile) estimated using LiDAR DEMs for Road for the 10-m buffer.

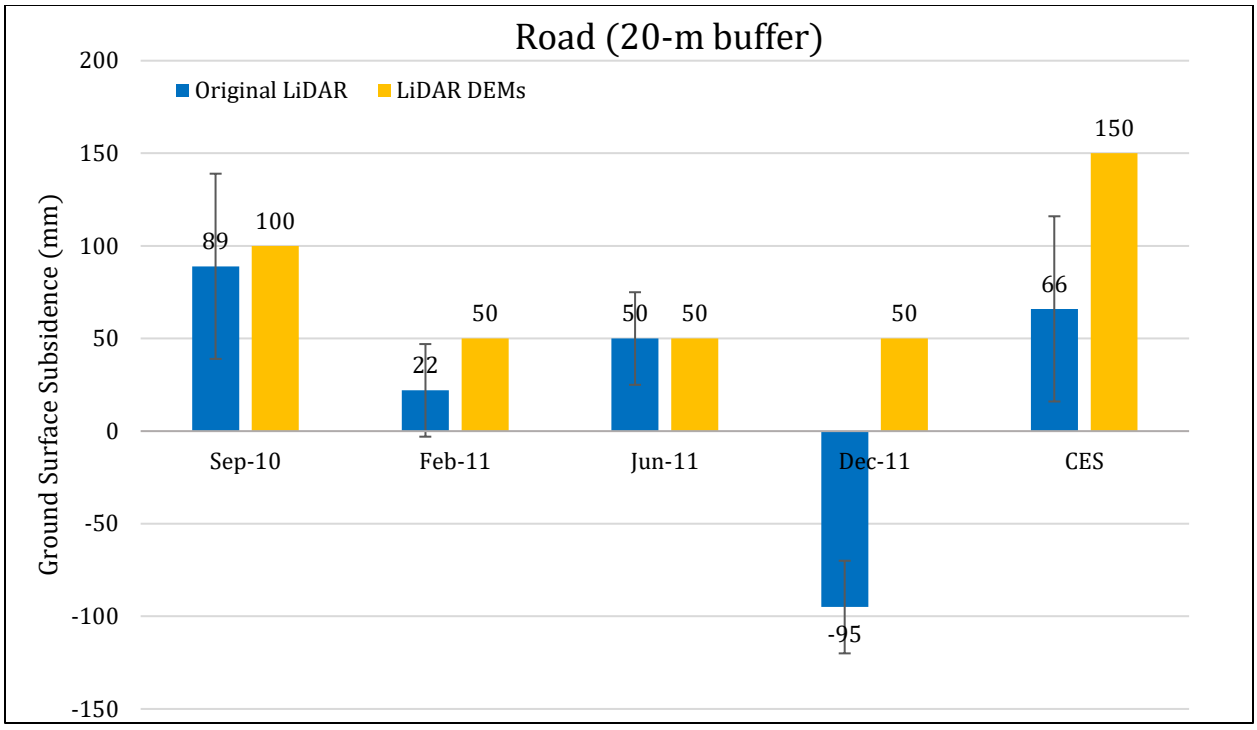

Figure 5: Comparison between ground surface subsidence determined from original LiDAR survey points and ground surface subsidence (50th %ile) estimated using LiDAR DEMs for Road for the 20-m buffer.

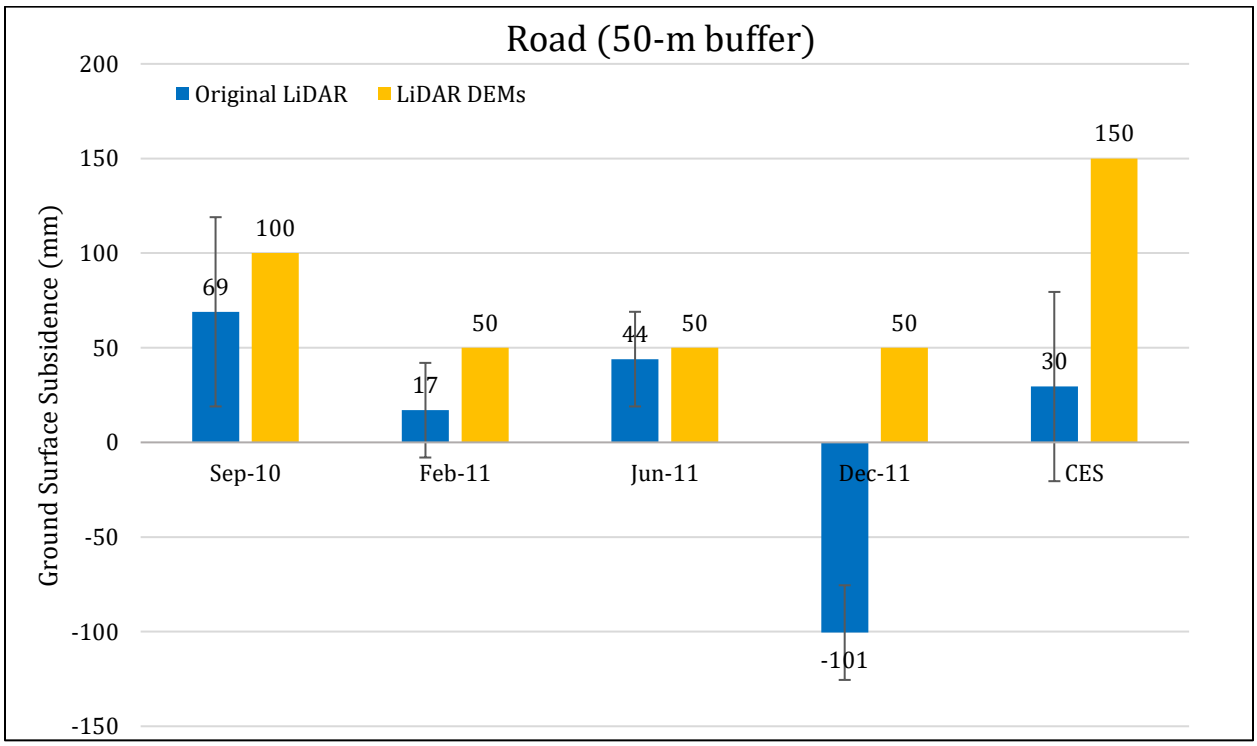

Figure 6: Comparison between ground surface subsidence determined from original LiDAR survey points and ground surface subsidence (50th %ile) estimated using LiDAR DEMs for Road for the 50-m buffer.

Note 2: The ground surface subsidence values determined from original LiDAR survey points are generally similar to the ground surface subsidence values estimated using LiDAR DEMs for all earthquake events. Discrepancy is evident for Patch B for the Feb-11 EQ – the ground surface subsidence based on LiDAR DEMs is two times smaller than that estimated using the original LiDAR points (50 mm versus 110 mm, respectively).

Table 8a: Ejecta-induced settlement for the top 20-m of the soil profile for Patch A for the 50th %ile PGA and P_L=50% using BI-2014, ZRB-2002, C_{FC} = 0.13, and I_C cutoff of 2.6.

Earthquake Event(s)	M_W	PGA (g)	Depth to Groundwater (m)	S_T (mm)	S_{V1D} (mm)	$S_{E,L}$ (mm)
Sep-10	7.1	0.17	1.5	NA	0±20	NA
Feb-11	6.2	0.35	1.5	92±25	4±50	88±56
Jun-11	6.2	0.21	1.5	63±25	0±25	63±35
Dec-11	6.1	0.31	0.5	-84±50	11±50	-95±71

Notes: S_T = Total settlement (Table 6); S_{V1D} = Average vertical settlement due to volumetric compression using Boulanger and Idriss (2014) (BI-2014), Zhang et al. (2002) (ZRB-2002) procedures and de Greef and Lengkeek (2018) thin-layer correction; $S_{E,L}$ = Ejecta-induced settlement as the difference between the LiDAR-based S_T and S_{V1D}.

Table 8b: Ejecta-induced settlement for the top 20-m of the soil profile for Patch B for the 50th %ile PGA and P_L=50% using BI-2014, ZRB-2002, C_{FC} = 0.13, and I_C cutoff of 2.6.

Earthquake Event(s)	M_W	PGA (g)	Depth to Groundwater (m)	S_T (mm)	S_{V1D} (mm)	$S_{E,L}$ (mm)
Sep-10	7.1	0.17	1.5	-63±50	0±20	-63±54
Feb-11	6.2	0.35	1.5	110±25	18±50	92±56
Jun-11	6.2	0.21	1.5	9±25	1±25	8±35
Dec-11	6.1	0.31	0.5	-91±25	30±50	-121±56

Notes: S_T = Total settlement (Table 6); S_{V1D} = Average vertical settlement due to volumetric compression using Boulanger and Idriss (2014) (BI-2014), Zhang et al. (2002) (ZRB-2002) procedures and de Greef and Lengkeek (2018) thin-layer correction; $S_{E,L}$ = Ejecta-induced settlement as the difference between the LiDAR-based S_T and S_{V1D}.

Table 8c: Ejecta-induced settlement for the top 20-m of the soil profile for Road within the 50-m buffer for the 50th %ile PGA and P_L=50% using BI-2014, ZRB-2002, C_{FC} = 0.13, and I_C cutoff of 2.6.

Earthquake Event(s)	M_W	PGA (g)	Depth to Groundwater (m)	S_T (mm)	S_{V1D} (mm)	$S_{E,L}$ (mm)
Sep-10	7.1	0.17	1.5	69±50	0±20	69±54
Feb-11	6.2	0.35	1.5	17±25	12±50	5±56
Jun-11	6.2	0.21	1.5	44±25	0±25	44±35
Dec-11	6.1	0.31	0.5	-101±25	23±50	-124±56

Notes: S_T = Total settlement (Table 6); S_{V1D} = Average vertical settlement due to volumetric compression using Boulanger and Idriss (2014) (BI-2014), Zhang et al. (2002) (ZRB-2002) procedures and de Greef and Lengkeek (2018) thin-layer correction; $S_{E,L}$ = Ejecta-induced settlement as the difference between the LiDAR-based S_T and S_{V1D}.

Note 3: The uncertainty for volumetric settlement was derived based on the sensitivity of volumetric settlement to PGA, C_{FC}, and P_L for each earthquake event for VsVp 57203 *Shirley Intermediate School* and CC LIQ 1 – CPT 5586 – *Vivian St* sites. Taking the 50th percentile as the baseline case, the minimum and maximum values corresponding to the difference between the 25th percentile and the 50th percentile and the 75th percentile and the 50th percentile were determined. The arithmetic mean of the range of the minimum and maximum difference was evaluated for each patch at the two sites. The maximum arithmetic mean for each earthquake event was rounded to the nearest five and used as the uncertainty value. Accordingly, the 1-D volumetric settlement uncertainties of ±20, ±50, ±25, and ±50 mm for the Sep-10, Feb-11, Jun-11, and Dec-11 earthquake events, respectively, were used for all sites in this study.

Table 9a: Coverage area and height of ejecta estimates for Patch A using photographs.

Earthquake Event	$A_{E,thick}$ (m^2)	$H_{E,thick}$ (mm)	$A_{E,thin}$ (m^2)	$H_{E,thin}$ (mm)	A_T (m^2)
Sep-10	0	0	0	0	13.8
Feb-11	0	0	1.31	10-50	13.8
Jun-11	0	0	0	0	13.8
Dec-11	0	0	0	0	13.8

Notes: $A_{E,thick/thin}$ = Coverage area of thick/thin ejecta layers; $H_{E,thick/thin}$ = Lower-upper estimate of height of thick/thin ejecta layers; A_T = Total assessment area of a buffer being considered; Thin and thick layers correspond to light gray and dark gray colors of ejecta observed in aerial photographs.

Table 9b: Coverage area and height of ejecta estimates for Patch B using photographs.

Earthquake Event	$H_{E,thin}$ (mm)	$A_{E,thin}$ (m^2)	$H_{E,thick}$ (mm)	$A_{E,thick}$ (m^2)	A_T (m^2)
Sep-10	0	0	0	0	33.0
Feb-11	0	0	0	0	33.0
Jun-11	0	0	0	0	33.0
Dec-11	0	0	0	0	33.0

Notes: $A_{E,thick/thin}$ = Coverage area of thick/thin ejecta layers; $H_{E,thick/thin}$ = Lower-upper estimate of height of thick/thin ejecta layers; A_T = Total assessment area of a buffer being considered; Thin and thick layers correspond to light gray and dark gray colors of ejecta observed in aerial photographs.

Table 9c: Coverage area and height of ejecta estimates for Road within the 50-m buffer using photographs.

Earthquake Event	Sep-10	Feb-11	Jun-11	Dec-11
$H_{E,thin}$ (mm)	0	5-10	5-10	3-6
$A_{E,thin}$ (m^2)	0	1183	48.8	58.2
$H_{E,thick}$ (mm)	0	20-40	0	0
$A_{E,thick}$ (m^2)	0	4.6	0	0
$H_{E,prism}$ (mm)	0	8-150	0	0
$V_{E,prism}$ (m^3)	0	5.71-9.78	0	0
$H_{E,cone}$ (mm)	0	150-250	0	0
$A_{E,\ cone}$ (m^2)	0	3.45	0	0
$H_{E,cc}$ (mm)	0	294-1028	0	0
$V_{E,cc}$ (m^3)	0	7.80	0	0
A_T (m^2)	1459	1383*	1449*	1459

Notes: $A_{E,thin/thick}$ = Coverage area of thin/thick ejecta layers; $H_{E,\ thin/thick}$ = Lower-upper estimate of height of thin/thick ejecta layers; $H_{E,prism}$ = Lower-upper estimate of ejecta height near the curb based on 2-4% cross slope of normal crown; $V_{E,prism}$ = Lower-upper estimate of total volume of prismatic-shape ejecta; $A_{E,cone}$ = Coverage area of conically shaped ejecta layers; $H_{E,cone}$ = Lower-upper estimate of height of conically shaped ejecta layers; $V_{E,cc}$ = Volume of conically shaped ejecta pile components; $H_{E,cc}$ = Lower-upper estimate of height of conically shaped ejecta pile components (based on the repose angle of 30°); A_T = Total assessment area of a buffer being considered; * indicates the reduction in A_T due to the presence of objects within the assessment area.

Note 4: The values in Table 9 correspond to the coverage area of ejecta outlined in aerial photographs (Figures 75 through 79) and the lower and upper estimates of ejecta height based on geometry and EQC LDAT property inspection notes (Figures 80 and 81) and reports from Aug 2011 (no lateral spreading was observed by the inspection team). The ejecta-induced settlement using photographs and engineering judgment, $S_{E,P}$, is estimated as

$$S_{E,P} = \frac{\sum_{i=1}^{a} A_{E,thick,i} * H_{E,thick,i} + \sum_{j=1}^{b} A_{E,thin,j} * H_{E,thin,j} + \frac{1}{3}\sum_{l=1}^{d} A_{E,cc,l} * R_{E,cc,l} * tan30°}{A_T} + \frac{\frac{1}{3}\sum_{m=1}^{e} A_{E,cone,m} * H_{E,cone,m} + \frac{1}{2}\sum_{n=1}^{f} W_{E,prism,n} * H_{E,prism,n} * L_{E,prism,n}}{A_T} = \frac{\sum_{i=1}^{a} V_{E,thick,i} + \sum_{j=1}^{b} V_{E,thin,j} + \sum_{l=1}^{d} V_{E,conical\ component,l} + \sum_{m=1}^{e} V_{E,cone,m} + \sum_{n=1}^{f} V_{E,prism,n}}{A_T}$$

where

- $A_{E,thick,i}$ and $H_{E,thick,i}$ are the area and the height of a thick ejecta layer, respectively;
- $A_{E,thin,j}$ and $H_{E,thin,j}$ are the area and the height of a thin ejecta layer, respectively;
- $A_{E,cc,l}$ and $R_{E,cc,l}$ are the area and the radius of an ejecta pile component, respectively, shaped as a cone with the repose angle of 30°;
- $A_{E,cone,m}$ and $H_{E,cone,m}$ are the aerea and the height of a conically shaped ejecta, respectively;
- $W_{E,prism,n}$ and $L_{E,prism,n}$ are the width and the length of the coverage area of a prismatically shaped ejecta layer, respectively, and $H_{E,prism,n}$ is the height of a prism-like ejecta layer;
- A_T is the total assessment area for a buffer being considered (Figure 1).

Table 10: Ejecta-induced settlement estimates for Patches A and B and Road based on photographs.

EQ Event	Patch A (10-, 20-, and 50-m buffers)		Patch B (50-m buffer)		Road (50-m buffer)	
	$S_{E,P,lower}$ (mm)	$S_{E,P,upper}$ (mm)	$S_{E,P,lower}$ (mm)	$S_{E,P,upper}$ (mm)	$S_{E,P,lower}$ (mm)	$S_{E,P,upper}$ (mm)
Sep-10	0	0	0	0	0	0
Feb-11	1	5	0	0	14	22
Jun-11	0	0	0	0	≈0	≈0
Dec-11	0	0	0	0	≈0	≈0

Note: $S_{E,P,lower}$ and $S_{E,P,upper}$ correspond to lower and upper estimates of $S_{E,P}$, respectively.

Table 11: Best final estimates of ejecta-induced settlement for Patches A and B and Road.

EQ Event	Patch A (10-, 20-, and 50-m buffers)			Patch B (50-m buffer)			Road (50-m buffer)		
	$S_{E,L}$ (mm)	$S_{E,P}$ (mm)	$S_{E,final}$ (mm)	$S_{E,L}$ (mm)	$S_{E,P}$ (mm)	$S_{E,final}$ (mm)	$S_{E,L}$ (mm)	$S_{E,P}$ (mm)	$S_{E,final}$ (mm)
Sep-10	NA	0	0	-63±54	0	0	69±54	0	0
Feb-11	88±56	3±2	5±5	92±56	0	0	5±56	18±4	15±20
Jun-11	63±35	0	0	8±35	0	0	44±35	≈0	<5
Dec-11	-95±71	0	0	-121±56	0	0	-124±56	≈0	<5

Notes: $S_{E,L}$ = Ejecta-induced settlement based on LiDAR data reported in Table 8; $S_{E,P}$ = Median ejecta-induced settlement for the range of values reported in Table 10; $S_{E,final}$ = Best final estimate of ejecta-induced settlement rounded to the nearest 5; Final plus/minus values are also rounded to the nearest 5.

Note 5:

- $S_{E,final}$ for Patch A is based solely on $S_{E,P}$ for all earthquake events.
- $S_{E,final}$ for Patch B is equal to $S_{E,P}$ for all earthquake events.
- $S_{E,final}$ for Road is a weighted average of $S_{E,L}$ and $S_{E,P}$ with weights of 1/3 and 2/3, respectively, for the Feb-11 EQ. For the Sep-10, Jun-11, and Dec-11 EQs, $S_{E,final}$ for Road is equal to $S_{E,P}$.
- The uncertainty associated with $S_{E,final}$ is also a weighted average of uncertainties associated with $S_{E,L}$ and $S_{E,P}$ with the same corresponding weights.
- The weights are based on the LiDAR error bands, LPI prediction error (Maurer et al. 2014[3]), presence of ejecta at the time of LiDAR surveys, density/quantity of LiDAR points, and completeness of visual evidence (i.e., ground and aerial photographs and EQC LDAT property inspection reports for the site). The Travis Country Dr site is in the apparent zone of higher ground surface subsidence for the Dec-11 EQ (i.e., the underestimate of the ground surface elevation by the Feb-12 LiDAR survey). The site is in the zone of accurate LPI prediction of liquefaction severity for the Sep-10 EQ and slight LPI underprediction of liquefaction severity for the Feb-11 EQ. The LDAT property inspection report is available for Patches A and B. There are no ground photographs of the road.

Summary 1:

- **The best estimate of the ejecta-induced free-field ground settlement at the Travis Country Dr site for the SEP 2010, FEB 2011, JUN 2011, and DEC 2011 earthquake is 0 mm, 5±5 mm, 0 mm, and 0 mm, respectively. About 95% of the site did not experience ejecta-induced ground settlement.**
- **The best estimate of the ejecta-induced free-field ground settlement of the road at the Bower Ave site for the SEP 2010, FEB 2011, JUN 2011, and DEC 2011 earthquake is 0 mm, 0-35 mm with the mean of 15 mm, <5 mm, and <5 mm, respectively.**

Note 6: CPT 29778 was initially named as CC LIQ 8.

Note 7: The PFY settlement assessment area visible in some of the following figures was later removed from the analysis.

[3] Maurer, B. W., Green, R. A., Cubrinovski, M., & Bradley, B. A. (2014). Evaluation of the Liquefaction Potential Index for Assessing Liquefaction Hazard in Christchurch, New Zealand. *Journal of Geotechnical and Geoenvironmental Engineering*, 140(7), 04014032-1-11. doi:10.1061/(asce)gt.1943-5606.0001117

Figure 7: Location of the site.

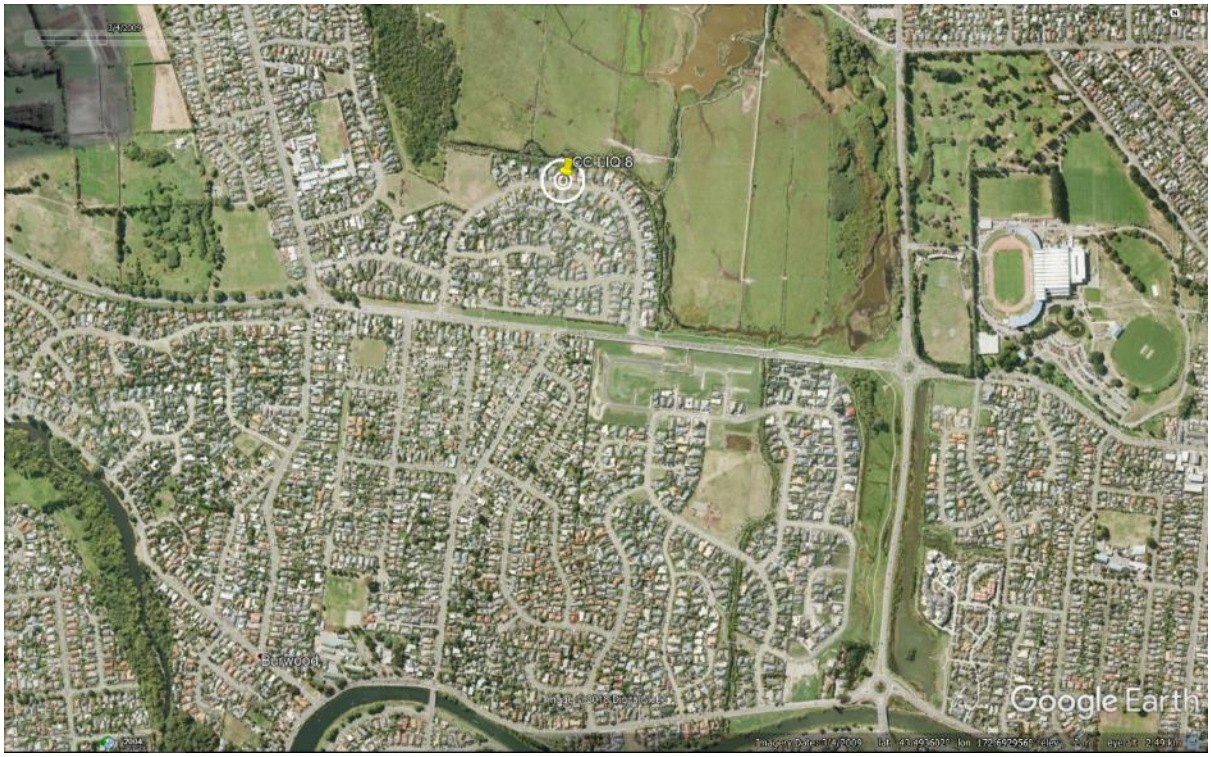

Figure 8: Position of the site relative to nearby buildings, vegetation, and free-face features.

Figure 9: Position of the site relative to swampy areas.

Figure 10: Street view of the site showing flat land.

Figure 11: Street view of the site showing patches of new asphalt pavement in Aug 2012.

Figure 12: Satellite image of the site taken in Dec 2004.

Figure 13: Satellite image of the site taken in Mar 2009.

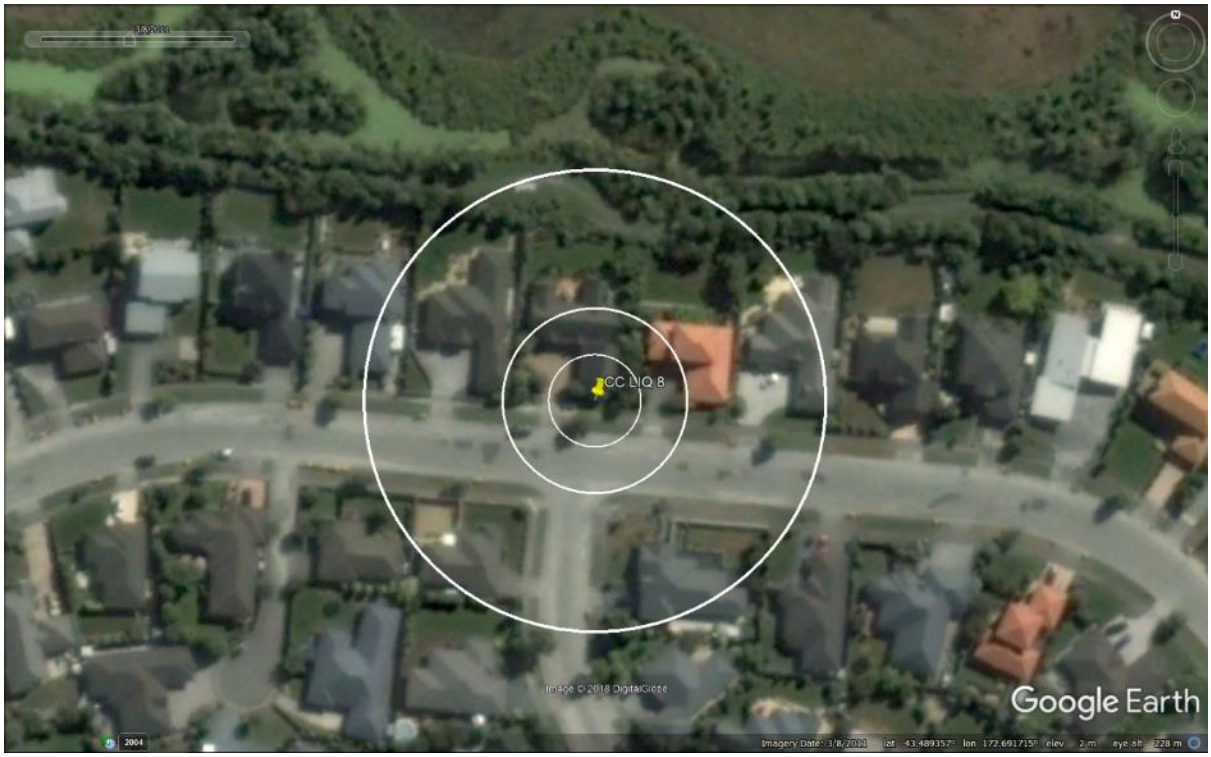

Figure 14: Satellite image of the site taken in Mar 2011.

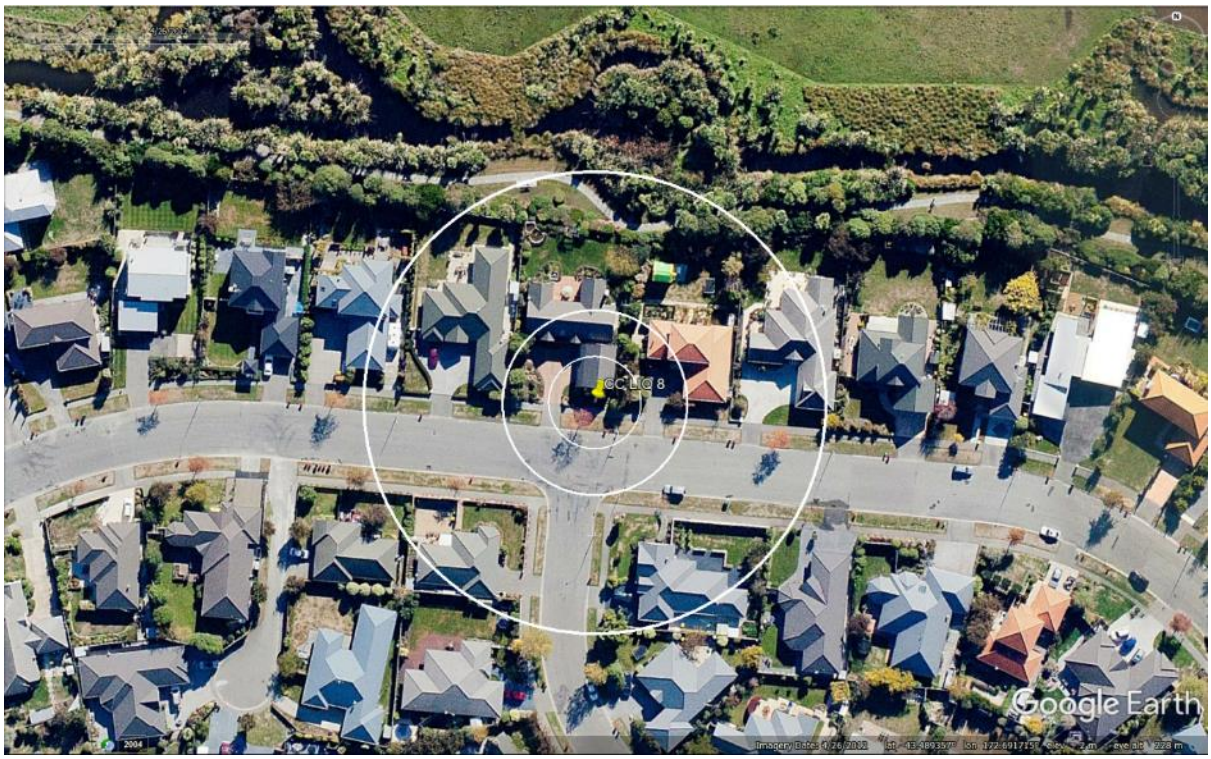

Figure 15: Satellite image of the site taken in Apr 2012.

Figure 16: Satellite image of the site taken in Sep 2015.

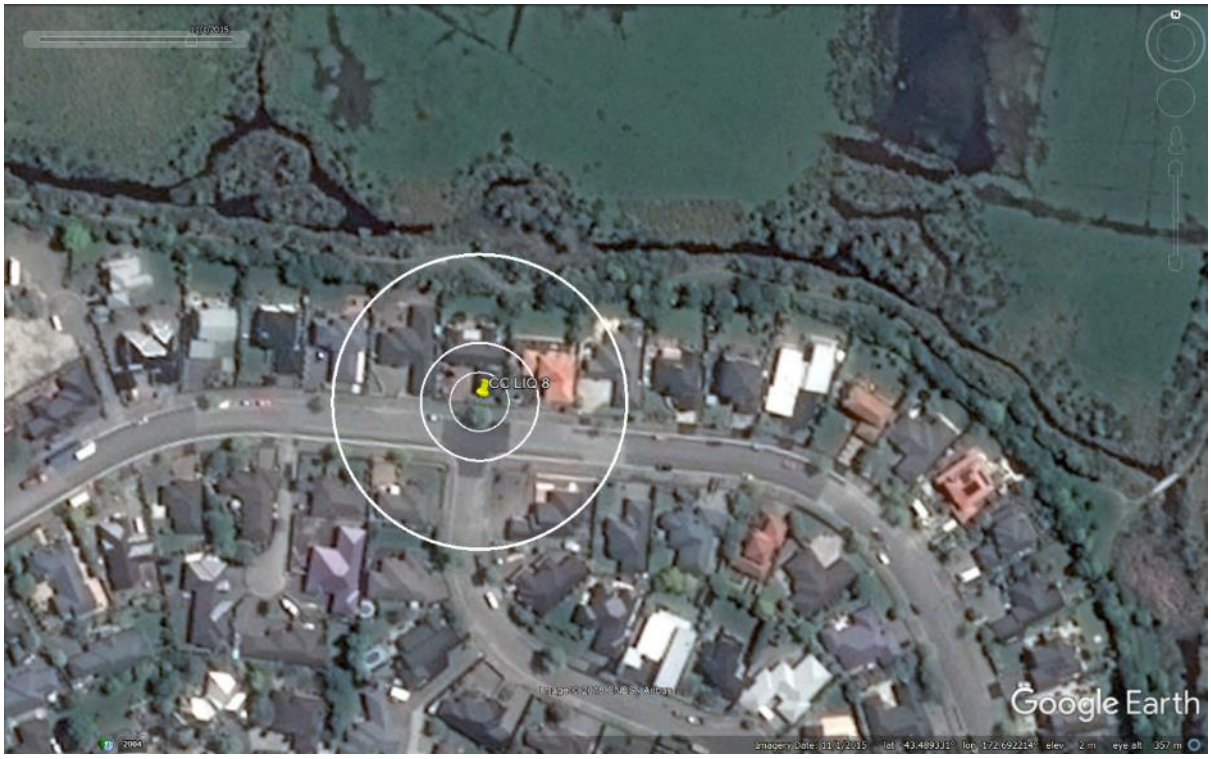

Figure 17: Satellite image of the site taken in Nov 2015.

Figure 18: Satellite image of the site taken in Jan 2016.

Figure 19: Aerial photograph of the site taken on Sep 4, 2010.

Figure 20: Aerial photograph of the site taken on Feb 24, 2011.

Figure 21: Aerial photograph of the site taken on June 14-15, 2011.

Figure 22: Aerial photograph of the site taken on June 16, 2011.

Figure 23: Aerial photograph of the site taken on Dec 24, 2011.

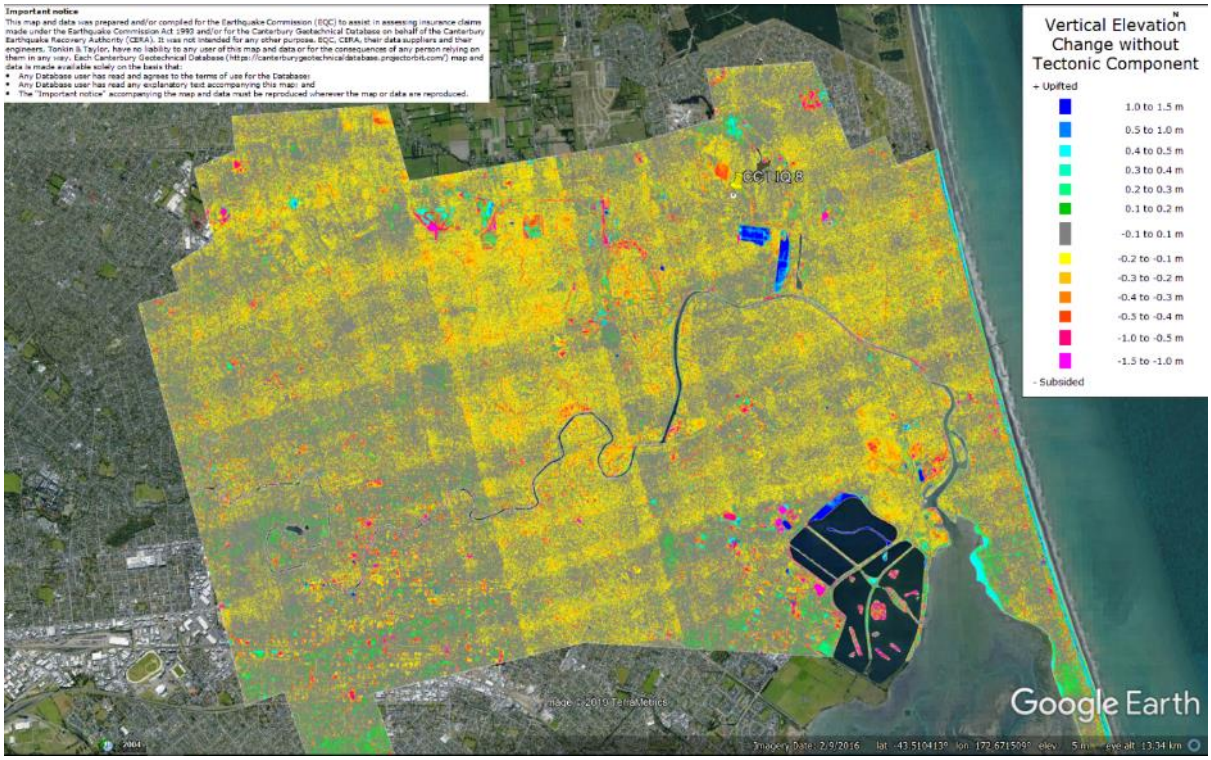

Figure 24: Vertical Ground Movements (Surface – Tectonic) for Sep 2010 Earthquake – the site is not in the apparent zone of overestimated ground surface subsidence.

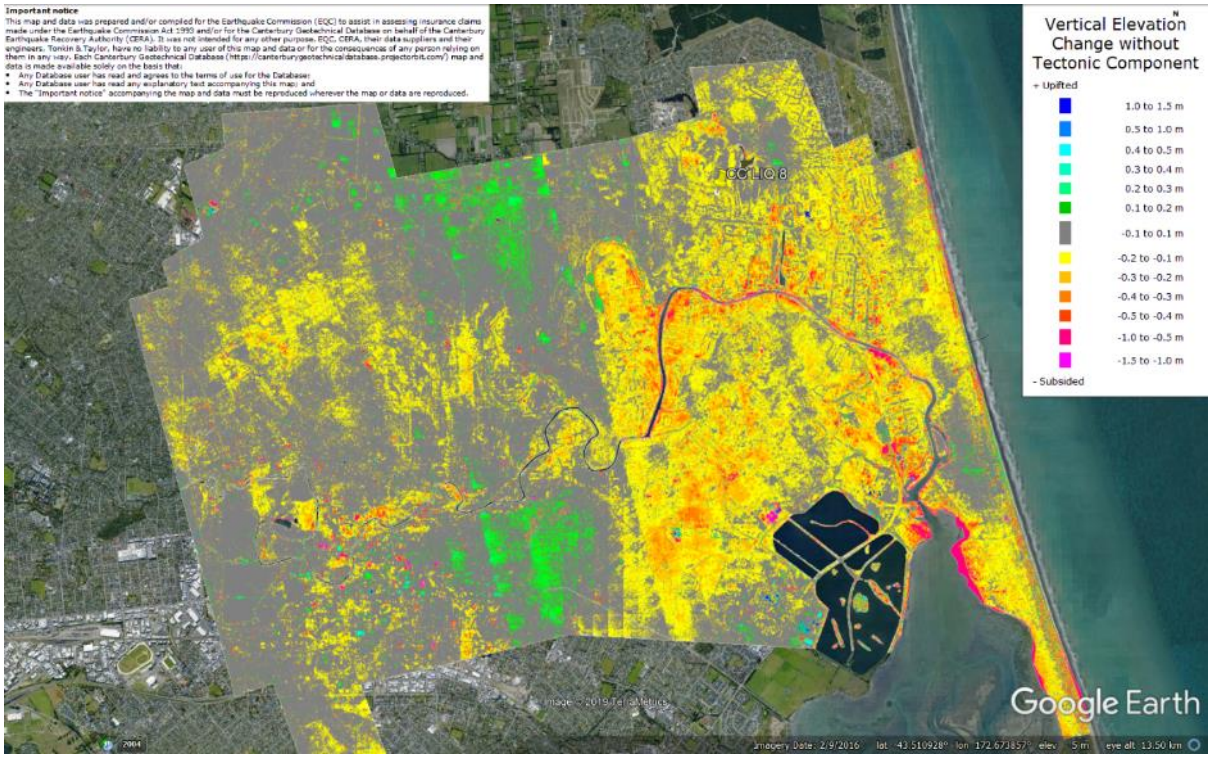

Figure 25: Vertical Ground Movements (Surface – Tectonic) for Feb 2011 Earthquake – the site is not in the apparent zone of underestimated ground surface subsidence.

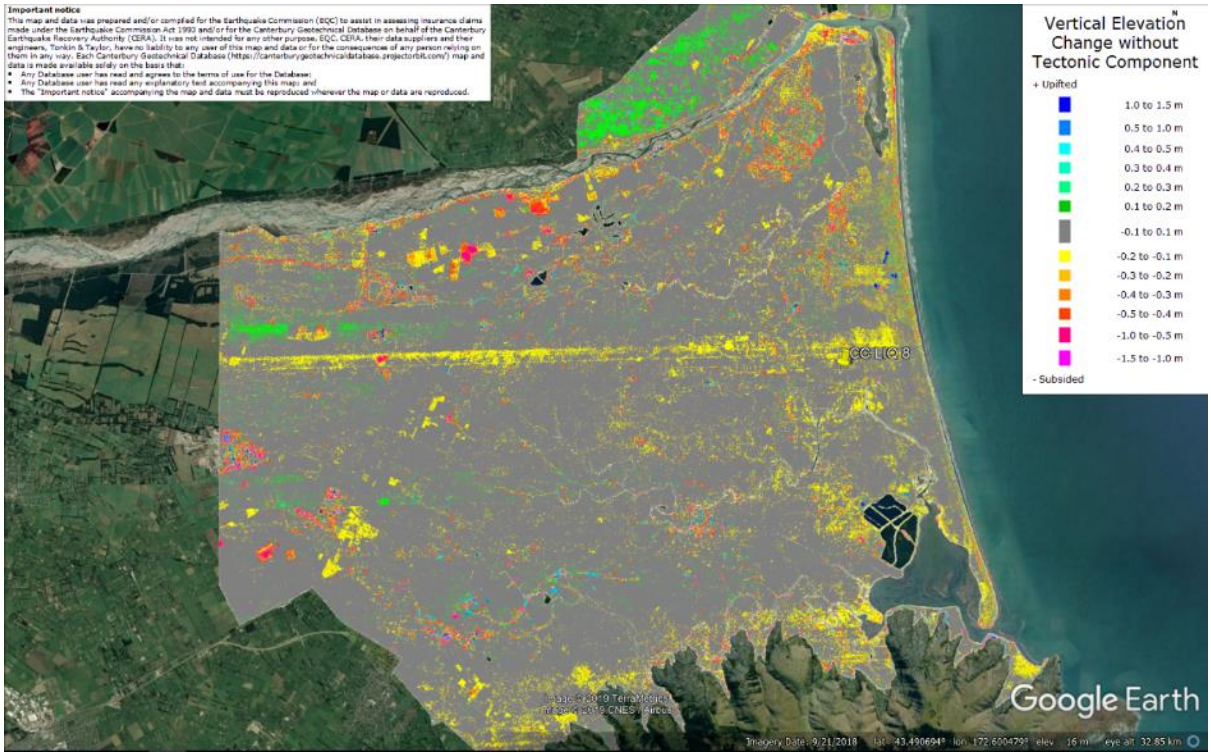

Figure 26: Vertical Ground Movements (Surface – Tectonic) for June 2011 Earthquake – the site is not in the apparent zone of overestimated or underestimated ground surface subsidence.

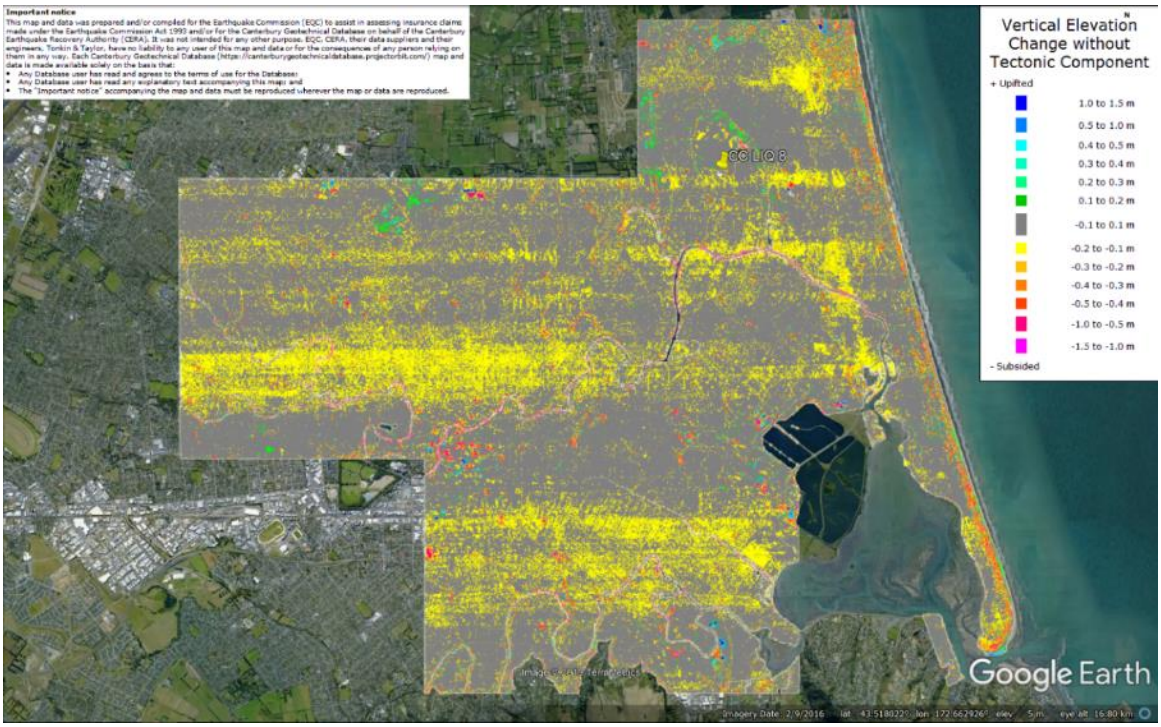

Figure 27: Vertical Ground Movements (Surface – Tectonic) for Dec 2011 Earthquake – the site is in the apparent zone of underestimated ground surface subsidence (i.e., Feb 2012 LiDAR flight error) .

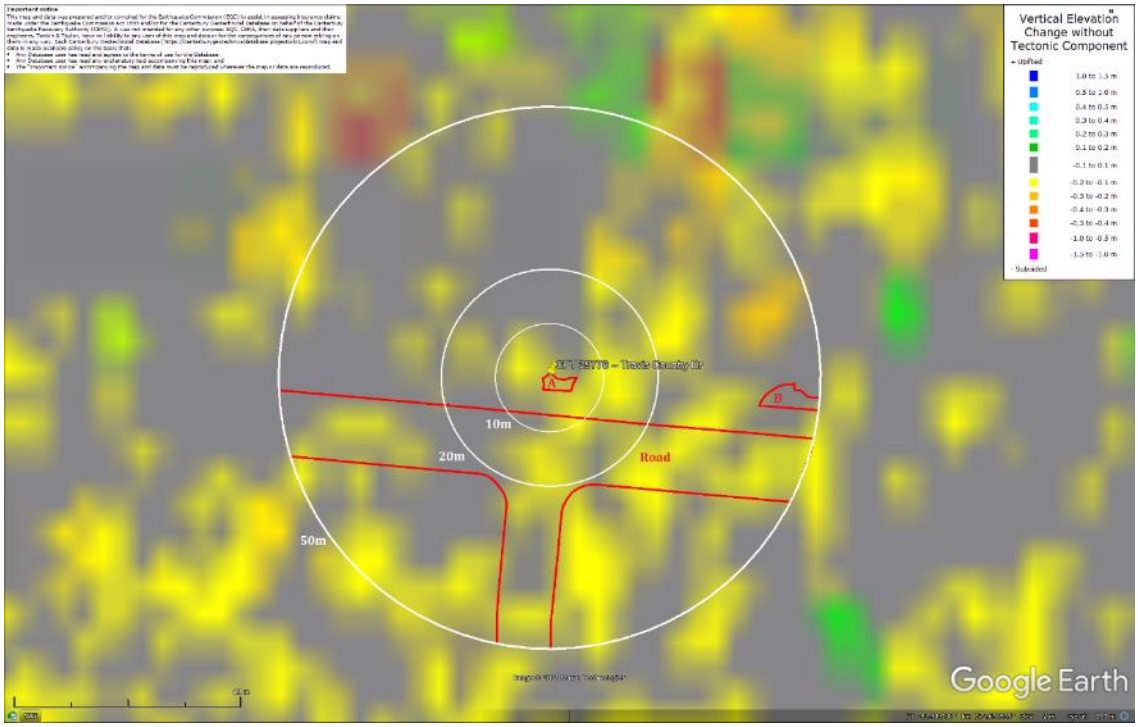

Figure 28: Ground surface subsidence without tectonic component for Sep 2010 Earthquake according to the LiDAR DEM.

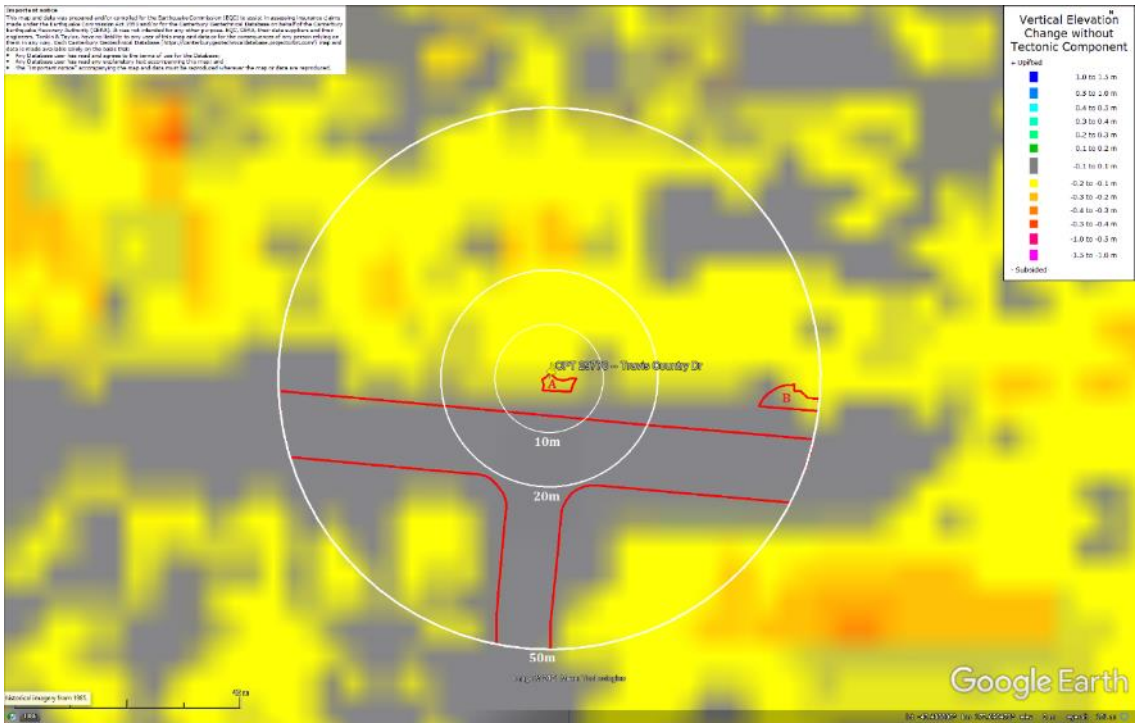

Figure 29: Ground surface subsidence without tectonic component for Feb 2011 Earthquake according to the LiDAR DEM.

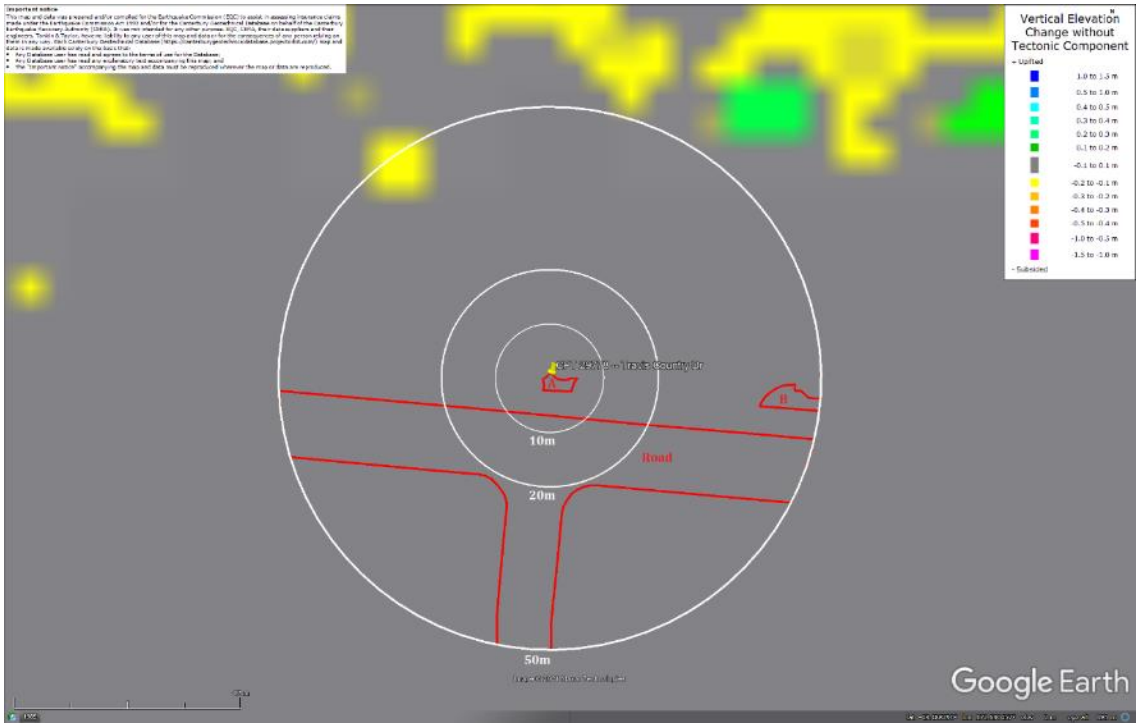

Figure 30: Ground surface subsidence without tectonic component for Jun 2011 Earthquake according to the LiDAR DEM.

Figure 31: Ground surface subsidence without tectonic component for Dec 2011 Earthquake according to the LiDAR DEM.

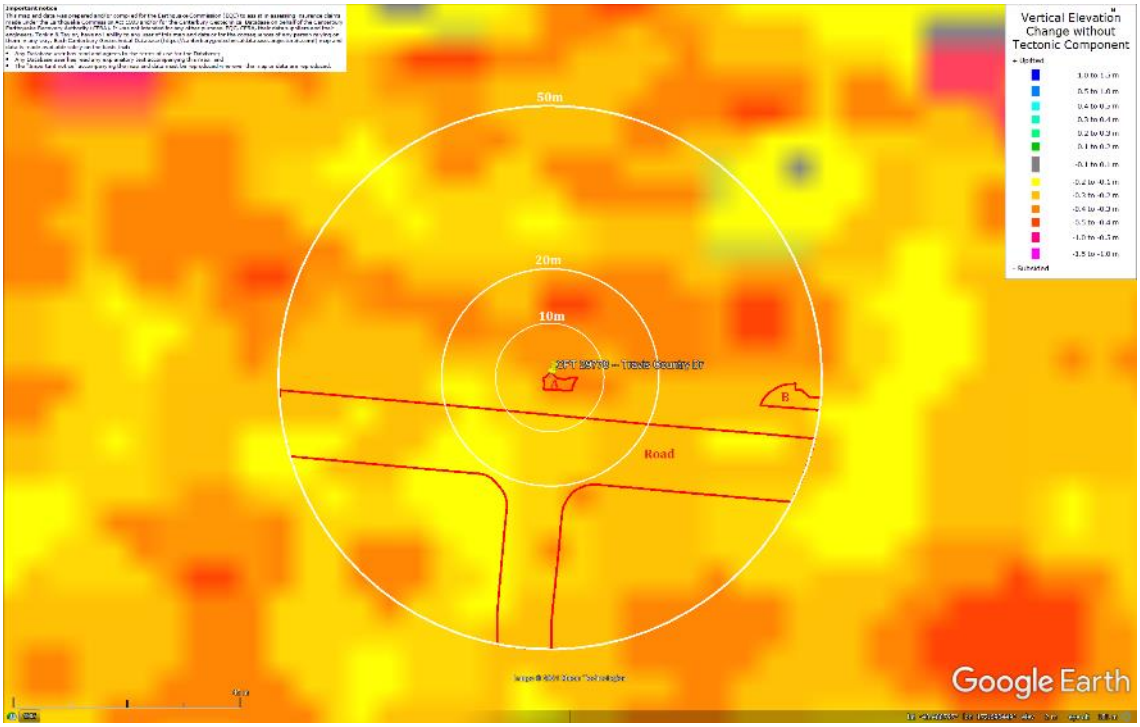

Figure 32: Ground surface subsidence without tectonic component for Canterbury Earthquake Sequence according to the LiDAR DEM.

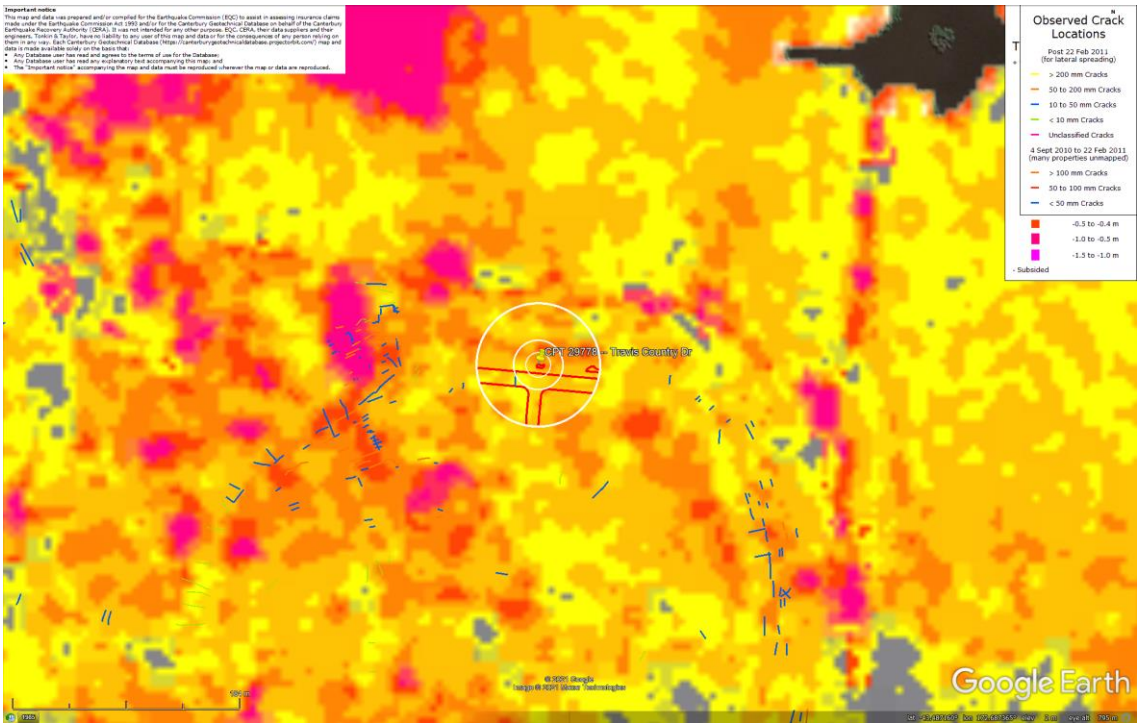

Figure 33: Absence of ground cracks indicates no lateral spreading for Canterbury Earthquake Sequence.

Figure 34: Vertical tectonic movements for Sep 2010 Earthquake.

Figure 35: Vertical tectonic movements for Feb 2011 Earthquake.

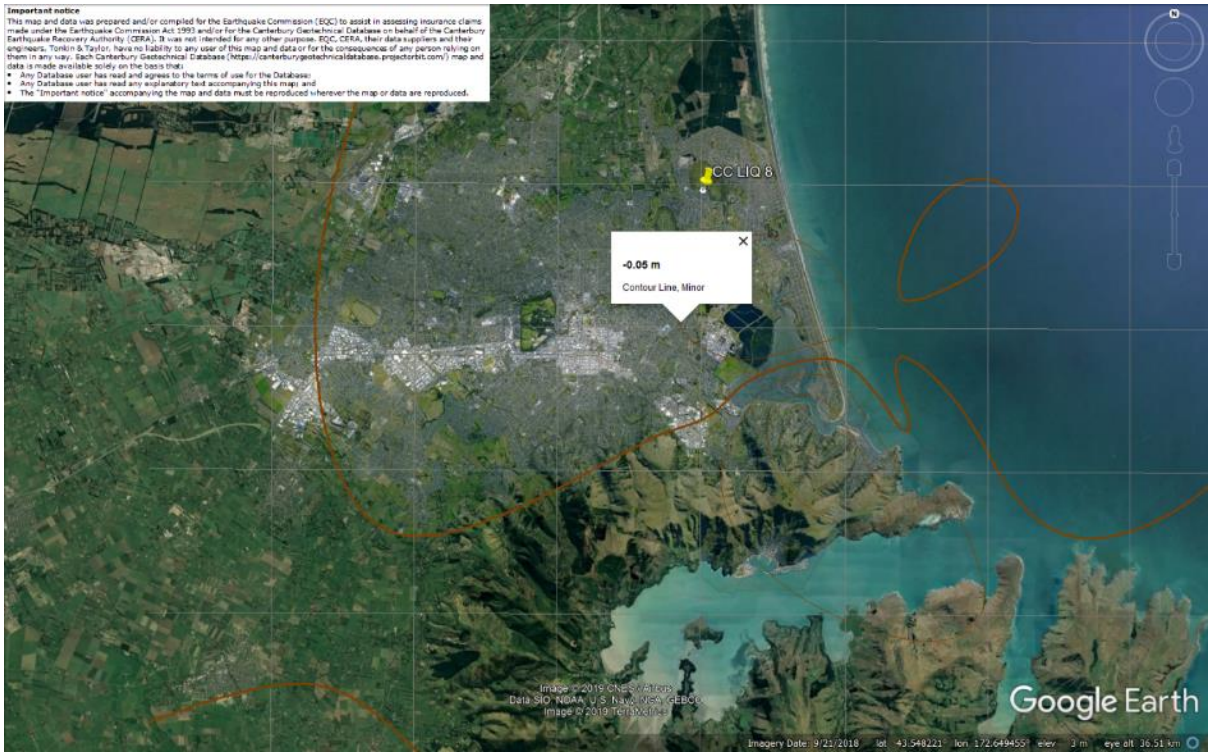

Figure 36: Vertical tectonic movements for June 2011 Earthquake.

Figure 37: Vertical tectonic movements for Dec 2011 Earthquake.

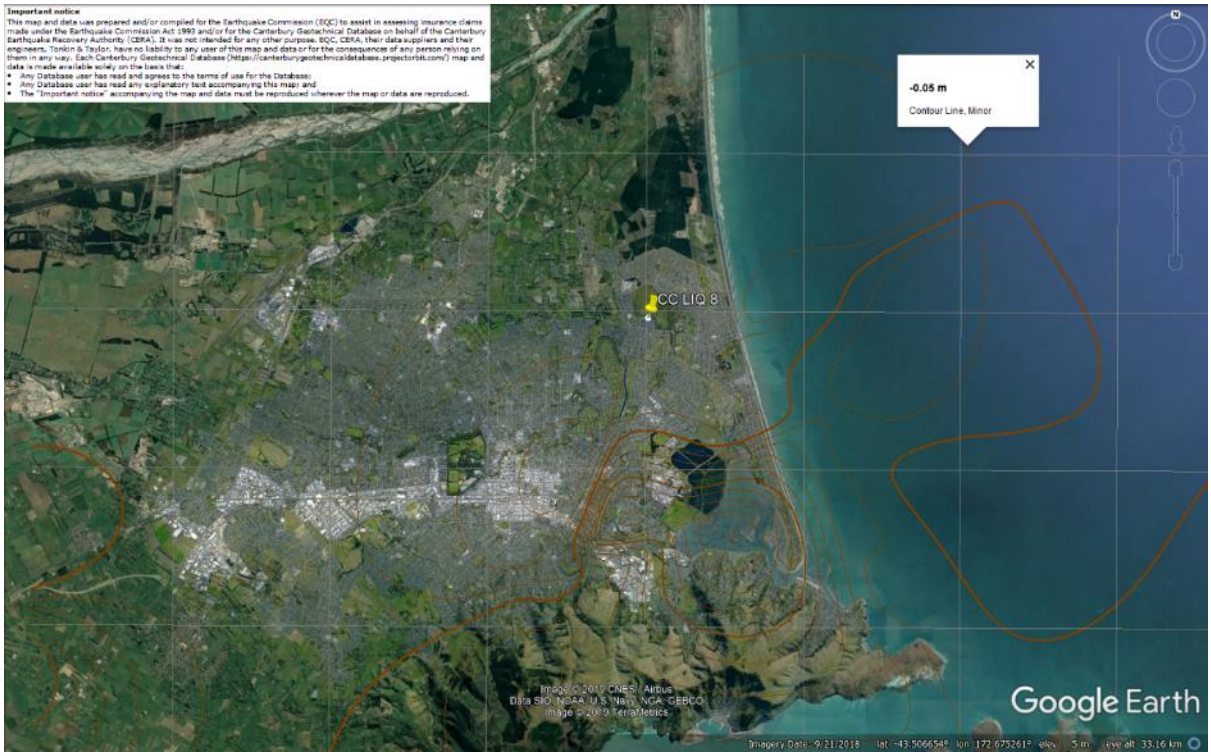

Figure 38: Vertical tectonic movements for Canterbury Earthquake Sequence.

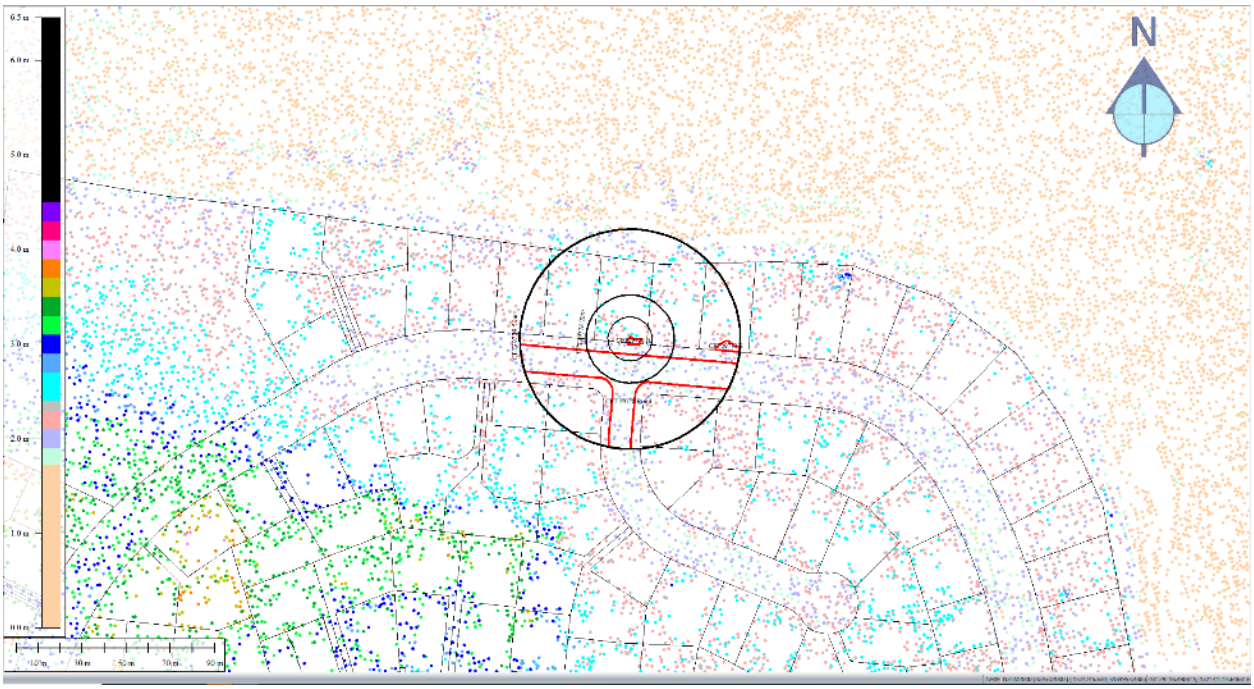

Figure 39: Jul 2003 LiDAR survey.

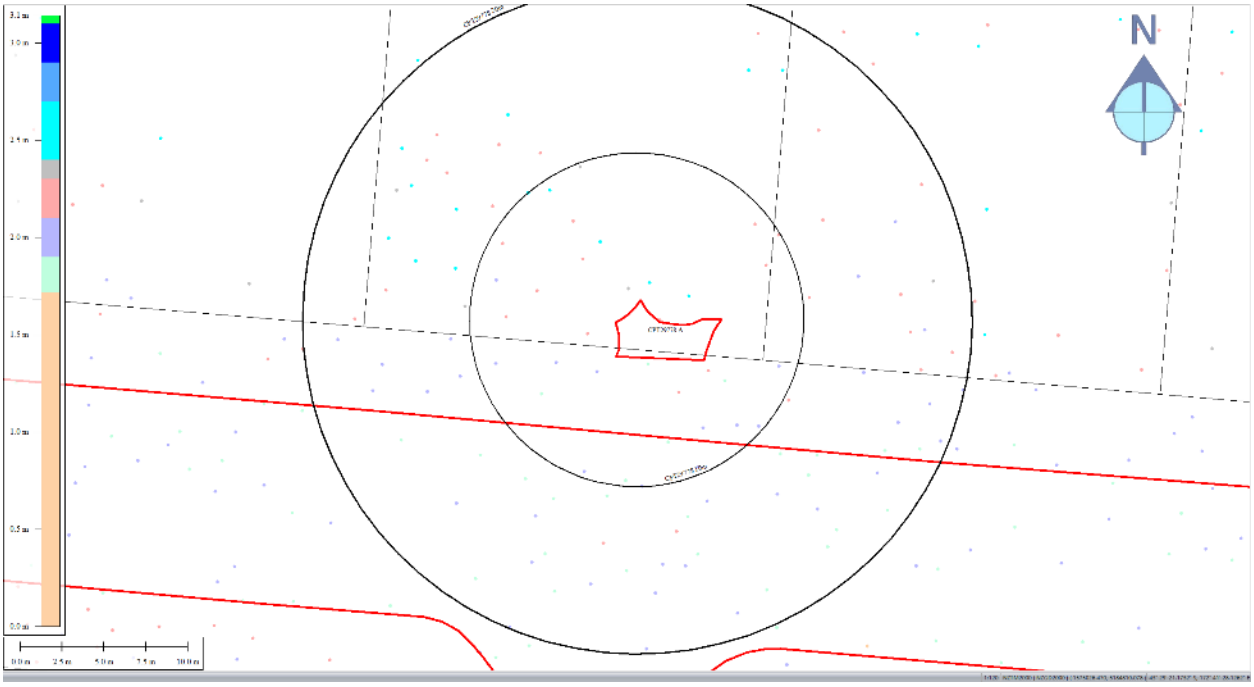

Figure 40: Ground surface elevation for Patch A for Jul 2003 LiDAR survey.

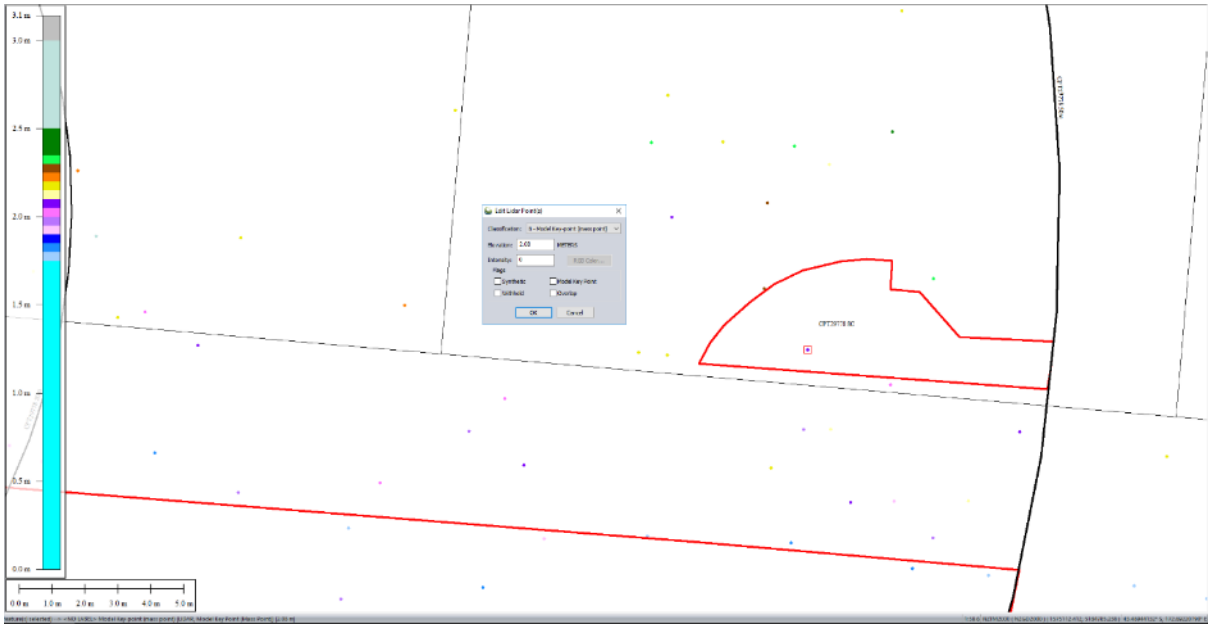

Figure 41: Ground surface elevation for Patch B for Jul 2003 LiDAR survey.

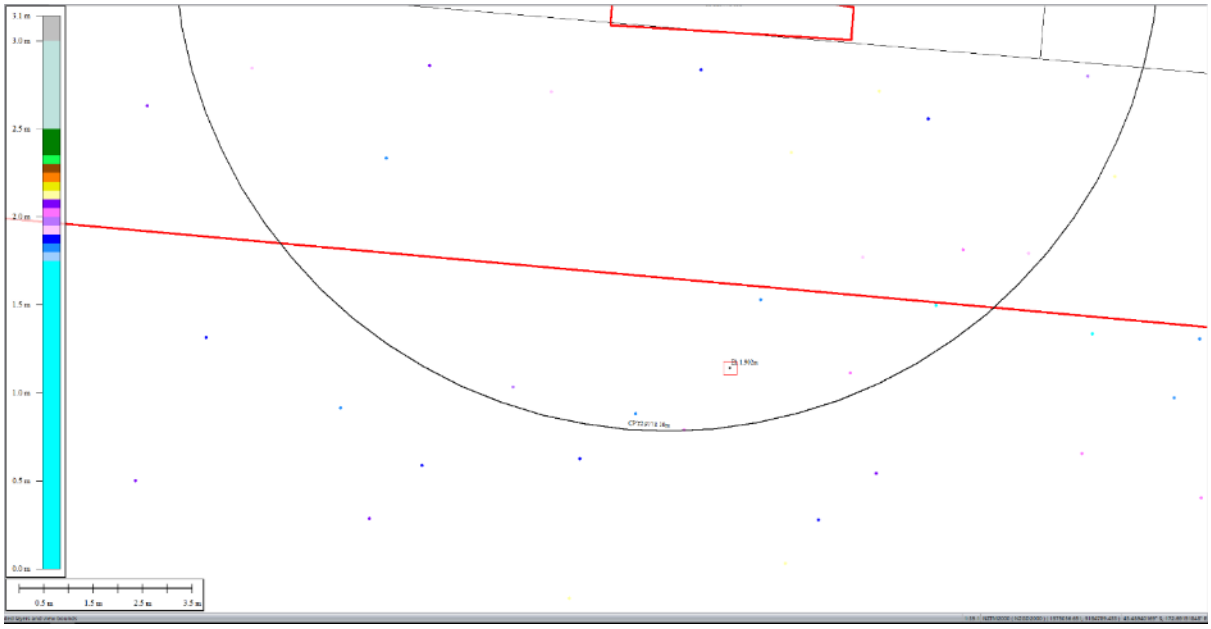

Figure 42: Ground surface elevation averaged over the 10-m buffer for Road for Jul 2003 LiDAR survey.

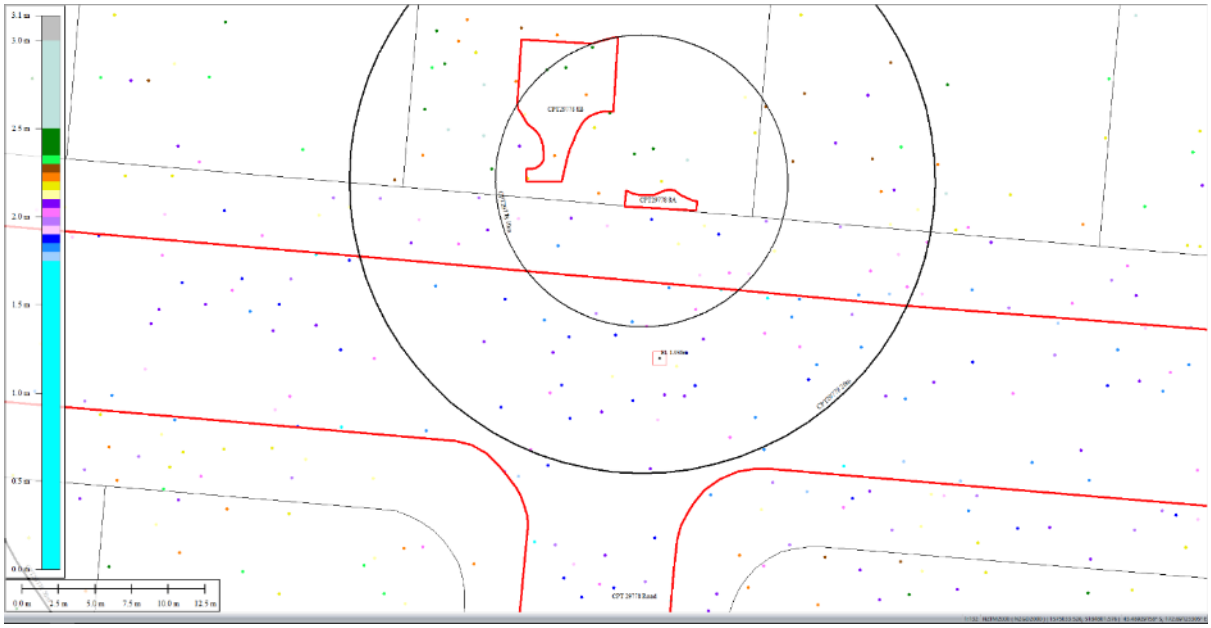

Figure 43: Ground surface elevation averaged over the 20-m buffer for Road for Jul 2003 LiDAR survey.

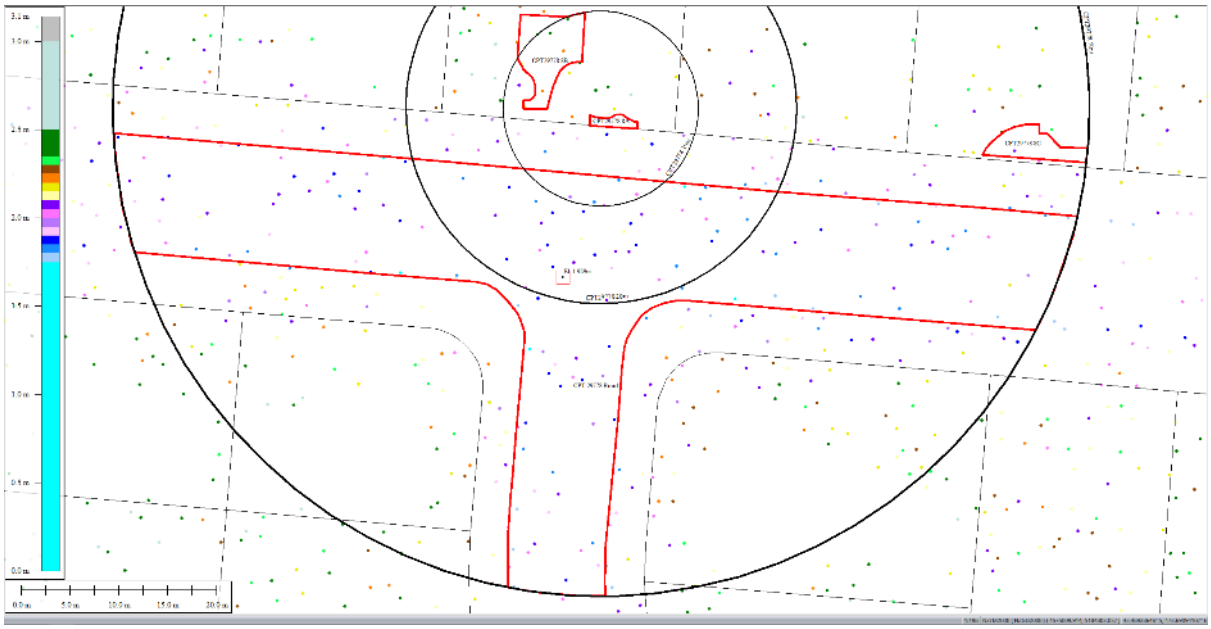

Figure 44: Ground surface elevation averaged over the 50-m buffer for Road for Jul 2003 LiDAR survey.

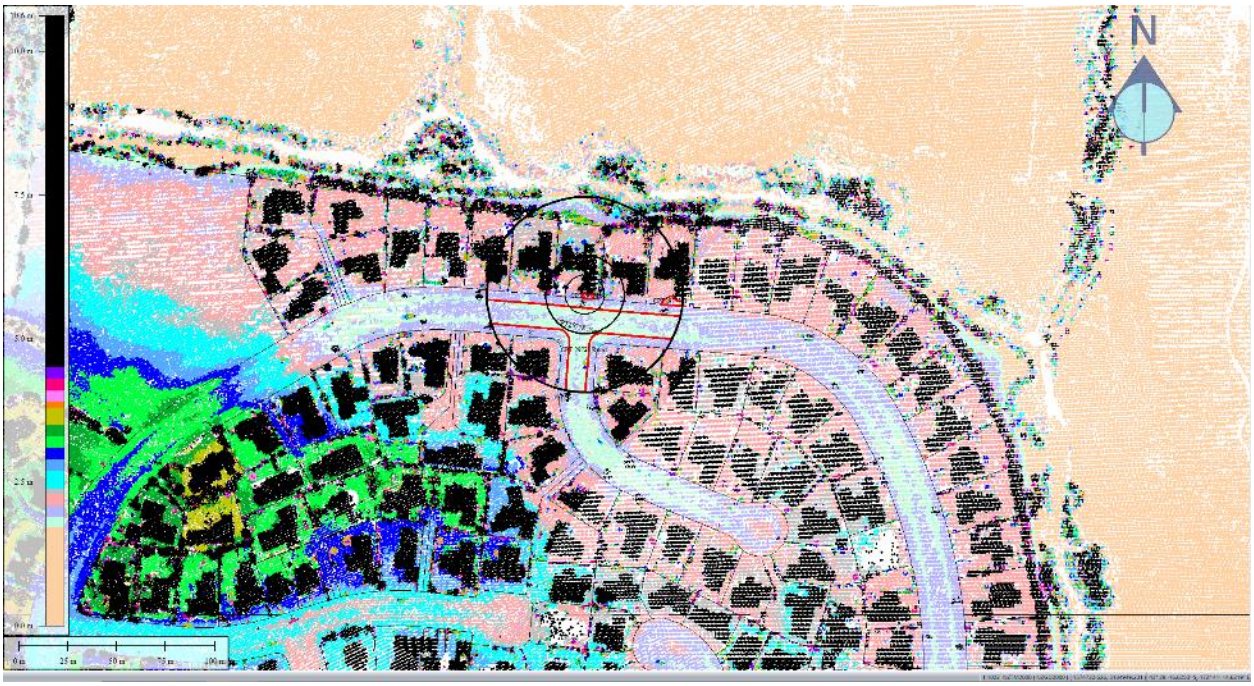

Figure 45: Sep 5, 2010 LiDAR survey.

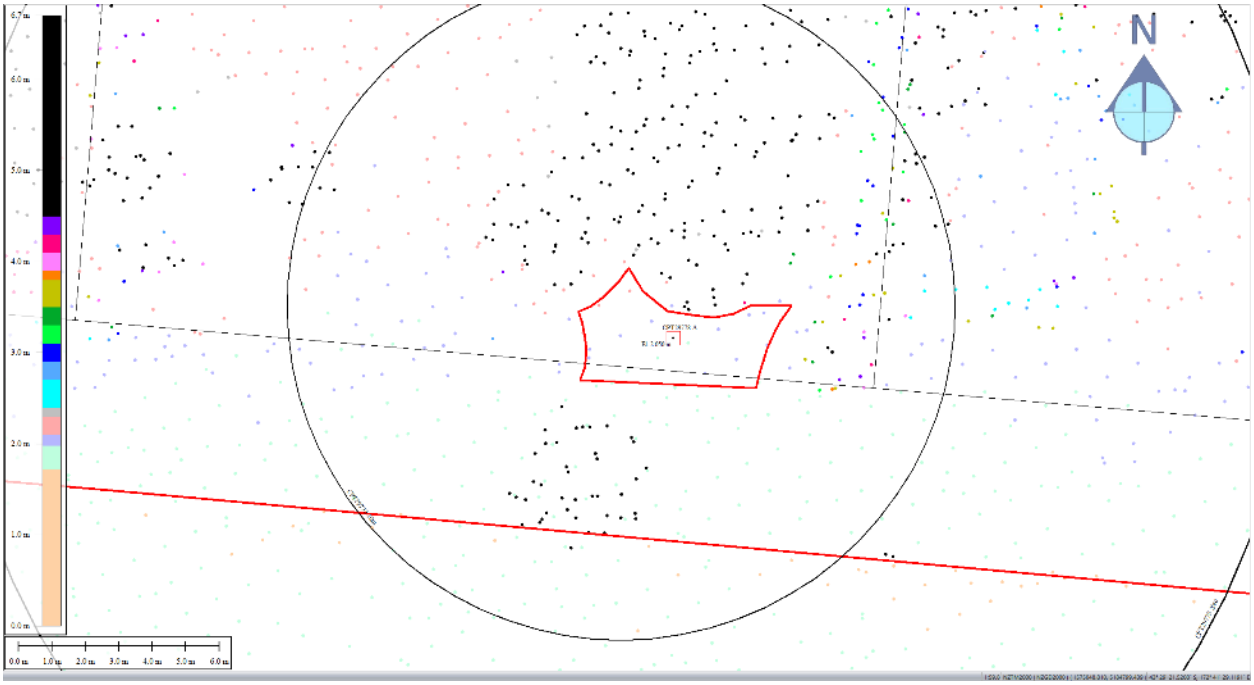

Figure 46: Ground surface elevation for Patch A for Sep 5, 2010 LiDAR survey.

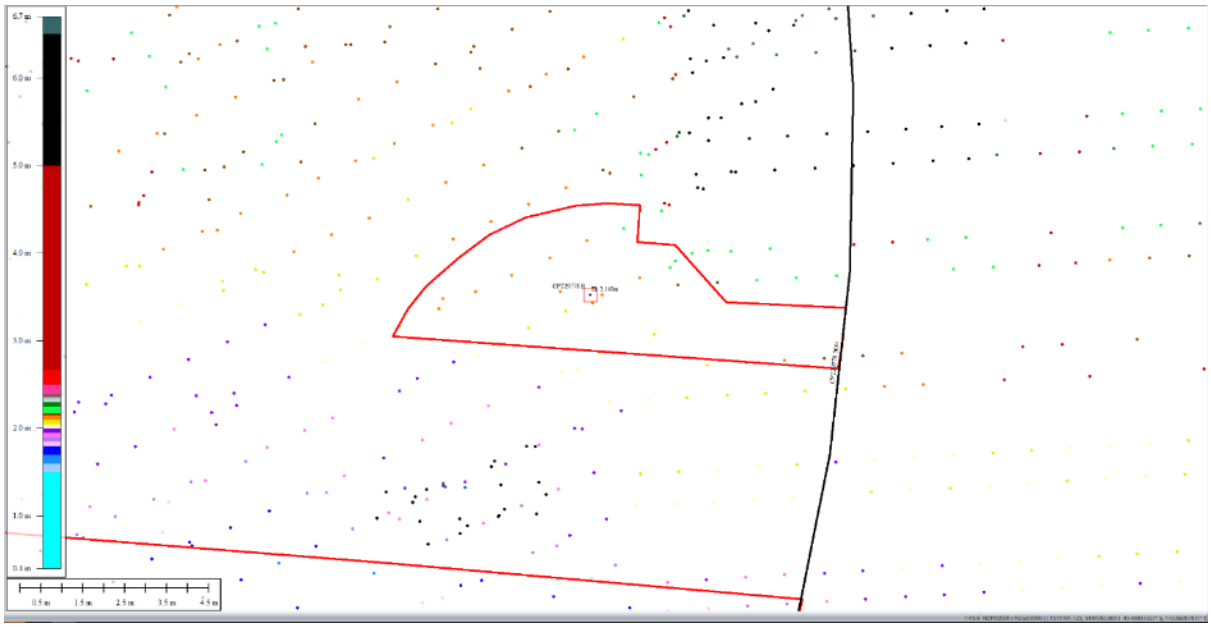

Figure 47: Ground surface elevation for Patch B for Sep 5, 2010 LiDAR survey.

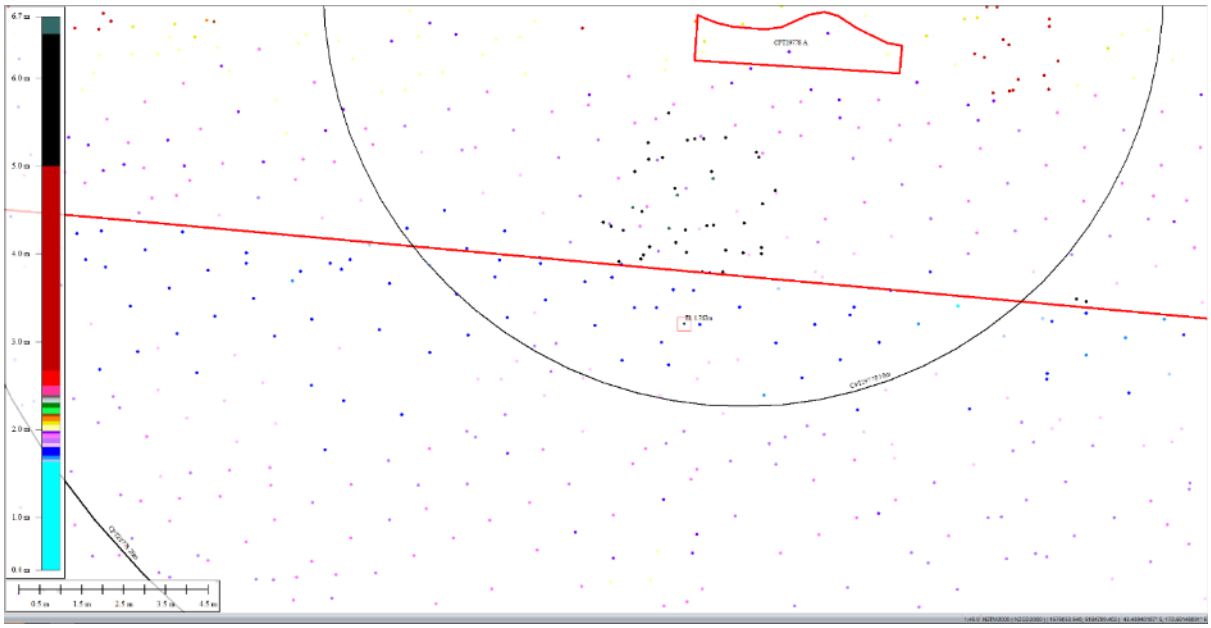

Figure 48: Ground surface elevation averaged over the 10-m buffer for Road for Sep 5, 2010 LiDAR survey.

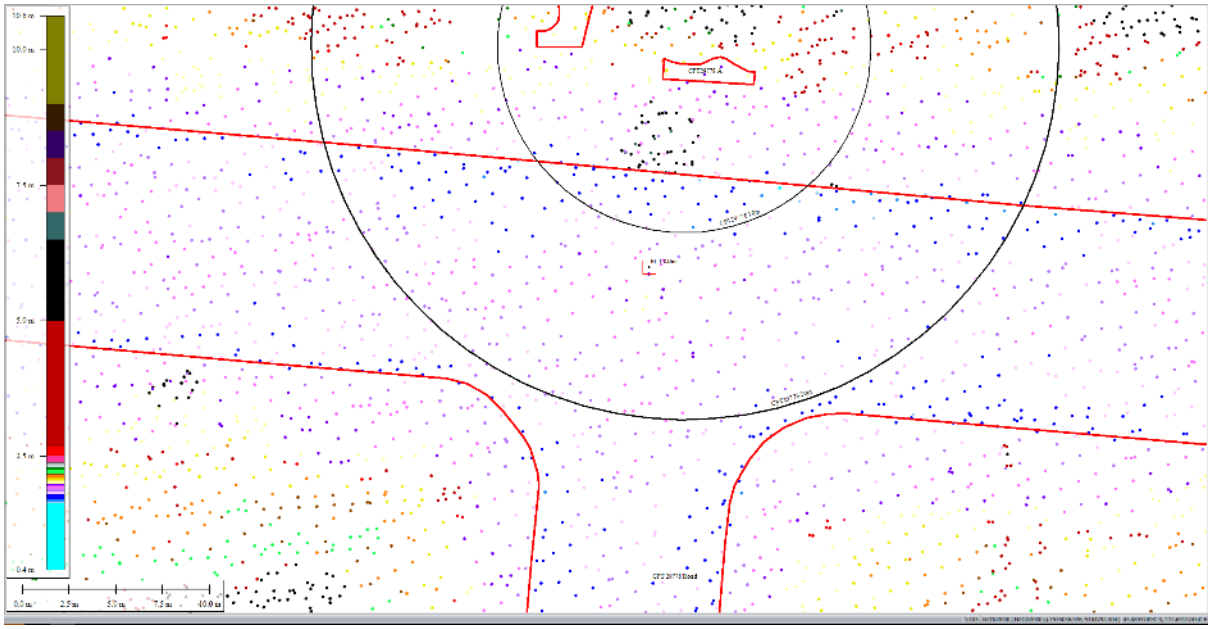

Figure 49: Ground surface elevation averaged over the 20-m buffer for Road for Sep 5, 2010 LiDAR survey.

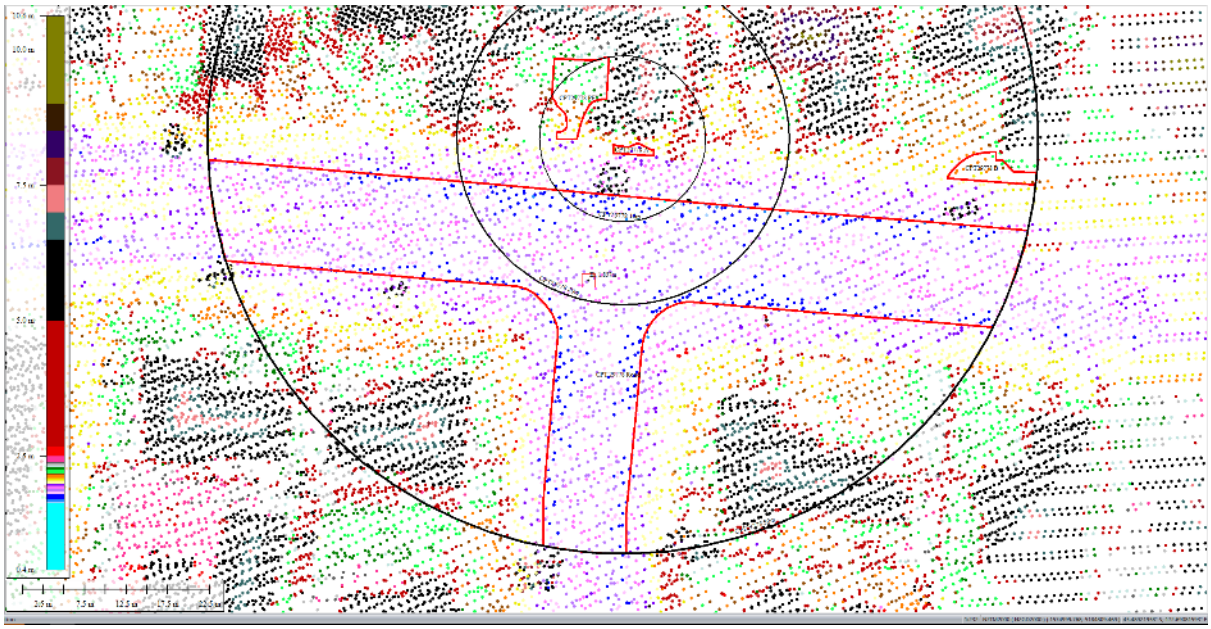

Figure 50: Ground surface elevation averaged over the 50-m buffer for Road for Sep 5, 2010 LiDAR survey.

Note 8: Mar 2011 LiDAR survey data are not available for the site.

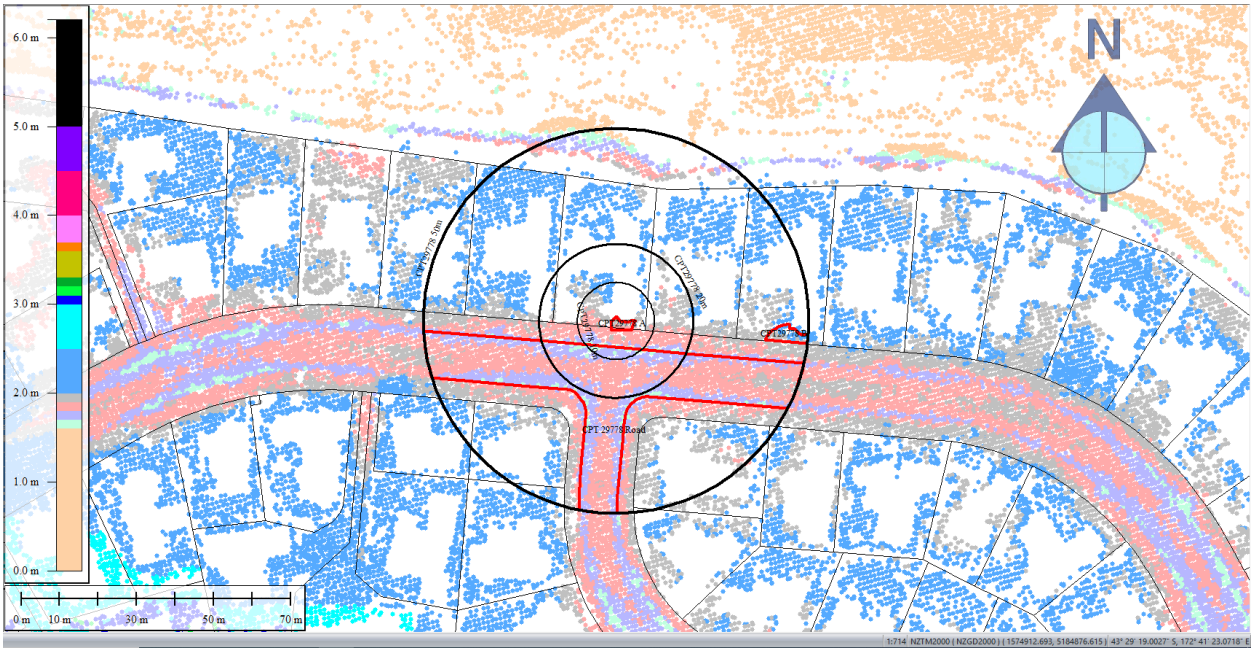

Figure 51: May 2011 LiDAR survey.

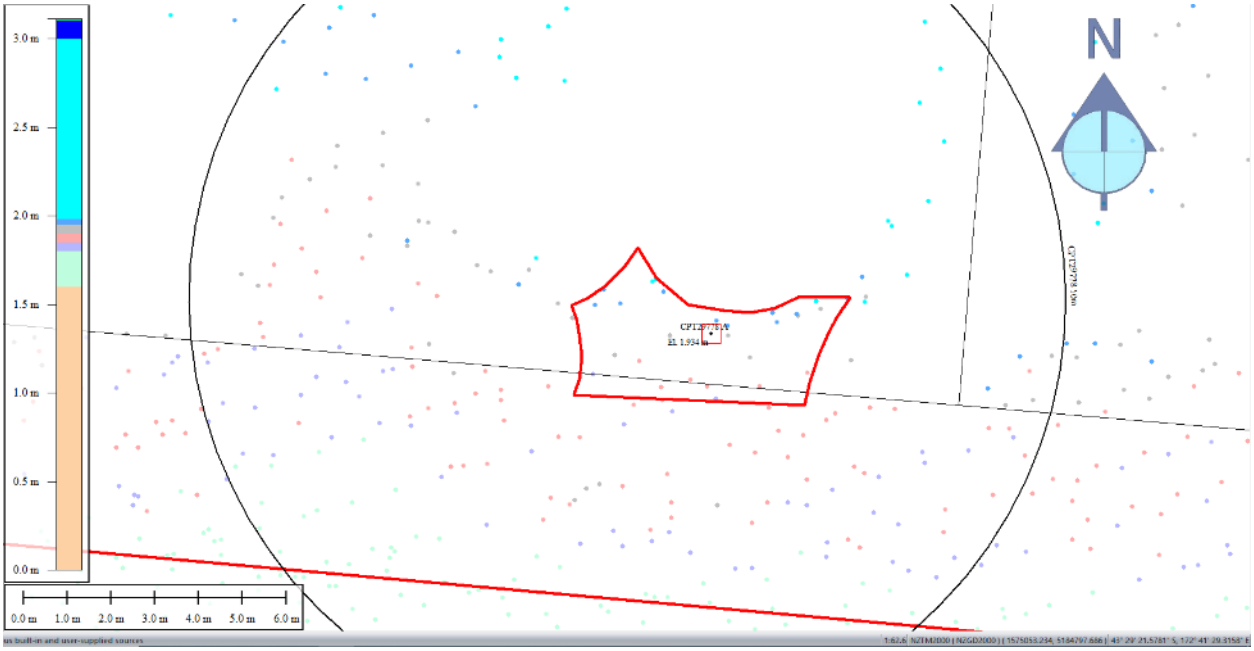

Figure 52: Ground surface elevation for Patch A for May 2011 LiDAR survey.

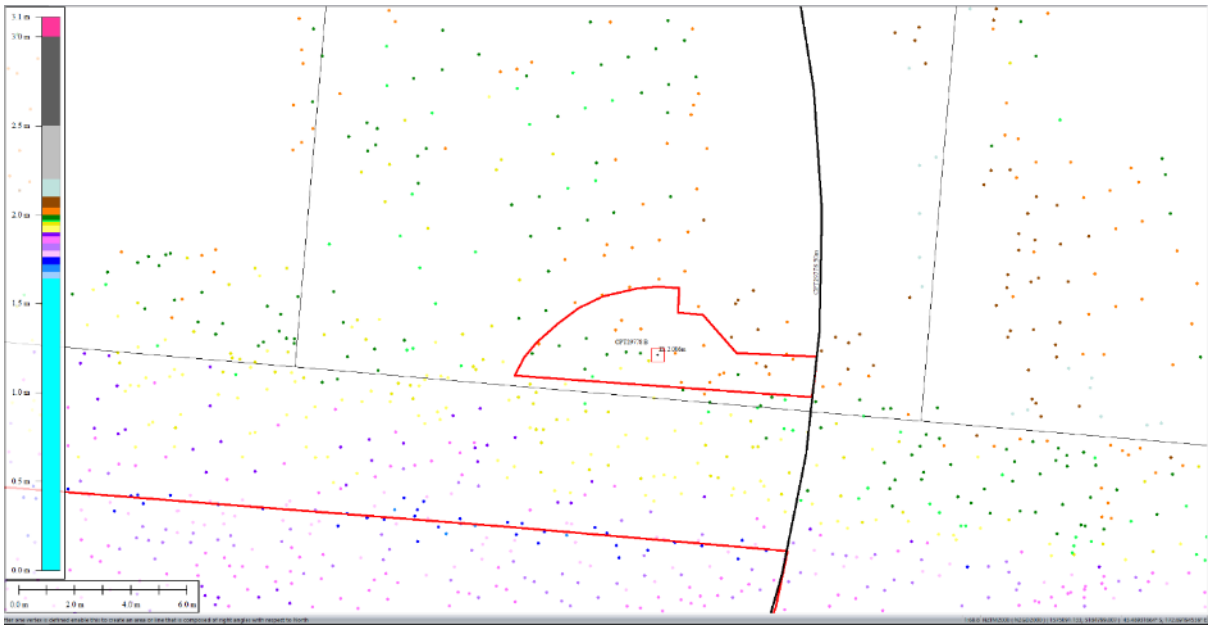

Figure 53: Ground surface elevation for Patch B for May 2011 LiDAR survey.

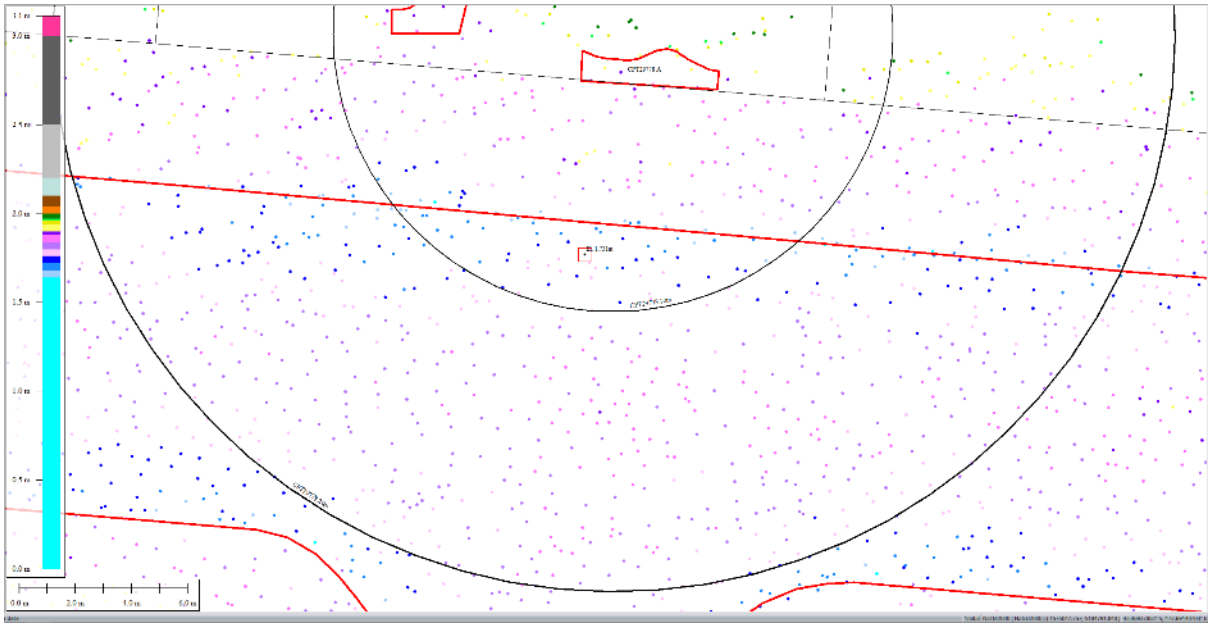

Figure 54: Ground surface elevation averaged over the 10-m buffer for Road for May 2011 LiDAR survey.

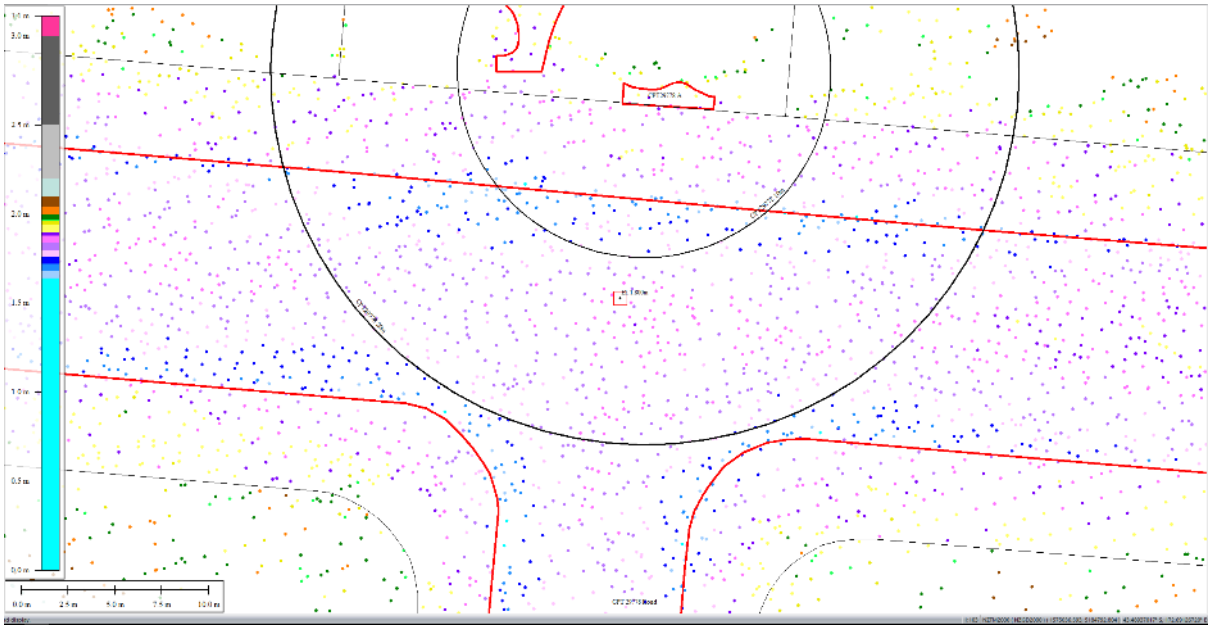

Figure 55: Ground surface elevation averaged over the 20-m buffer for Road for May 2011 LiDAR survey.

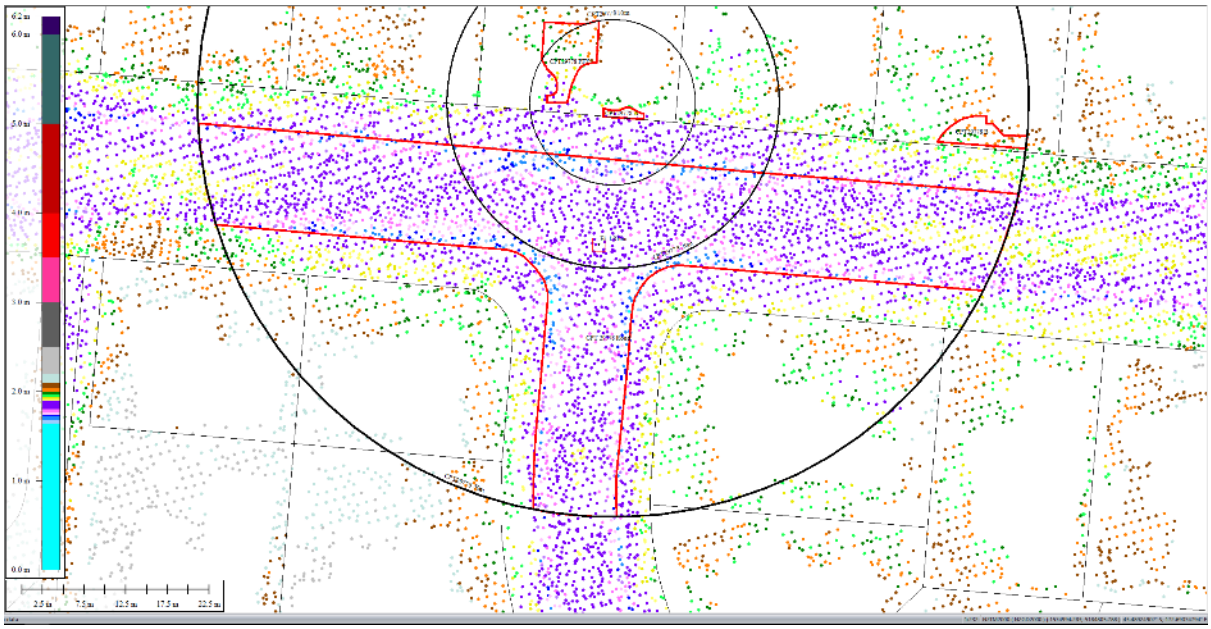

Figure 56: Ground surface elevation averaged over the 50-m buffer for Road for May 2011 LiDAR survey.

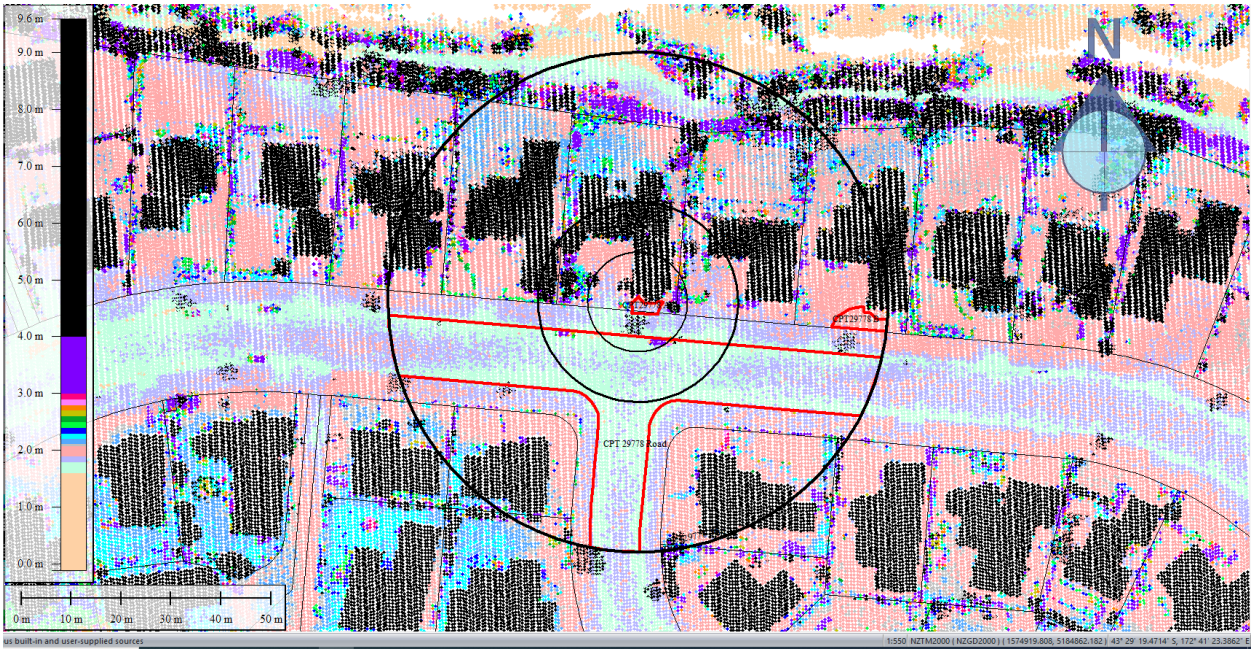

Figure 57: Sep 2011 LiDAR survey.

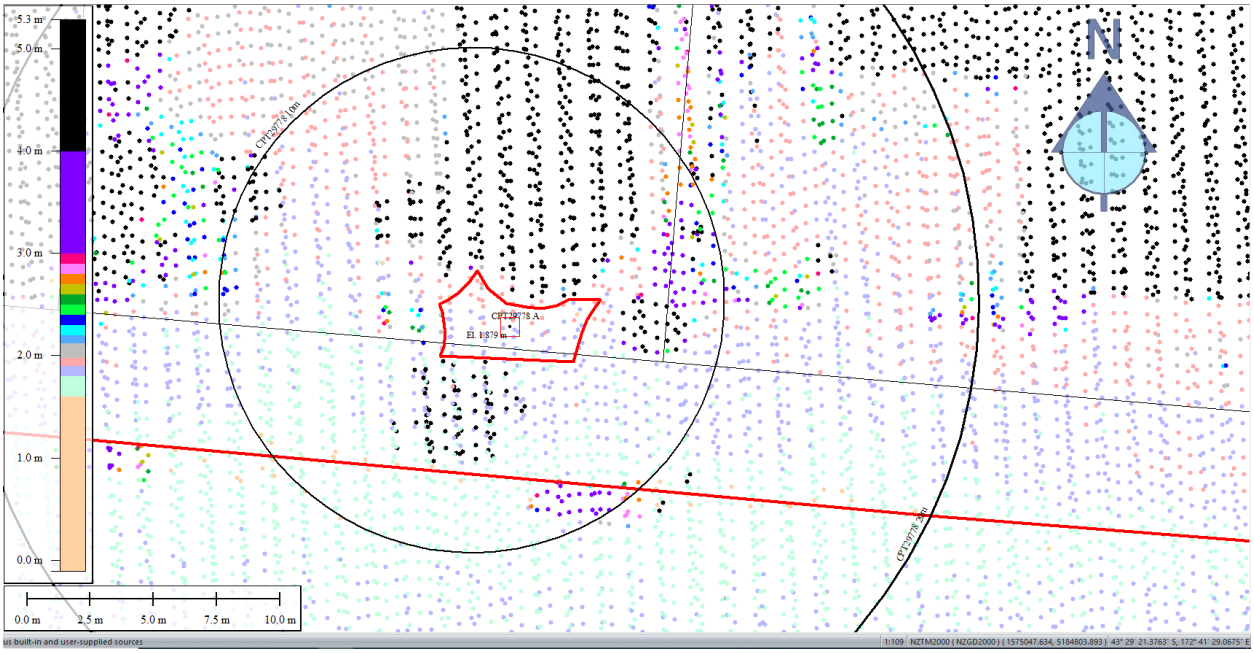

Figure 58: Ground surface elevation for Patch A for Sep 2011 LiDAR survey.

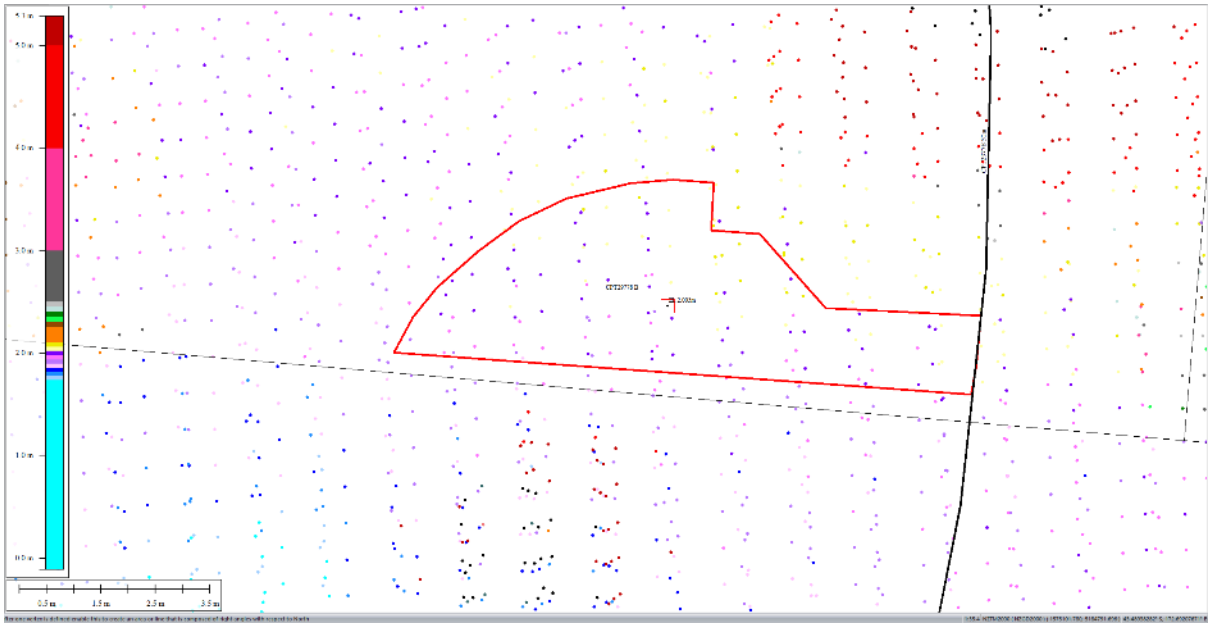

Figure 59: Ground surface elevation for Patch B for Sep 2011 LiDAR survey.

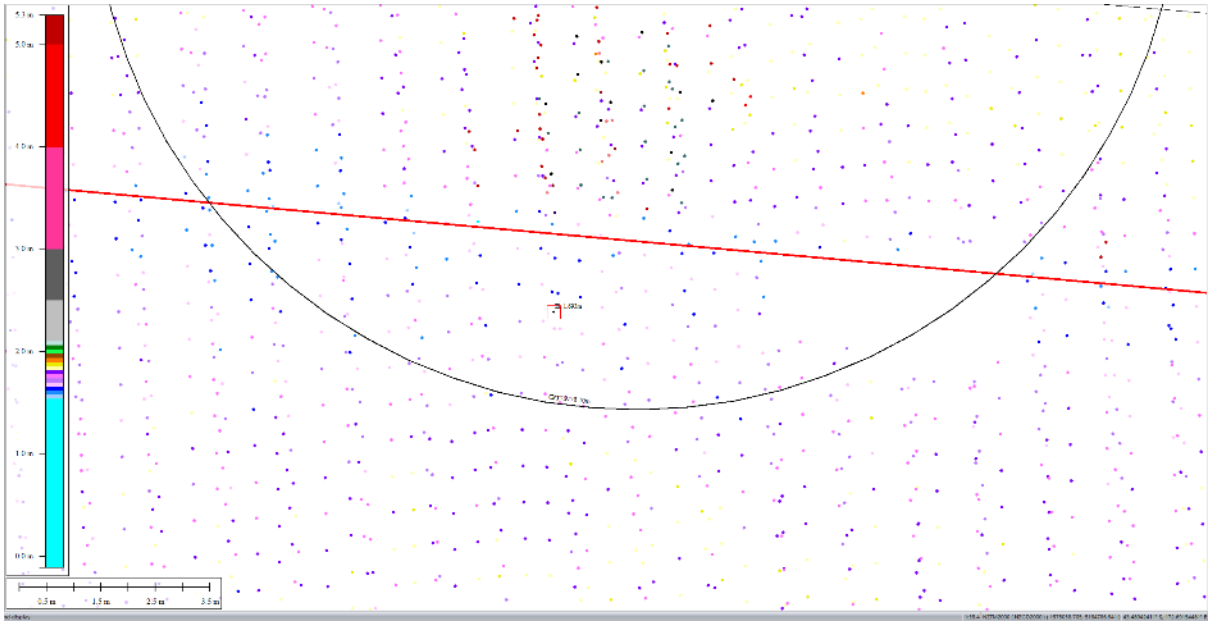

Figure 60: Ground surface elevation averaged over the 10-m buffer for Road for Sep 2011 LiDAR survey.

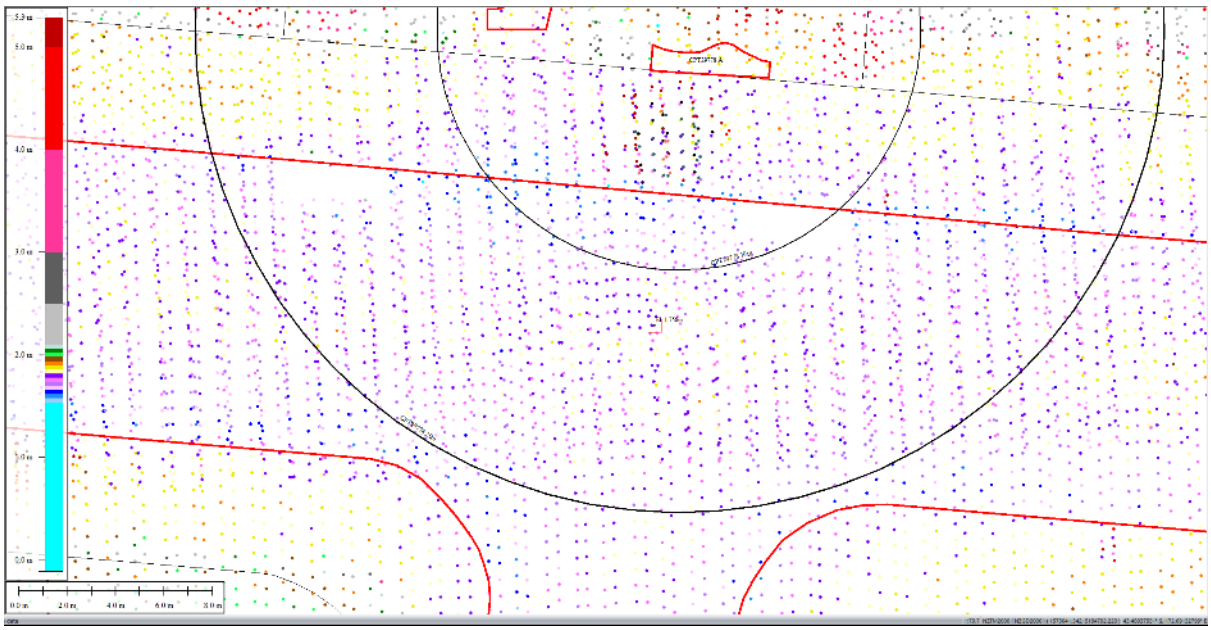

Figure 61: Ground surface elevation averaged over the 20-m buffer for Road for Sep 2011 LiDAR survey.

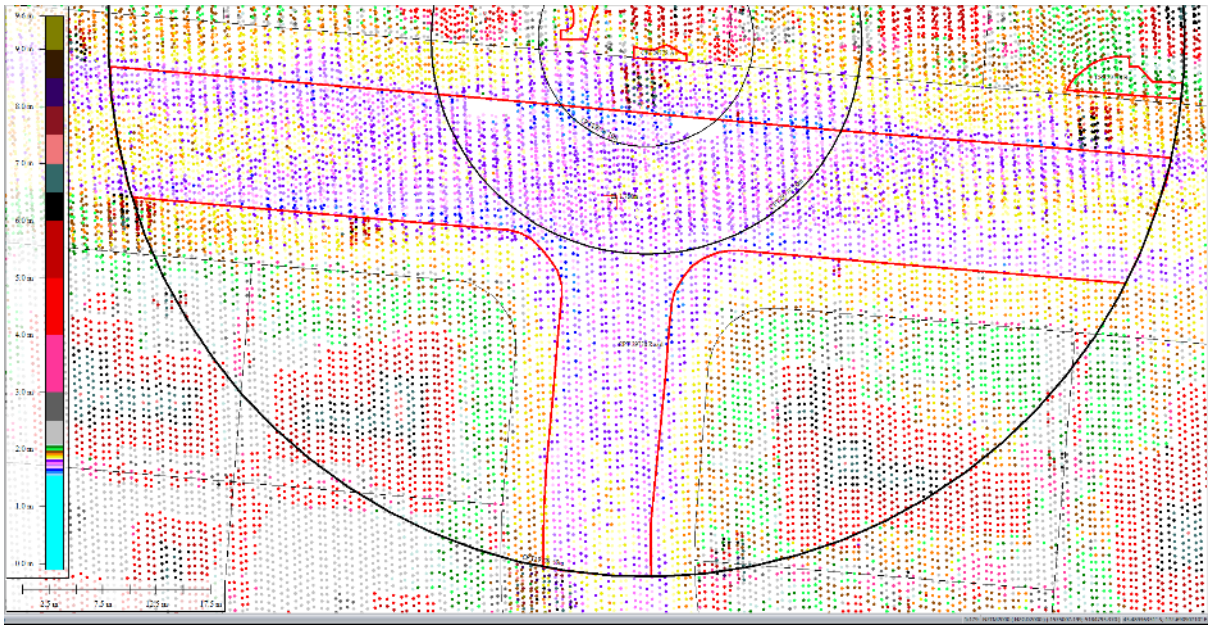

Figure 62: Ground surface elevation averaged over the 50-m buffer for Road for Sep 2011 LiDAR survey.

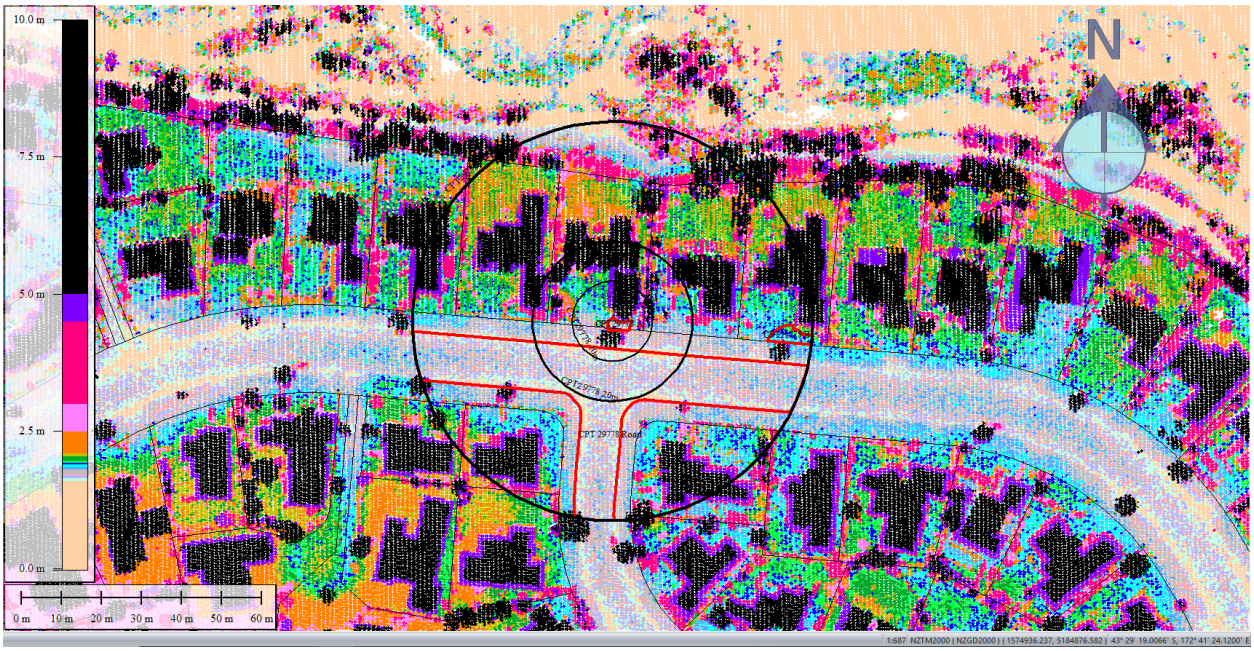

Figure 63: Feb 2012 LiDAR survey.

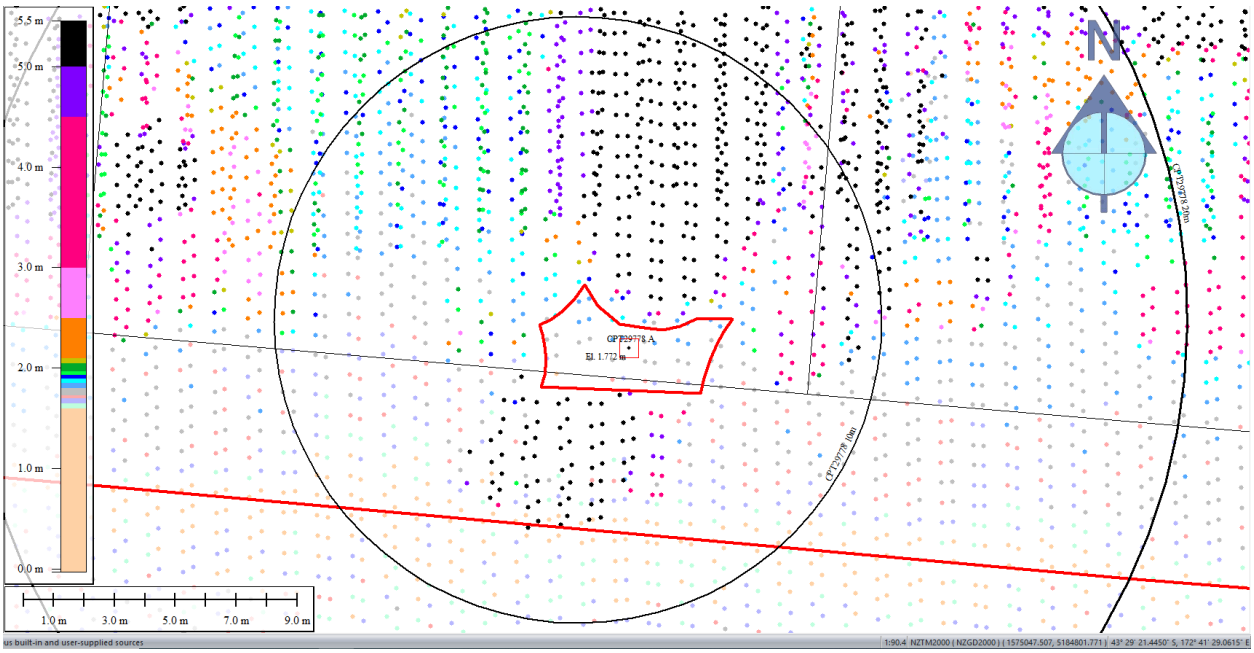

Figure 64: Ground surface elevation for Patch A for Feb 2012 LiDAR survey.

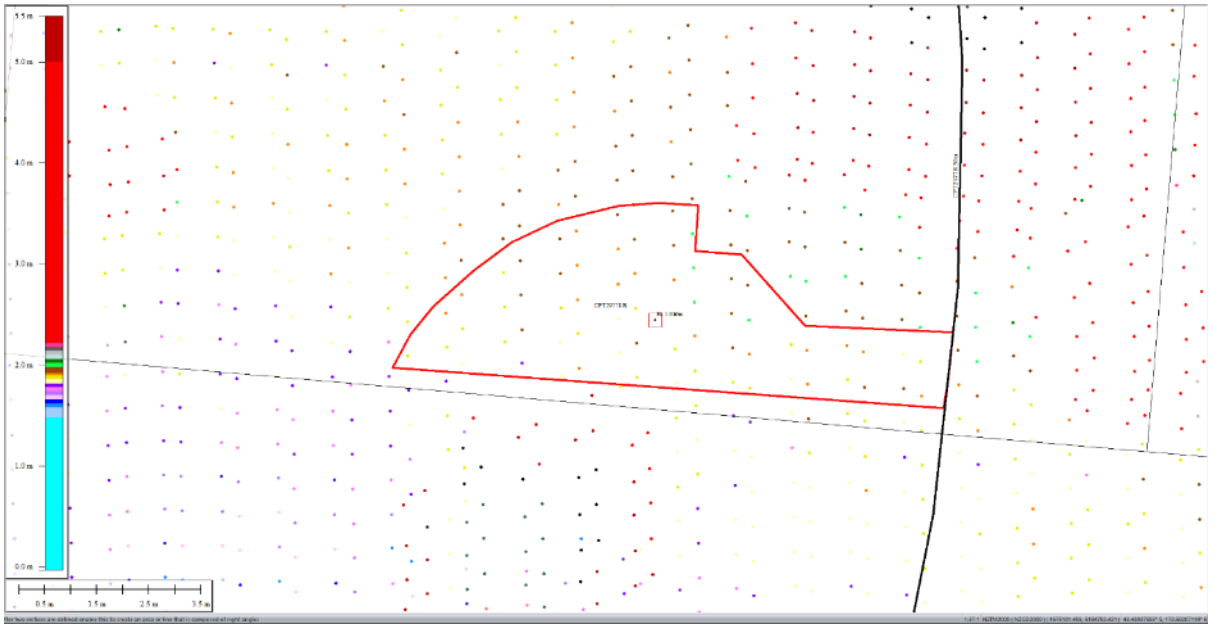

Figure 65: Ground surface elevation for Patch B for Feb 2012 LiDAR survey.

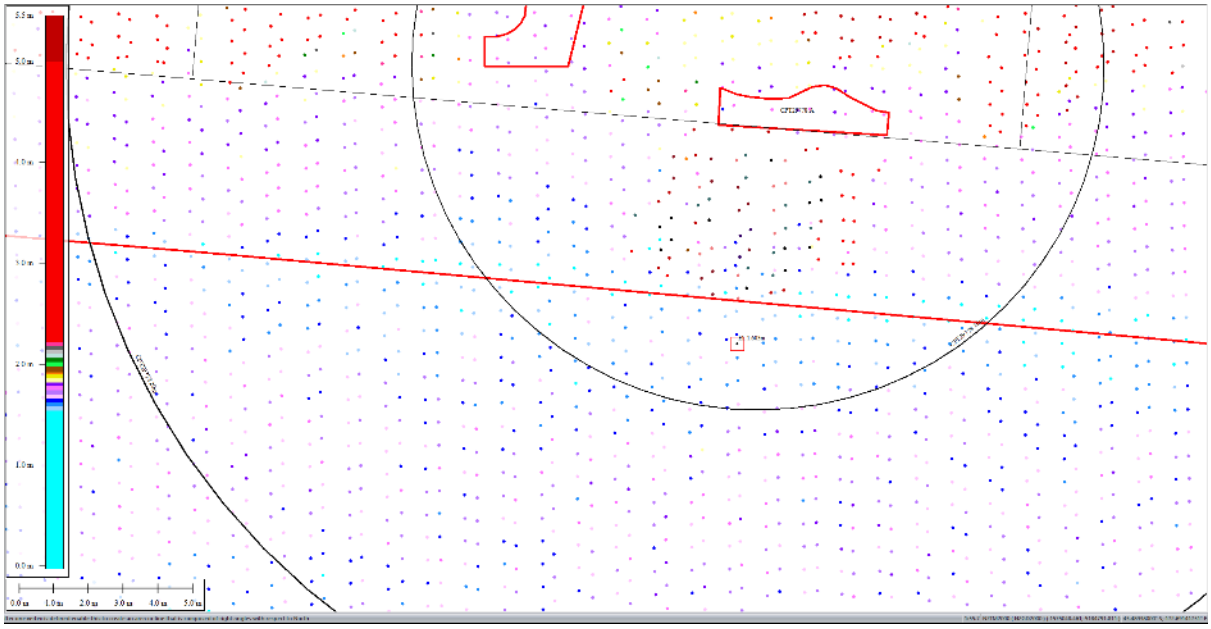

Figure 66: Ground surface elevation averaged over the 10-m buffer for Road for Feb 2012 LiDAR survey.

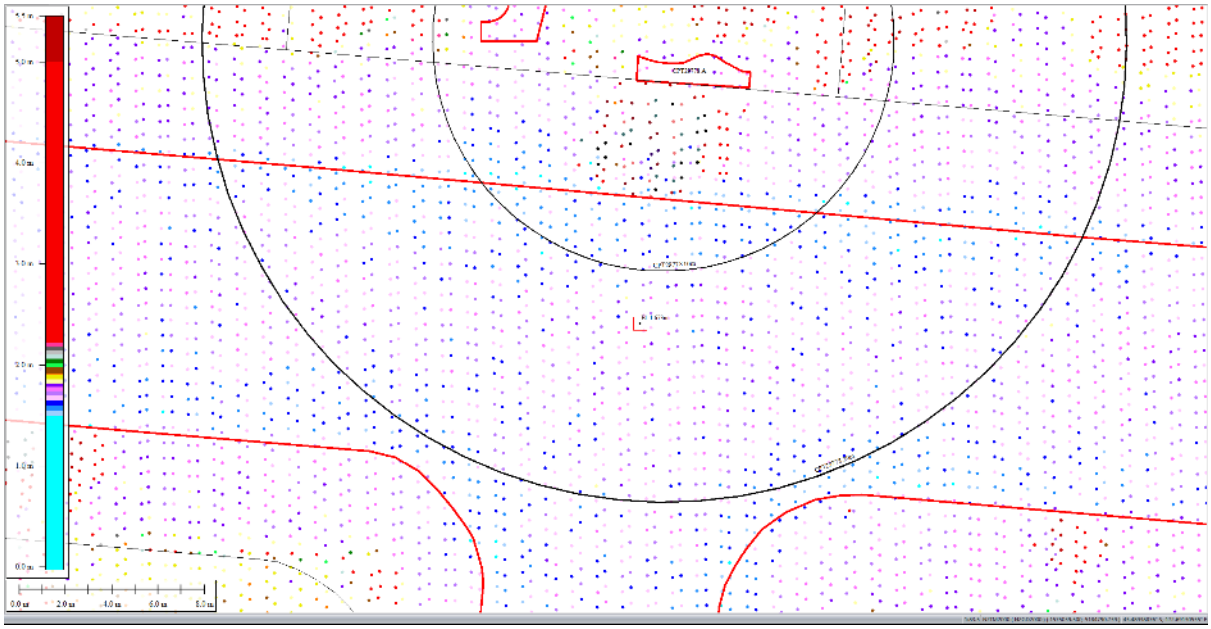

Figure 67: Ground surface elevation averaged over the 20-m buffer for Road for Feb 2012 LiDAR survey.

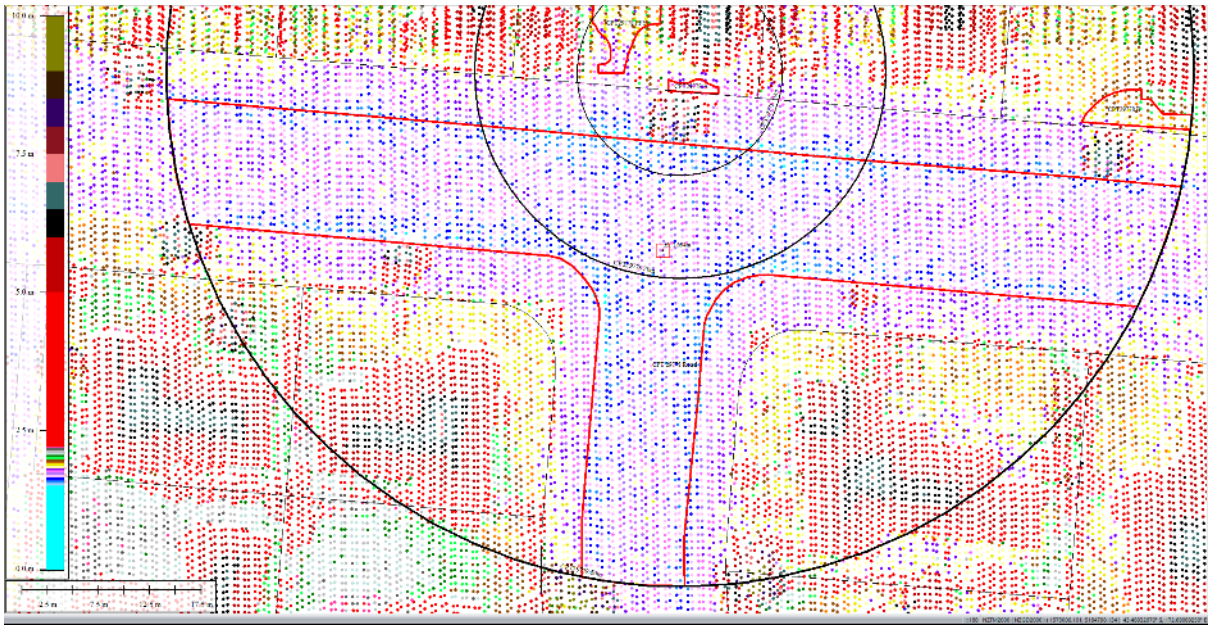

Figure 68: Ground surface elevation averaged over the 50-m buffer for Road for Feb 2012 LiDAR survey.

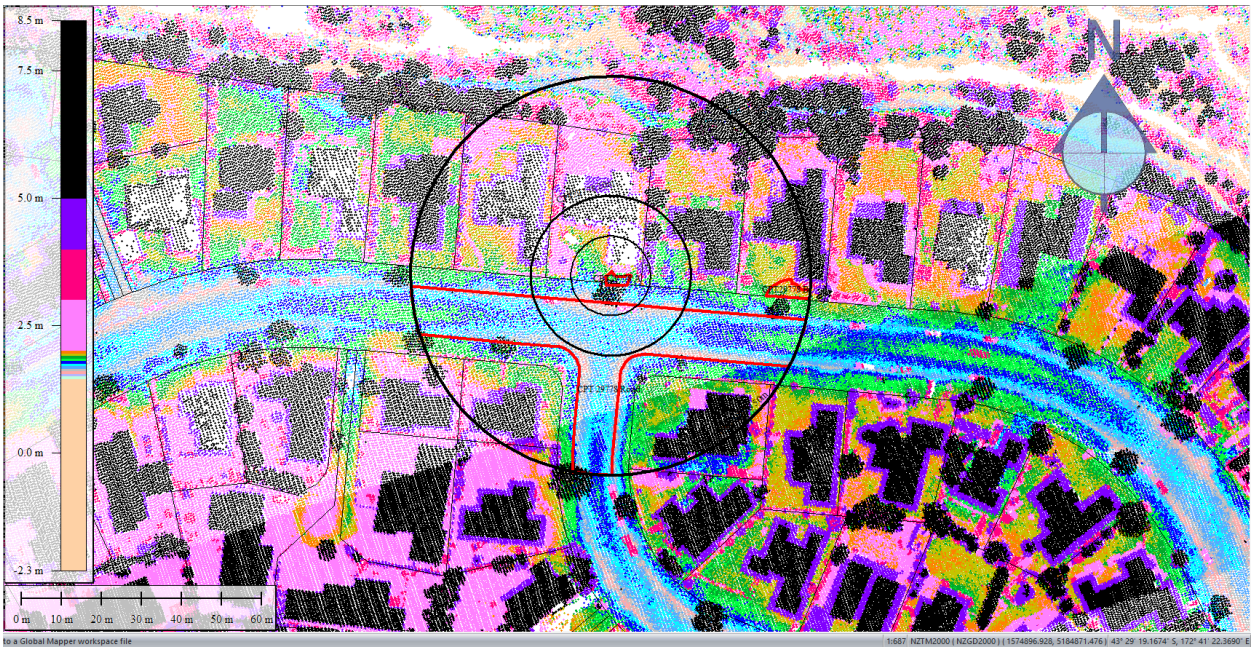

Figure 69: Oct 2015 LiDAR survey.

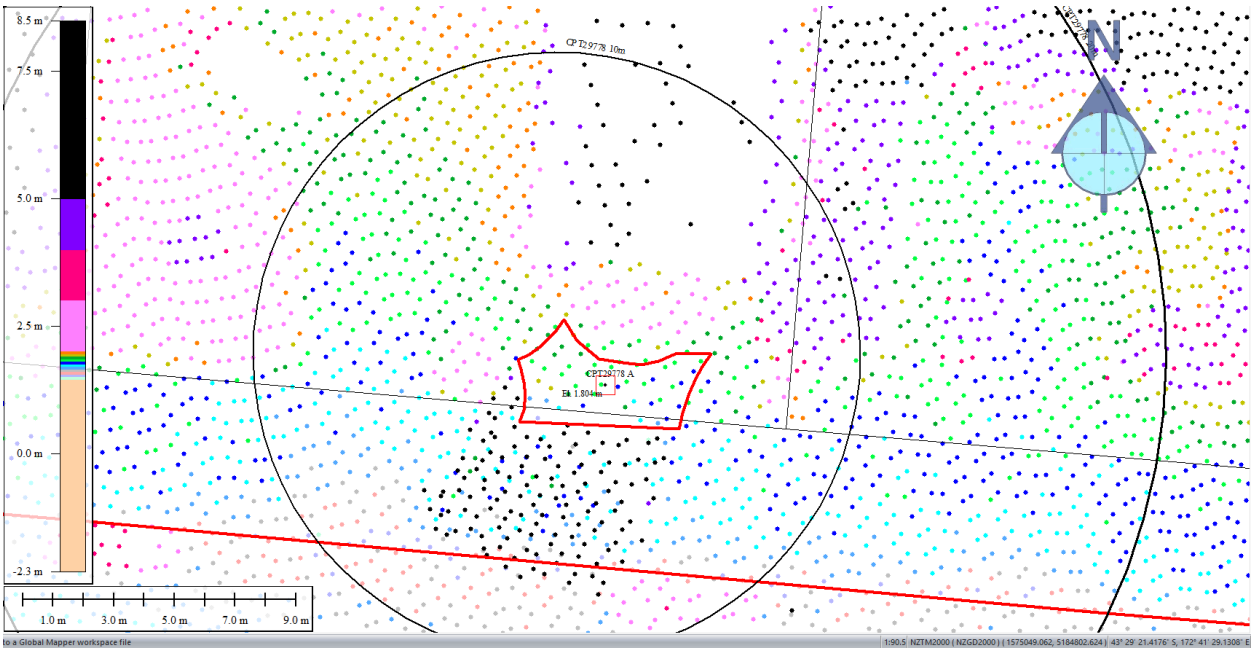

Figure 70: Ground surface elevation for Patch A for Oct 2015 LiDAR survey.

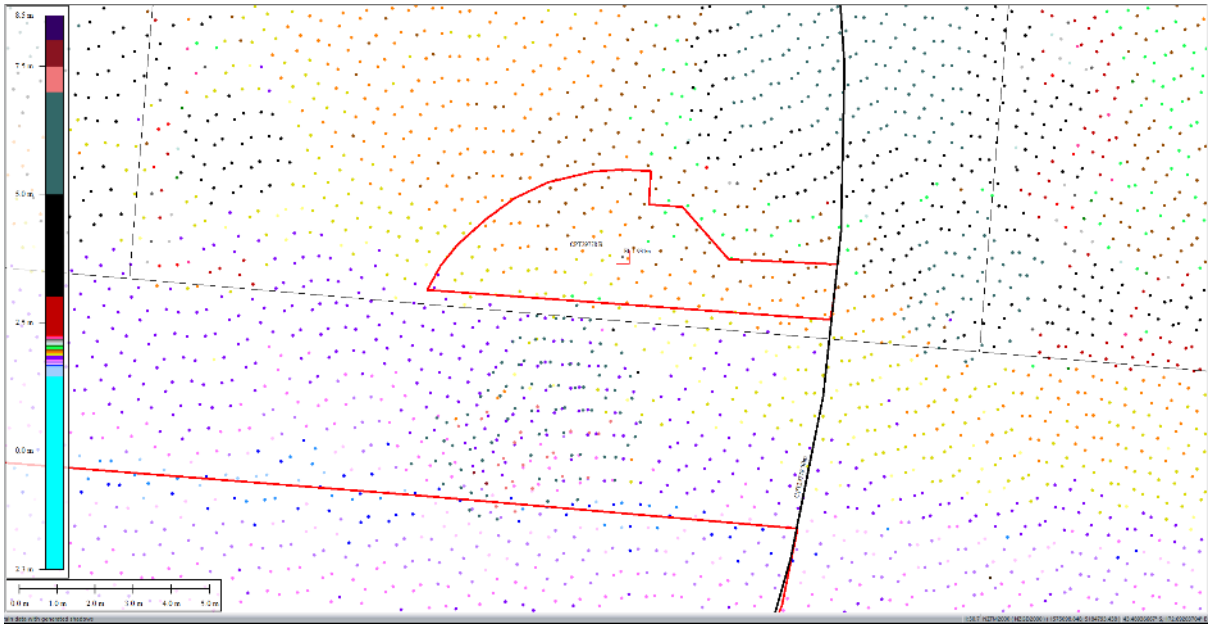

Figure 71: Ground surface elevation for Patch B for Oct 2015 LiDAR survey.

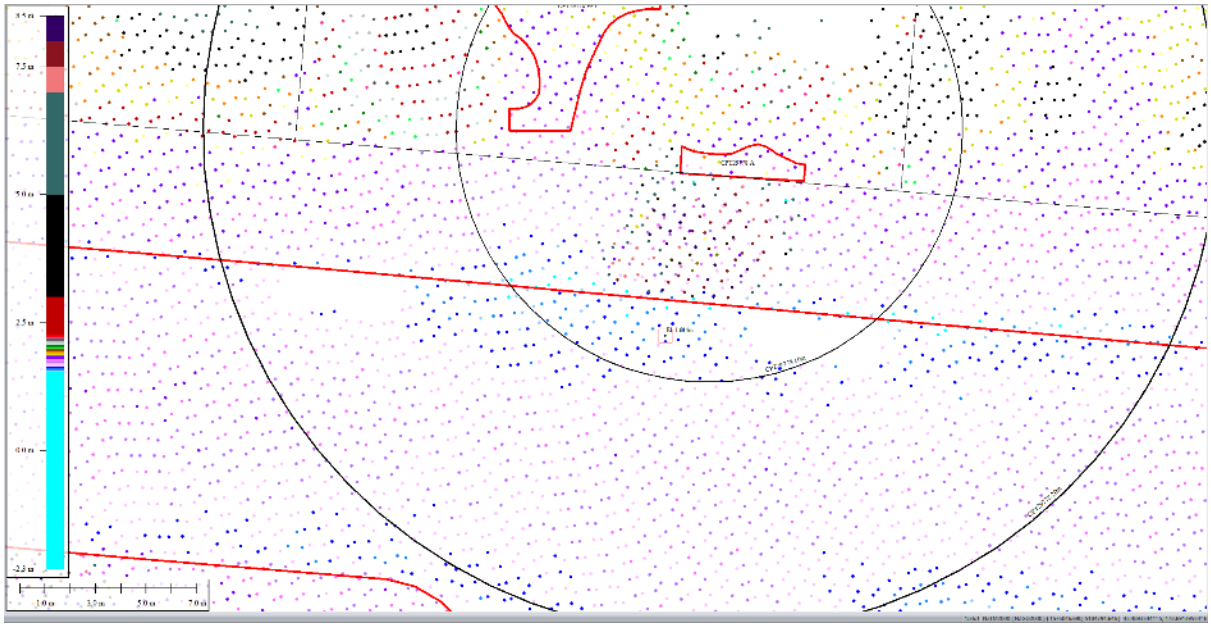

Figure 72: Ground surface elevation averaged over the 10-m buffer for Road for Oct 2015 LiDAR survey.

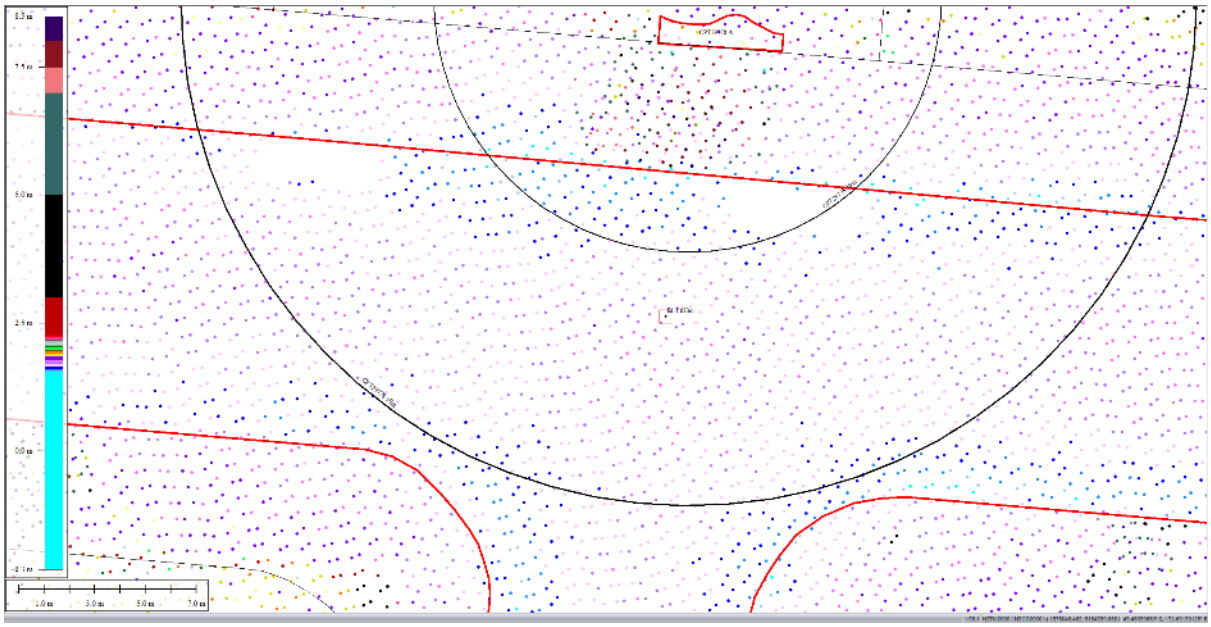

Figure 73: Ground surface elevation averaged over the 20-m buffer for Road for Oct 2015 LiDAR survey.

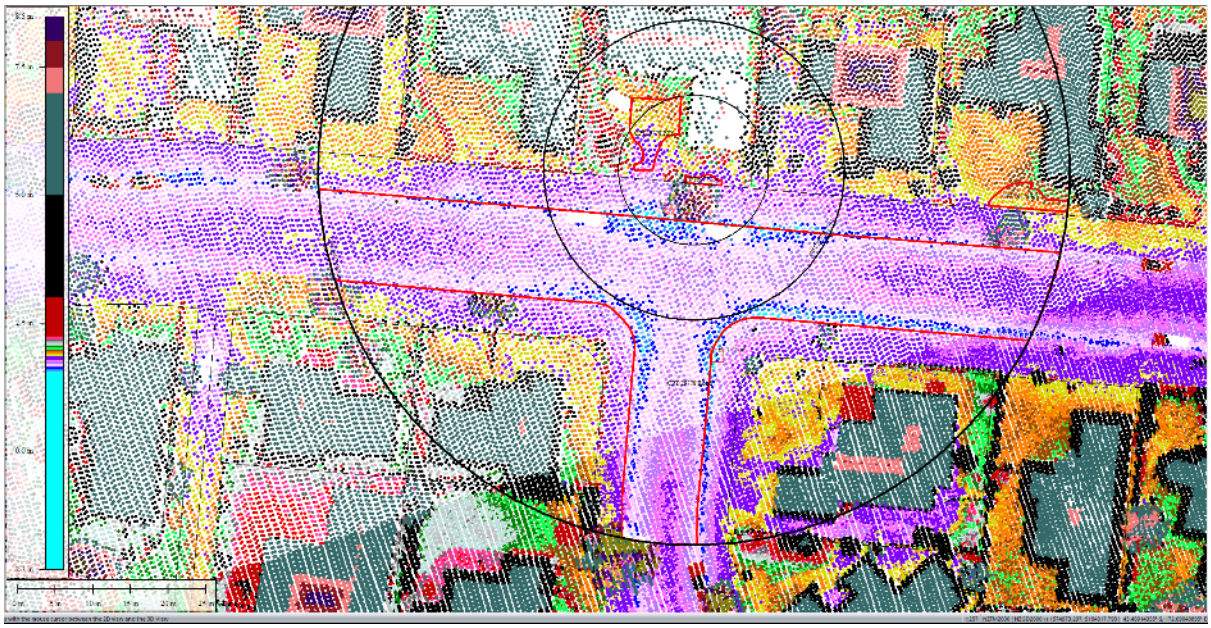

Figure 74: Ground surface elevation averaged over the 50-m buffer for Road for Oct 2015 LiDAR survey.

Figure 75: Absence of ejecta at the site for Sep-10 EQ.

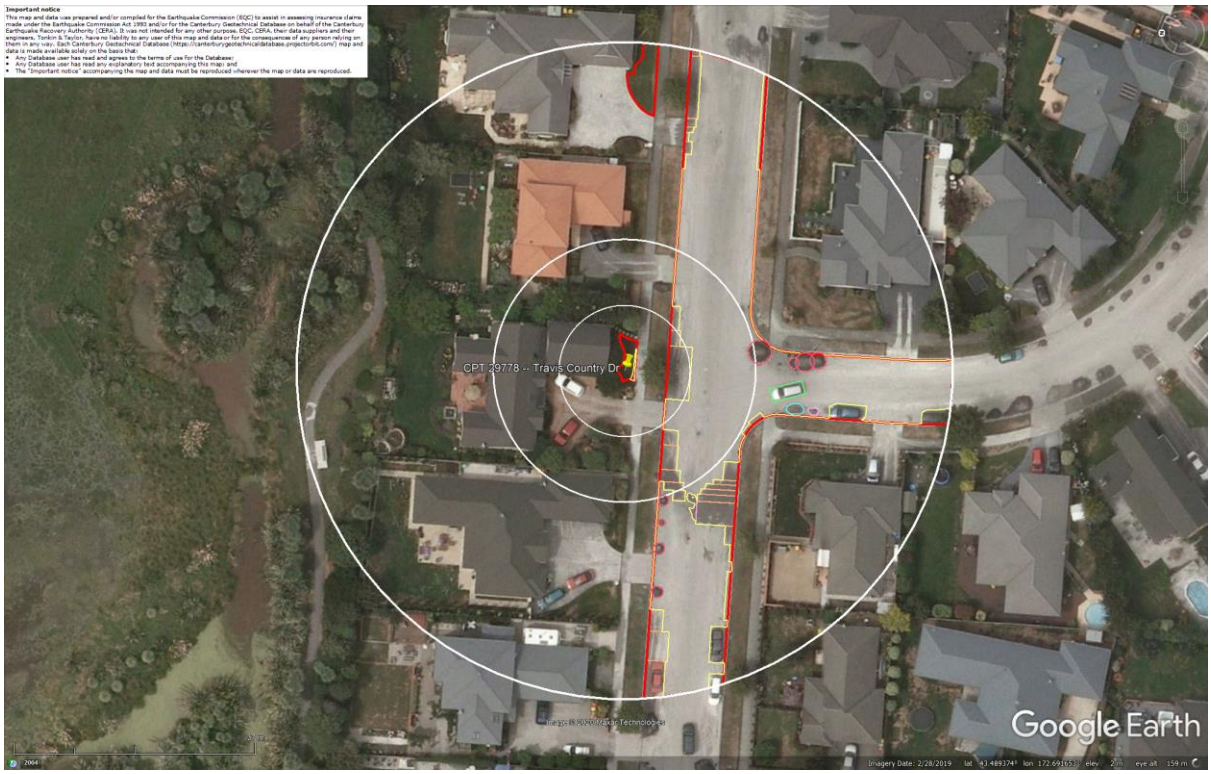

Figure 76: Ejecta outline for Feb-11 EQ.

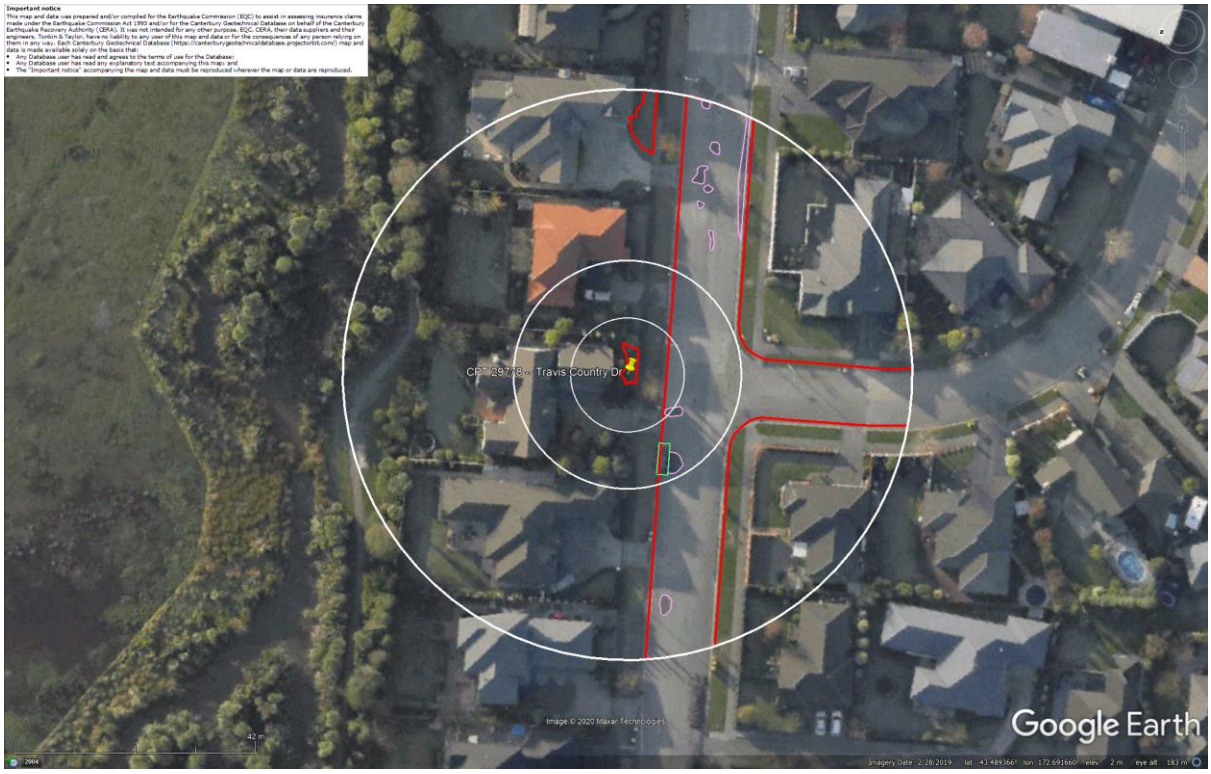

Figure 77: Ejecta outline for Jun-11 EQ in the aerial photograph acquired on Jun 14-15, 2011.

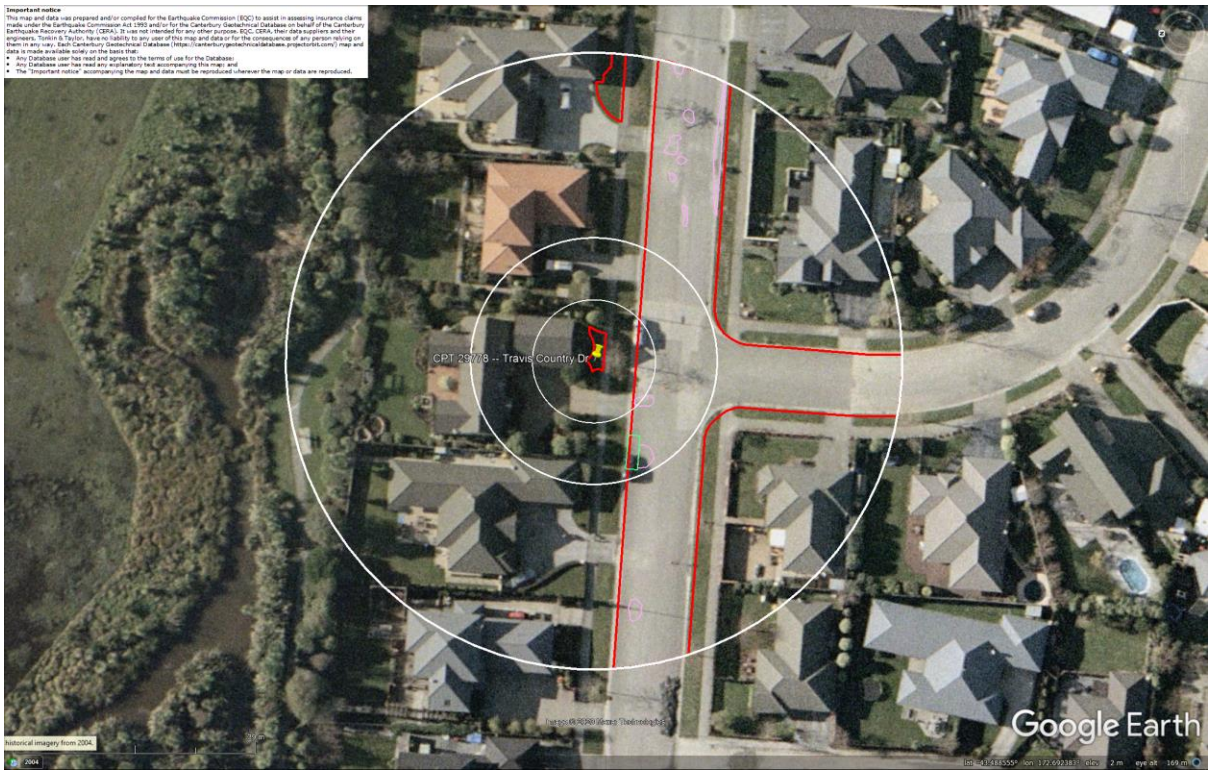

Figure 78: Aerial photograph acquired on Jun 16, 2011, showing ejecta outline for Jun-11 EQ based on the aerial photograph from Jun 14-15, 2011 (Figure 87).

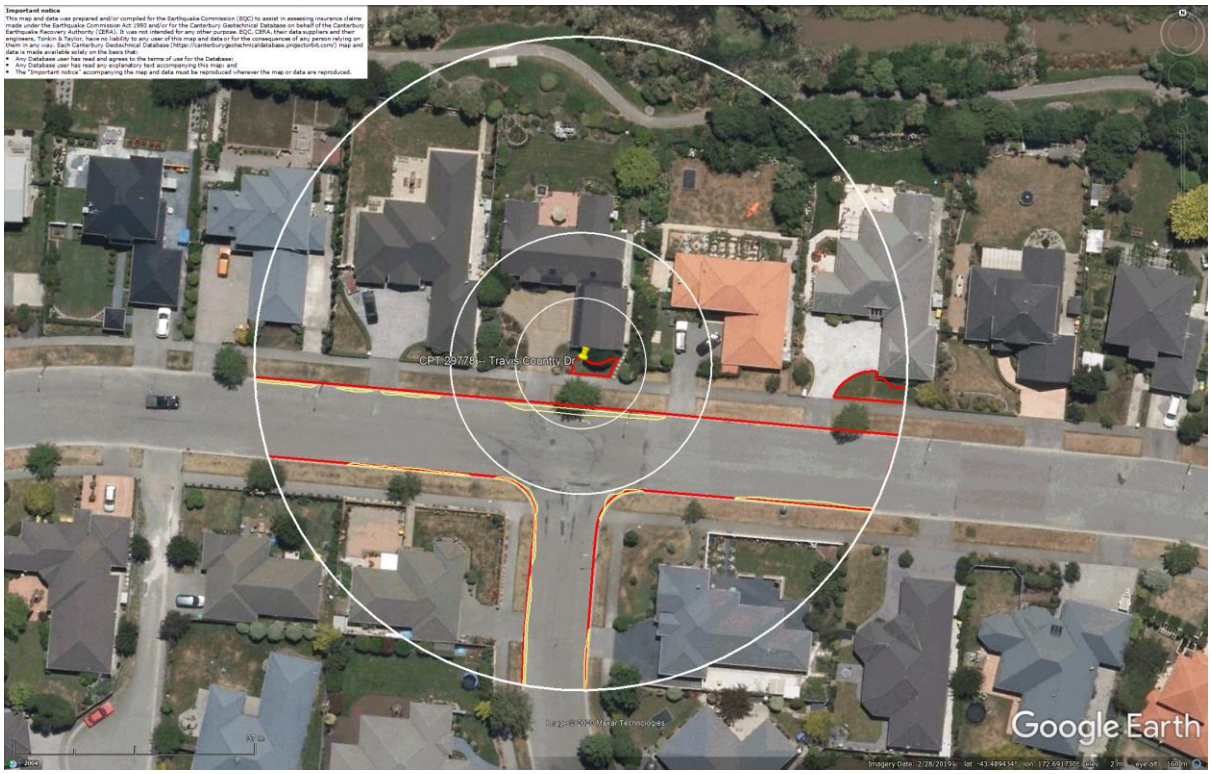

Figure 79: Ejecta outline for Dec-11 EQ.

Contents of this figure cannot be shared as doing so is restricted by a Non-Disclosure Agreement.

Figure 80: LDAT property inspection notes for Patch A (the dotted lines symbolize ejected sand).

Contents of this figure cannot be shared as doing so is restricted by a Non-Disclosure Agreement.

Figure 81: LDAT property inspection notes for Patch B (no signs of liquefaction according to the inspection team).

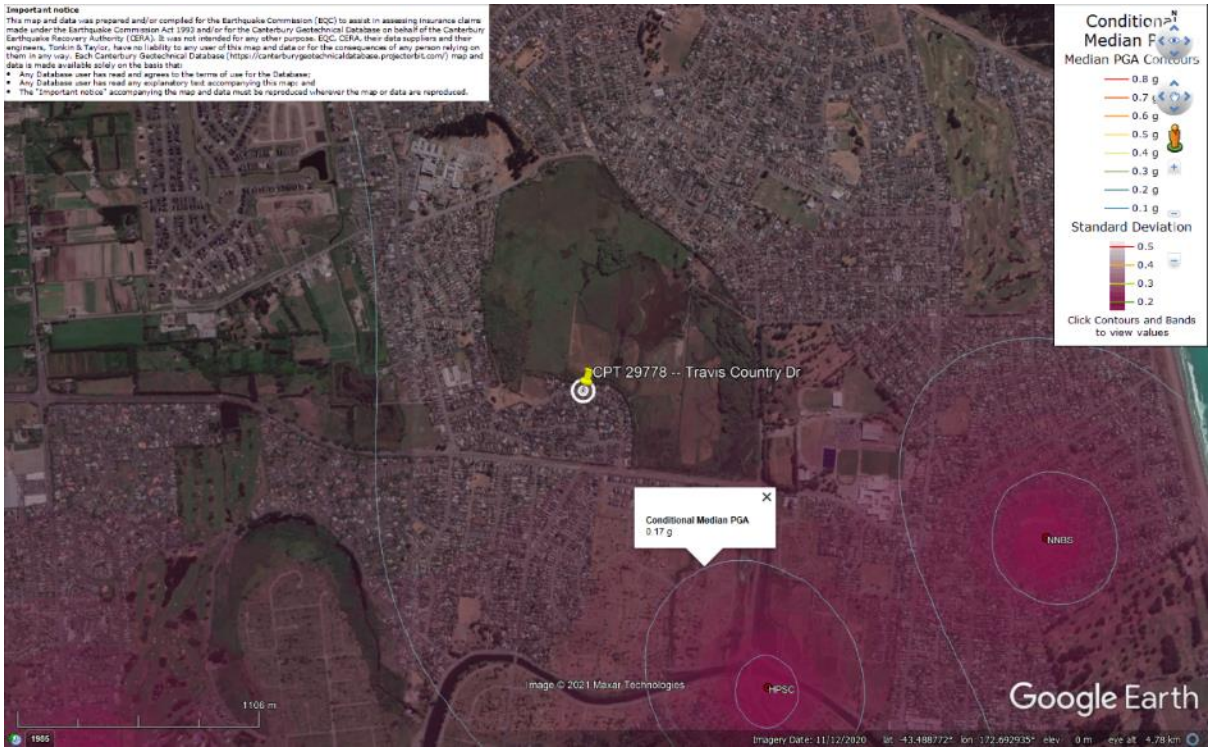

Figure 82: PGA for Sep-10 EQ (st. dev. = 0.325-0.350 ln units).

Figure 83: PGA for Feb-11 EQ (st. dev. = 0.350-0.375 ln units).

Figure 84: PGA for Jun-11 EQ (st. dev. = 0.375-0.400 ln units).

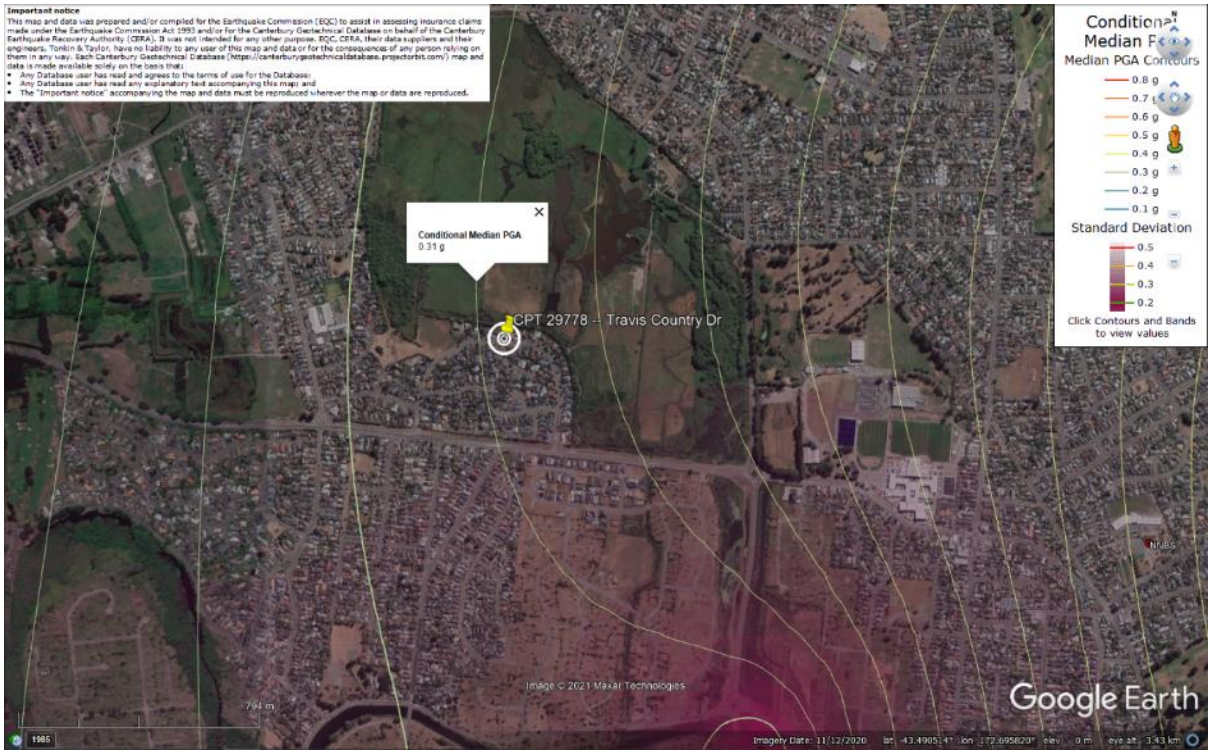

Figure 85: PGA for Dec-11 EQ (st. dev. = 0.375-0.400 ln units).

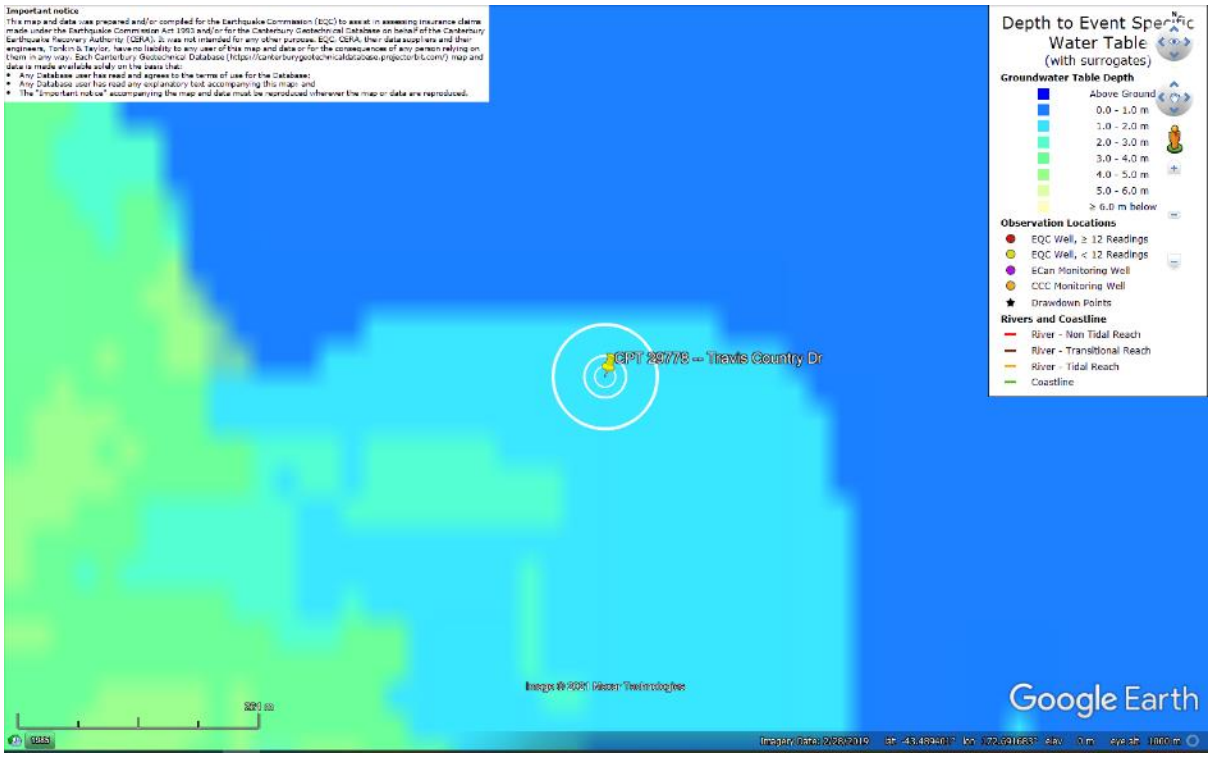

Figure 86: Depth to groundwater table for Sep-10 EQ.

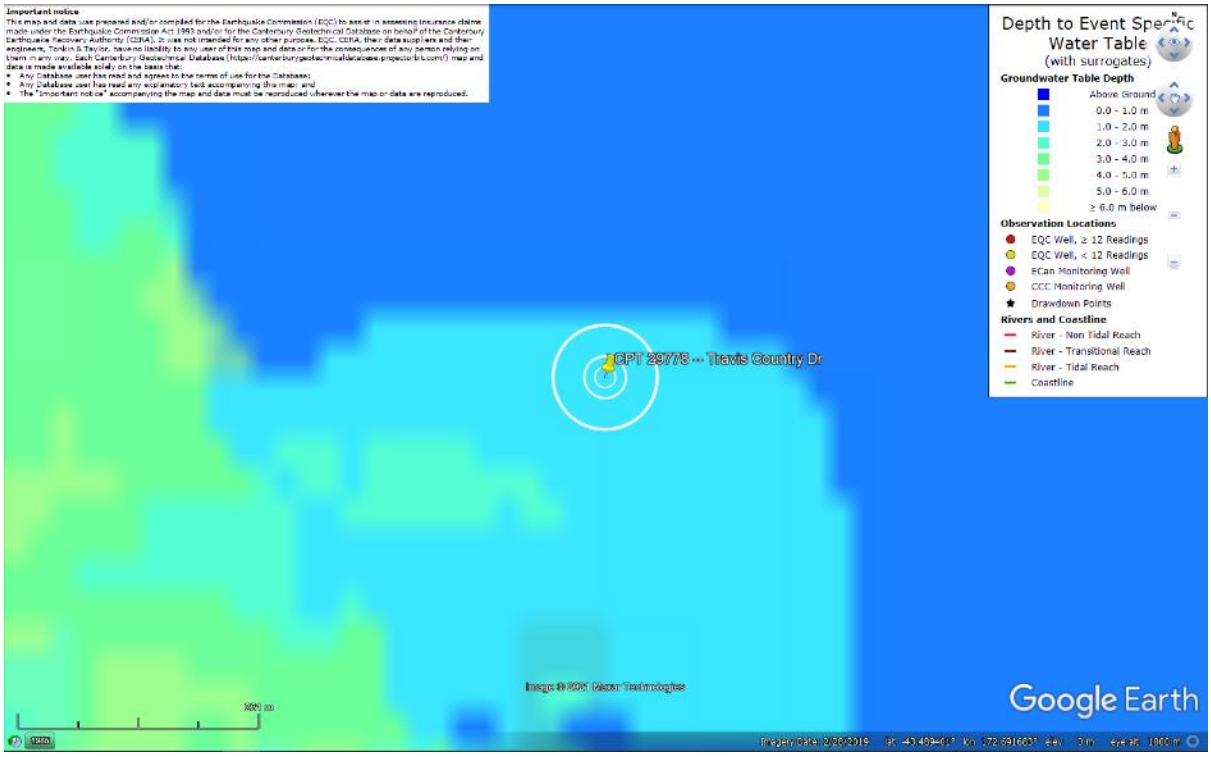

Figure 87: Depth to groundwater table for Feb-11 EQ.

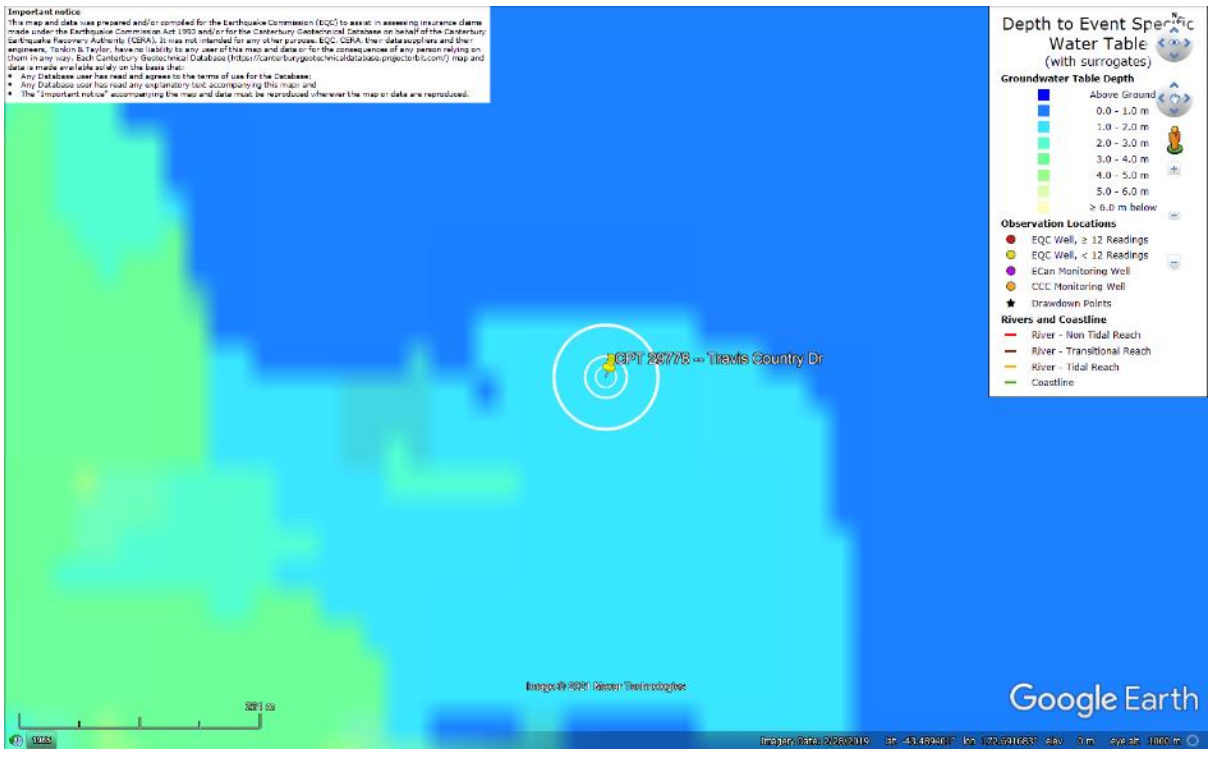

Figure 88: Depth to groundwater table for Jun-11 EQ.

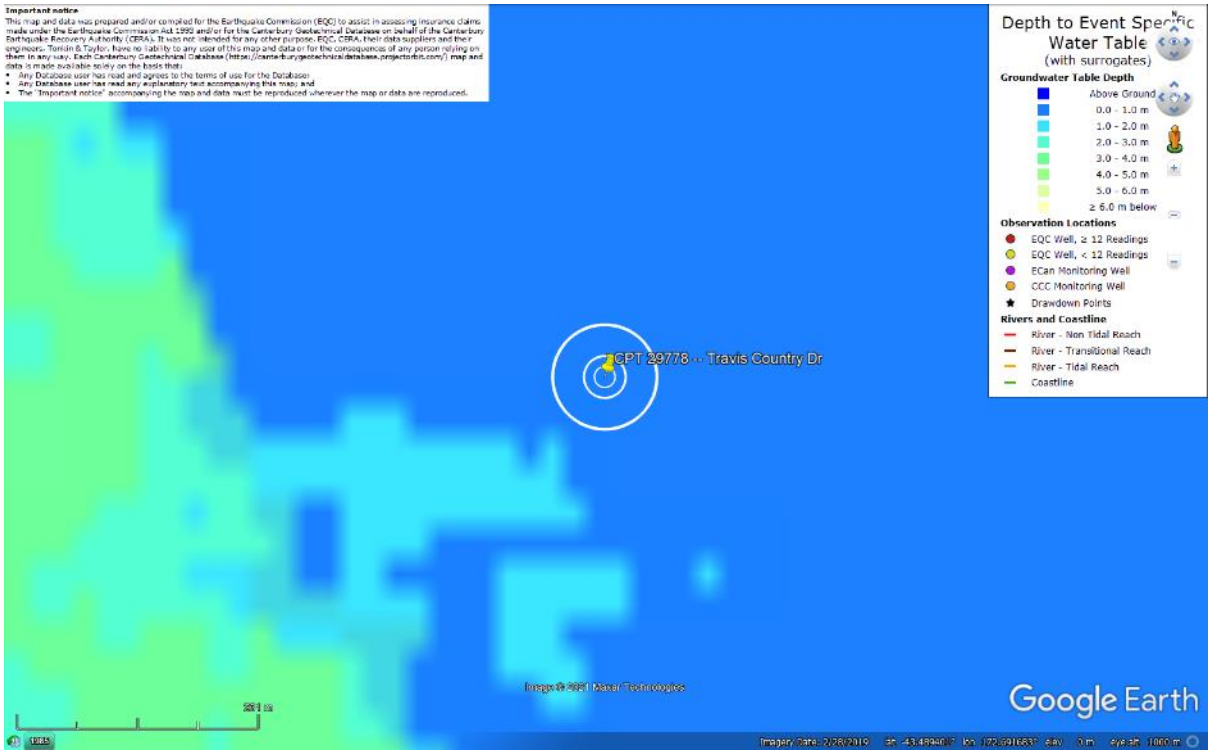

Figure 89: Depth to groundwater table for Dec-11 EQ.

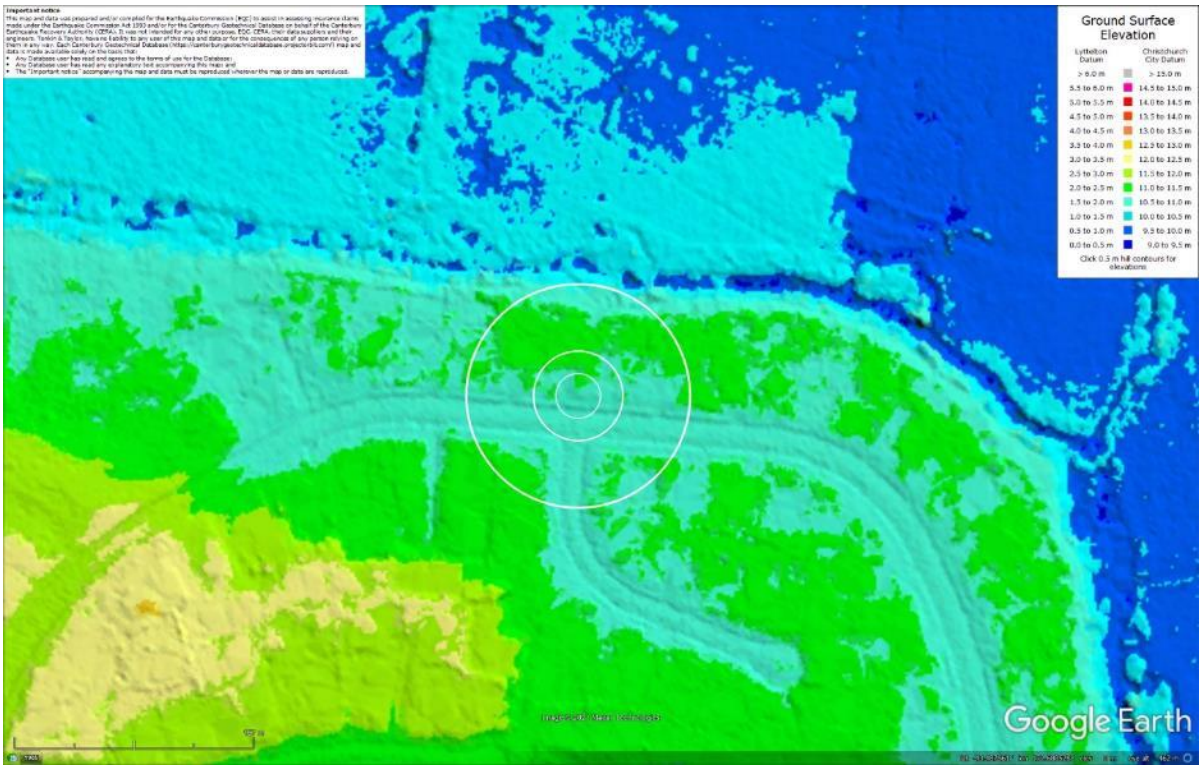

Figure 90: Ground surface elevation according to the Sep-11 LiDAR survey.

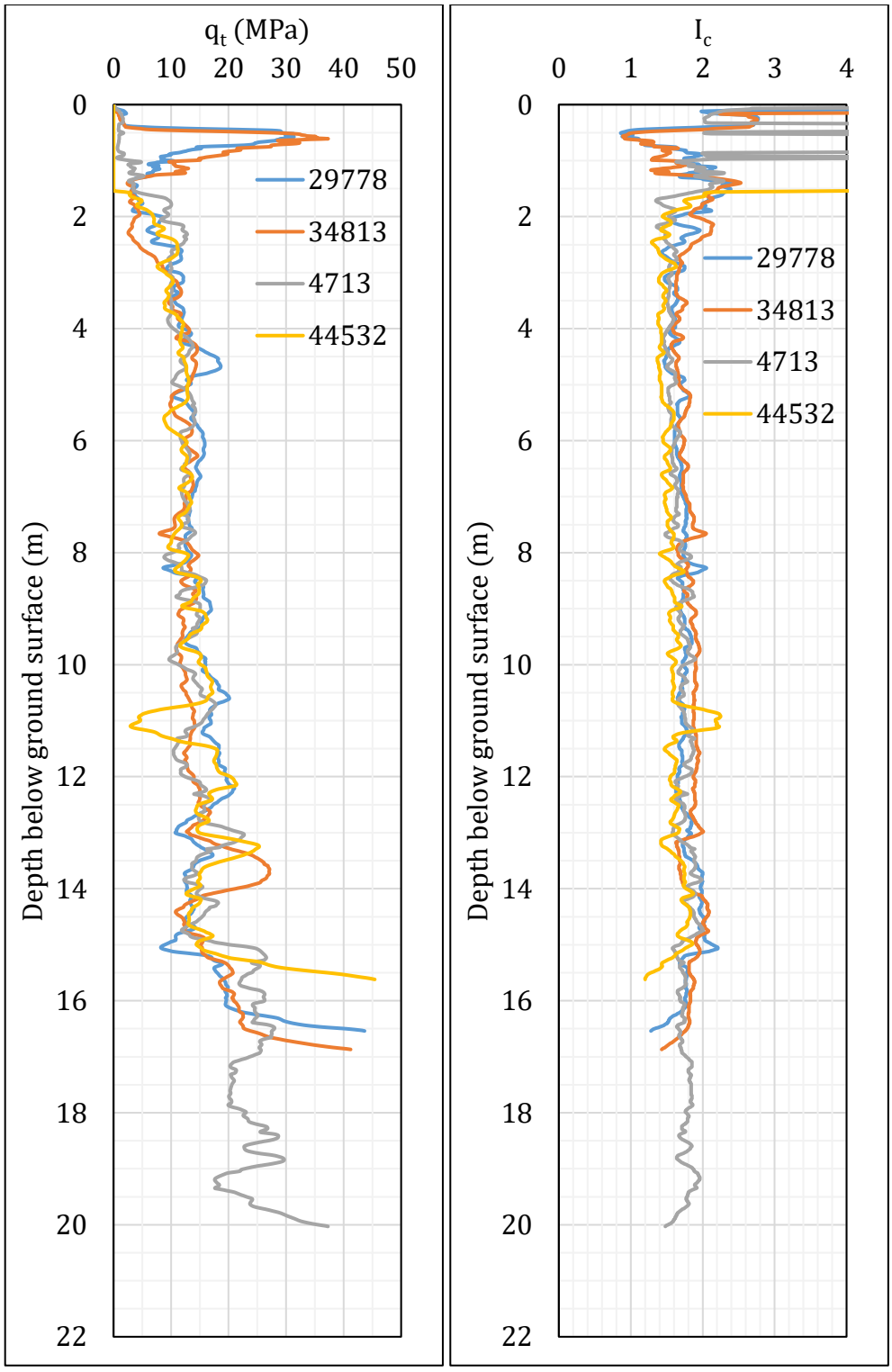

Figure 91: q_t and I_c profiles.

Note 9: The selection of CPTs for the area considered for settlement assessment (Figure 1) is based on the proximity of the CPTs to the considered areas. In accordance with that, the following table shows CPTs that were used for the volumetric settlement analysis in *Cliq v.3.0.3.2*, a CPT soil liquefaction software developed by GeoLogismiki. (The average volumetric settlements were reported in Table 8.)

Table 12: CPT profiles used in volumetric settlement analysis for areas selected for settlement assessment.

CPT ID No.	Patch A	Patch B	Road
29778	✓		✓
34813		✓	✓
4713			✓
44532			

Note: CPT 4713 was used to estimate the volumetric settlement between the 15-m and 20-m depth for CPTs 29778 and 34813.

Table 13: CPT-based results.

		CPT ID				
EQ Event	Parameter	29778	34813	4713	44532	$\Delta_{15m-20m}$*
Sep-10	S_{V1D} (mm)	0	0	0	9	0
	LSN	0	0	0	1	0
	LPI	0	0	0	0	0
	LPI_{ish}	0	0	0	0	--
	$D_{FS<1}$ (m)	undet.	undet.	undet.	undet.	--
Feb-11	S_{V1D} (mm)	4	18	14	48	0
	LSN	1	8	2	10	0
	LPI	0	1	0	3	0
	LPI_{ish}	0	1	0	1	--
	$D_{FS<1}$ (m)	undet.	1.87	undet.	1.58	--
Jun-11	S_{V1D} (mm)	0	1	0	10	0
	LSN	0	0	0	1	0
	LPI	0	0	0	0	0
	LPI_{ish}	0	0	0	0	--
	$D_{FS<1}$ (m)	undet.	undet.	undet.	undet.	--
Dec-11	S_{V1D} (mm)	11	30	29	51	0
	LSN	6	15	17	12	0
	LPI	1	4	3	4	0
	LPI_{ish}	1	5	2	3	--
	$D_{FS<1}$ (m)	undet.	1.34	0.97	0.52	--

Notes: $D_{FS<1}$ = Depth to the first liquefiable layer ($FS_L<1$) that is at least 200-mm thick, as determined by the Boulanger and Idriss (2016) liquefaction-triggering procedure (P_L=50%, C_{FC}=0.13, and $I_{c,cutoff}$ =2.6), and exported from *Cliq v.3.0.3.2*; undet. = the specified soil layer was not detected; * indicates the amount of S_{V1D}, LSN, and LPI to be added for CPTs 29778 and 34813 due to their penetration depths being shallower than 20 m.

Note 10: Based on the borehole log (BH 14719, Figure 1), the groundwater table is at a depth of 2.6 m below the ground surface. The soil profile consists of (1) fill (silty fine to coarse gravel) to a depth of 2.65 m, (2) silty fine to medium sand, SM, of the Christchurch formation to a depth of 3.05 m, and (3) fine to medium sand, SP, of the Christchurch formation to a depth of 20 m.

Note 11: The ejecta-induced free-field settlement provided in Table 11 is an areal average settlement due to ejecta, which is based on the total settlement assessment area, A_T (provided in Table 9 and repeated in Table 14). However, the considered area was not always covered completely with ejecta; thus, it is important to provide the localized ejecta-induced settlement, too. The localized settlement due to ejecta is estimated using photographic evidence only as

$$S_{E,P\_localized} = \frac{V_E}{A_E}$$

where V_E is the total volume of ejecta within A_T and A_E is the total coverage area of ejecta within A_T. Please note that the areal ejecta-induced settlement provided in Table 14 as S_{E,P_areal} is the same as $S_{E,P}$ in Table 11, which was estimated as

$$S_{E,P\_areal} = S_{E,P} = \frac{V_E}{A_T}$$

where V_E is the total volume of ejecta within A_T and A_T is the total settlement assessment area.

Table 14a: Areal and localized ejecta-induced settlement estimates for Patch A (10-, 20-, and 50-m buffers) based on photographic evidence.

Earthquake Event	A_T (m^2)	A_E (m^2)	V_E (m^3)	S_{E,P_areal} (mm)	$S_{E,P\_localized}$ (mm)
Sep-10	13.8	0	0	0	0
Feb-11	13.8	1.3	0.01-0.07	5±5	30±20
Jun-11	13.8	0	0	0	0
Dec-11	13.8	0	0	0	0

Notes: $S_{E,P\_areal} = S_{E,P}$ reported in Table 11 = areal ejecta-induced settlement; $S_{E,P\_localized}$ = localized ejecta-induced settlement; A_T = total settlement assessment area; V_E = total volume of ejecta within A_T; A_E = total area of ejecta within A_T; The estimates of both areal and localized ejecta-induced settlement are rounded to the nearest 5; Final plus/minus values are also rounded to the nearest 5; NA = Not available.

Table 14b: Areal and localized ejecta-induced settlement estimates for Road (50-m buffer) based on photographic evidence.

Earthquake Event	A_T (m^2)	A_E (m^2)	V_E (m^3)	S_{E,P_areal} (mm)	$S_{E,P\_localized}$ (mm)
Sep-10	1459	0	0	0	0
Feb-11	1383	1383	19.7-29.9	20±5	20±5
Jun-11	1449	48.8	0.2-0.5	<5	10±5
Dec-11	1459	58.2	0.2-0.4	<5	5±5

Notes: S_{E,P_areal} = $S_{E,P}$ reported in Table 11 = areal ejecta-induced settlement; $S_{E,P\_localized}$ = localized ejecta-induced settlement; A_T = total settlement assessment area; V_E = total volume of ejecta within A_T; A_E = total area of ejecta within A_T; The estimates of both areal and localized ejecta-induced settlement are rounded to the nearest 5; Final plus/minus values are also rounded to the nearest 5; NA = Not available.

Summary 2:

- **The best estimate of the localized ejecta-induced free-field ground settlement at the Travis Country Dr site for the SEP 2010, FEB 2011, JUN 2011, and DEC 2011 earthquake is 0 mm, 30±20 mm, 0 mm, and 0 mm, respectively.**
- **The best estimate of the localized ejecta-induced settlement of the road at the Travis Country Dr site for the SEP 2010, FEB 2011, JUN 2011, and DEC 2011 earthquake is 0 mm, 20±5 mm, 10±5 mm, and 5±5 mm, respectively.**